HIZIR EKŞİ

M.S. Thesis

2019

SEISMIC BEHAVIOR OF FIFTEEN YEARS OLD RC FRAME

HIZIR EKŞİ

IŞIK UNIVERSITY

2019

SEISMIC BEHAVIOR OF FIFTEEN YEARS OLD RC FRAME

HIZIR EKŞİ

B.S., Civil Engineering, IŞIK UNIVERSITY, 2016

Submitted to the Graduate School of Science and Engineering
in partial fulfillment of the requirements for the degree of
Master of Science
in
Civil Engineering

IŞIK UNIVERSITY
2019

IŞIK UNIVERSITY

GRADUATE SCHOOL OF SCIENCE AND ENGINEERING

SEISMIC BEHAVIOR OF FIFTEEN YEARS OLD RC FRAME

HIZIR EKŞİ

APPROVED BY:

Prof. Dr. Faruk KARADOĞAN   Işık University   _____

(Thesis Supervisor)

Prof. Dr. Esin İNAN   Işık University   _____

Prof.Dr. O.Cem ÇELİK   Istanbul Thecnical University   _____

APPROVAL DATE: ..../..../....

SEISMIC BEHAVIOR OF FIFTEEN YEARS OLD RC FRAME

Abstract

It is known that during the construction process of significant part of RC structure stock, mild steel and aggregates coming from sea bed used before the existing code proposals and standards in Turkey. Low concrete quality, mild-nonribbed reinforcement and sea type of aggregates are some of the under design features of those structures. This study mainly focused on seismic behaviour of this type of RC frame as experimentally and analytically.

Especially in humid environments, reinforcement corrosion probably occurs when the concrete quality is low and it includes aggregates coming from sea bed. The reinforcement corrosion can cause a lot of structural problems such as cracking of concrete, bond lost and decreasing of effective cross sectional area of rebar during the service life of RC structure. These destructive corrosion results limit the service life of existing structure stock. Depending on the degree of natural corrosion attack, the adherence between the reinforcement and concrete is adversely affected, the effective reinforcement cross section is reduced as a function of time and the cracking of the concrete cover can be seen as the main structural damages.

Within the scope of this study, the fifteen years old RC frames were tested to represent the structures which are naturally corroded and constructed before recent earthquake codes and standards. Nearly 1/3 scale one RC frames and one reference frame (15 years ago) were tested under the cyclic horizontal loads and constant axial forces in the İstanbul Technical University Building and Earthquake Engineering Laboratory. The seismic behavior of reinforced concrete frames has been tried to be explained by analysing the strength development, displacement capacity, ductility, lost of effective cross sectional area of reinforcement, stiffness, moment-curvature relations and displacement components obtained under cyclic load procedures. The poisson ratio of fifteen years old confined and unconfined concrete in descending branch of stress-strain diagrams was another topic for which only limited amount of literature is available.

In the theoretical part of this study; non-linear pushover analysis of the structural frame was investigated using by DC2B-v2 which include distributed plasticity theory, Sap2000 and SeismoStruct that are based on concentrated plasticity theory computer programs. The outputs obtained from these programs by using theoretical models and the results of the experimental behavior are compared. There is a special purpose computer program has been developed for finding the buckling load parameters of a frame with and without plastic hinges.

According to the experimental and analytical results; strength development, lateral and vertical displacement capacity, ductility and moment curvature relationships have been measured, evaluated and compared. The tested frame specimen did not reach its theoretical load capacity and drift level due to decrement of effective cross sectional area of reinforcement and decrement of adherence between the concrete and rebar. Displacement capacity of tested corroded frame was reduced visibly when compared with uncorroded reference frame. Some of the reinforcing bars of stirrups which are closer to the outer joints were ruptured at 4% story drift that indicate a loss in displacement capacity and shear capacity due to high corrosion attack on those outer stirrups reinforcements.

Keywords: Natural corrosion, Seismic Behaviour, Poisson's ratio

ONBEŞ YILLIK BETONARME ÇERÇEVELERİN DEPREM DAVRANIŞI

Özet

Ülkemizde bir çok kontrollü ve kontrolsüz yapı üretilmiş ve üretilmeyede devam etmektedir. Günümüzde yönetmelik ve standartlarından önce üretilen bu betonarme yapı stokunun önemli bir kısmının inşaası esnasında düz yüzeyli yumuşak betonarme çeliği ve beton üretiminde tuz muhtevası yüksek deniz kumu kullanıldığı bilinmektedir. Bu özellikleri taşıyan betonarme malzeme ile inşaa edilen mevcut yapı stokunun bir kısmı ise önemli depremlerde yapısal zarar görmüş veyahut kullanılamaz hale gelmiştir.

Özellikle rutubetli ortam şartlarında, kullanılan beton kalitesinin düşük olduğu hallerde veya beton içeriğinde kullanılan su veya agreganın korozyon tetikleyici bileşenleri içermesi durumunda ortaya çıkan yapısal korozyon ve süreç esnasında betonda meydana gelen çekme çatlakları ve dayanımdaki azalış yapının servis ömrünü etkileyen hasarların arasında en önemlilerinden bazılarıdır. Korozyon evresine bağlı olarak betonarme eleman bileşenleri arasındaki aderans bağını azaltması, etkili donatı kesit alanının azalması ve beton örtüsünün zarar görmesi başlıca yıkıcı etkili donatı kesit alanının azalması ve beton örtüsünün çatlayarak ayrılması başlıca yıkıcı yapısal etkiler olarak görülebilir.

Çalışmamız kapsamında ülkemizdeki var olan bu yapı stokunu temsil edebilmesi amacıyla yaklaşık 15 yıllık süreç ve doğal dış ortam koşulları içerisinde korozyona uğramış düz yüzeyli yumuşak betonarme donatısı ve deniz kumu kullanılarak üçe bir ölçekte üretilmiş betonarme çerçevelerin yatay yükler altındaki davranışı analitik ve deneysel olarak irdelenmiştir. İstanbul Teknik Üniversitesi Yapı ve Deprem Mühendisliği Labratuvarında gerçekleştirilen deneysel çalışmalar için 15 yıl önce üretilen ve doğal korozyon sürecine maruz bırakılan 3 adet numune ve 15 yıl önce aynı deney düzeneği ile denenmiş olan referans numunesi kullanılmıştır. Betonarme numuneler, kolon tepe noktalarına aynı anda etkiyen sabit düşey yükler ve her iki yönde etkitilen çevrimsel yükleme ile deneye tabi tutulmuştur. Kullanılan numuneler, ülkemizdeki yapı rezervinde sıklıkla karşılaşılan, standart ve yönetmeliklere uygun olmayan şekilde inşaa edilmiş; beton mukavemeti yetersiz, nervürsüz yumuşak çelik, deniz kumu ve agregası, yetersiz enine donatı gibi

özellikleri taşıyan yapı sistemlerini temsil etmektedir. Sargı ekisinin gözetildği onbeşyıllık beton/betonarme numune setleri ise gerilme-şekildeğiştirme bağıntılarından yararlanmak maksadı ile deneysel çalışma kapsamında denenmiş, iniş kolunda Poisson oranının davranışı gözlemlenmiştir. Deneysel çalışma ile elde edilen yapısal dayanım, deplasman kapasitesi, yapısal ve eleman sünekliği, donatı ve beton gerilme-şekil değiştirme bağıntıları, moment-eğrilik ve açısal yerdeğiştirme verileri ile doğal korozyon sürecine maruz bırakılmış betonarme elemanların deprem etkisi altında yapısal davranışı irdelenmiştir.

Bu çalışmanın kuramsal bölümünde ise; yapısal sistemin doğrusal olmayan analizi DC2B(v2), Sap2000 ve SeismoStruct programları kullanılarak incelenmiştir. Kuramsal modeller kullanılarak bu programla çalışılan yapısal davranışa ait veriler, labaratuvar çalışmasıyla elde edilen sonuçlar ile karşılaştırılmış ve irdelenmiştir.

Sonuç olarak, onbeş yıllık doğal korozyon sürecinin yapısal davranışta büyük önem derecesinde etki etmediği, net beton örtüsünün az olduğu sargı donatısı kısımlarında daha etkili olduğu görülmüştür. %4 kat ötelemesi oranına ulaşıldığında bu sargı donatılarındaki etkili çapın azalması ve kesme kuvvetini karşılayamadığından yapısal göçmeler oluştuğu görülmüştür. Analitik çalışmalar ile deneysel çalışmaların sonuçlarının uyum içerisinde olduğu görülmüştür. Gerilme şeklideğiştirme bağıntılarında iniş kolu esnasında beton numuneler üzerindeki yanal şekildeğiştirmenin büyük mertebelere ulaşması ve kabuk betonunun çatlama/ezilme suretiyle ayrışmasından dolayı Poisson oranının elde edilmesini olumsuz yönde etkilemiştir.

Anahtar kelimeler: Doğal korozyon, Deprem davranışı, Poisson oranı

Acknowledgements

To...

Table of Contents

List of Tables

List of Figures

List of Abbreviations

RC   **R**einforced **C**oncrete

FEMA   **F**ederal **E** **M** **A**gency

LVDT   **L**inear **V**ariable **D**isplacement **T**ransducers

TEC   **T**urkish **E**arthquake **C**ode

STEEL ITU **S**tructural and **E**arthquake **E**ngineering **L**aboratory

DC   **D**irect **C**urrent

Chapter 1

Introduction

1.1   Objectives and Scope of the Thesis

There are a lot of vulnerable RC buildings in earthquake zones built many years ago using the available materials at that time and referring to existing engineering codes in the time of design and construction. Especially in Turkey, during the recent destructive earthquakes such as 1992 Erzincan, 1999 Düzce&Kocaeli and 2011 Van earthquakes many structures had greater damage then expected. Turkey has very high seismicity due to active faults and huge amount of existing low-rise RC structure stock around the fault zones. There are many crucial mistakes done to come up with these unexpected damages observed on those buildings. Inadequate static design based on the early version of codes, insufficient concrete compressive strength obtained in the site, poor workmanship and other negative factors caused the unexpected damages on the structures. Reinforcement corrosion is another crucial point which causes this type of unpredictable collapses of RC structures. Because of that, natural corrosion of rebar has rising attention in widespread occurrence at RC structures such as buildings, viaducts, concrete covered roads etc.

Natural corrosion process has many destructive effects on decrement in capacity of structures and expected service life. It is known that rust which has been developed around the reinforcement bars causes increment in the size of original

bars and simply because of that high tensile stresses causes cracks in the concrete which will be another reason to increase the corrosion of bars. Also the effective cross sectional area of the reinforcement reduces due to this formation of rust and the bond between reinforcement and concrete is lost in corroded RC structures [1]. There are some studies carried on corrosion effets on RC structures, says that corrosion deterioration process of reinforcement bar that can affect the bond relations behavior and anchorage capacity of reinforcing bars with concrete [2]. These studies indicate that significant loss of bond strength observed between concrete and reinforcement during the corrosion process and the longitudinal cracks effects the bond behavior of reinforcing bars in concrete.

RC structures designed for the same seismic capacity could have different lifetime seismic performance and service life depending on their structural features at that time and environmental conditions. It is known that rebar corrosion leads to lost of bond between rebar and concrete, decrement in effective cross sectional area of reinforcement bars and decrement of total load bearing capacity at corroded sections rather than uncorroded sections. Consequently, corrosion reaction process effects the structural behavior of the RC structures that's why the RC structures designed for the same seismic capacity could have different seismic performance especially during the earthquakes.

Reinforced concrete 1/3 scale frame specimens were prepared and released by a team fifteen years ago at the main campus of Istanbul Technical University. Several of them were tested for some other purposes and rest of them were exposed to natural environment conditions to observe corrosion formation behavior on RC structures. In this study three of the one story-one bay, fifteen years old and naturally corroded specimens were tested by three different master students under constant vertical loads acting on the top of the both columns and lateral reversed cyclic loads which represents the earthquakes. The RC frame specimens have special structural features such as their concrete mixture which includes aggregate and sand coming from sea bed and non-ribbed mild steel used. This type of RC structures was widely constructed in Turkey before the existing earthquake codes

and standards. This study is composed of primarily the theoretical and analytical works mainly based on experimental works. 15 years old RC frame exposed the corrosion were tested and confined/unconfined concrete cylinder specimens were tested as well. The confined and unconfined concrete cylinder specimens were tested for working on poisson ratio and stress strain relationships in descending branch. Concrete core and reinforcement bar specimens were tested to have an idea about the material mechanical properties. By the help of this additional material tests, characteristics of actual concrete and reinforcement model behaviour defined and used in analyses to obtain the analytical results in the second stage of the main study. Different computer programs were used to analyse the structure and compare the overall results in some parameters such as ductility and displacement capacity in terms of natural corrosion time effect.

The main objectives of this study defined as fallows:

1. A comprehensive literature survey has been completed for the topic natural and accelerated corrosion which is an important topic as the rehabilitation of existing RC building which are poorly designed and poorly constructed in our country,

2. To learn how tests can be carried out in Structural Mechanics Labs: Preparations of specimens to test, instrumentation and measuring systems, loading schedule, interpretation of the data collected etc.

3. The main experimental program covers the test of one of the three 15 years old one story one bay 1/3 scale RC frame which is made from mild steel and aggregates obtained from sea bed to find out the earthquake behavior,

4. To observe the effect of natural corrosion on the earthquake behaviour of an RC frame first experimentally and then theoretically;Theoretical part will contain not only the material nonlinearity but also the geometrical nonlinearity to observe the loss of safety margin against buckling due to the material nonlinearity,

5. For doing that a lot of tests on 15 years old cylindrical 15/30 cm specimens has been conducted first. The results have been compared by code proposals, the stress-strain relationships of confined/unconfined specimens have been compared paying attention on the descending branches,

6. The poisson ratio of fifteen years old confined and unconfined concrete in descending branch of stress-strain diagrams was another topic for which only limited amount of literature is available,

7. Several computer programs such as **Sap2000**, **SeismoStruct** and **DC2B(v2)** were used to analytical works of modelling the corroded RC frame and a special purpose computer program has been developed for finding the buckling load parameters of a frame with and without plastic hinges.

1.2   Organization of the Thesis

This study include six chapters, list of references and appendices. The first chapter include the objectives with an introduction and scope of the thesis. In chapter two and three, corrosion in reinforced concrete structures, corrosion effects on structures, timeline, accelerated corrosion, natural corrosion, and natural corrosion evaluation techniques are explained. In those chapters, literature survey related to the topics of corrosion, destructive effects of natural corrosion process on structural features of RC structures, previous experimental and theoretical works on different bond behavior models, studies on corrosion analysis of reinforced concrete systems and reinforcement corrosion related codes are explained. Poisson ratio of confined and unconfined concrete related literature survey also introduced in those chapters.

In chapter four, experimental works are introduced. The preparation of RC frame and cylindrical specimens, the special characteristics of tested frame and specimens, the testing procedures and loading protocol, test setup with its instrumentation and test results are introduced in this chapter. Test results of corroded

reinforcement and core concrete specimens, RC frame specimens with compared reference frame, moment-curvature relationships and results of uniaxial tension tests are reported. Poisson ratio related test results are also given in this chapter.

In chapter five, the description and numerical representation of the prepared analytical model is submitted, respectively. This section also includes information on comparison of the theoretical and experimental outputs. Three different type of analytical study was performed with three different computer program to work on the destructive effect of corrosion process on RC structures. The conclusions, references and appendices are given, respectively.

Chapter 2

Literature Surveyo on Corrosion Behavior of Reinforced Concrete Structures

2.1 Corrosion

Corrosion reaction can be explained as an deteriation process of a metallic type of materials. Corrosion of reinforcing steel occurs due to several environmental reasons such as ingress of corrosion causing substances and causing material inside the concrete proportion.

Figure 2.1: Natural corrosion process and cover concrete cracking.

2.1.1 Corrosion Formation and RC Structures

There are a lot of destructive damages process effects the RC structures such as corrosion of rebar. RC structures include two main components which are concrete and reinforcement steel. There is a layer between them which has high PH zone features in the natural environment of concrete. This layer protect rebar from external effects by covering with an passive zone. Corrosion process can initialize by several reasons such as concrete permeability level, aggregates coming from sea bed and sea water inside the concrete. Also another effect can be given as RC structures may not designed and constructed suitable enough for the natural environment conditions to resist from corrosion attack such as insufficient concrete clear cover.

The main part of natural corrosion reaction is the formation of rust material on reinforcement steel as mentioned before. Rebar steel turn into the rust type of materials when it faced with air and water because of cracks on the concrete

surface. The important stages in corrosion reaction process of steel bars given in representative Fig 2.2 as below. First of all, air reached to the steel surface with the help of surface cracks, reinforcement steel begins corrosion chemical reaction process with the decreasing of pH value of protective layer surrounding as given Fig 2.2.
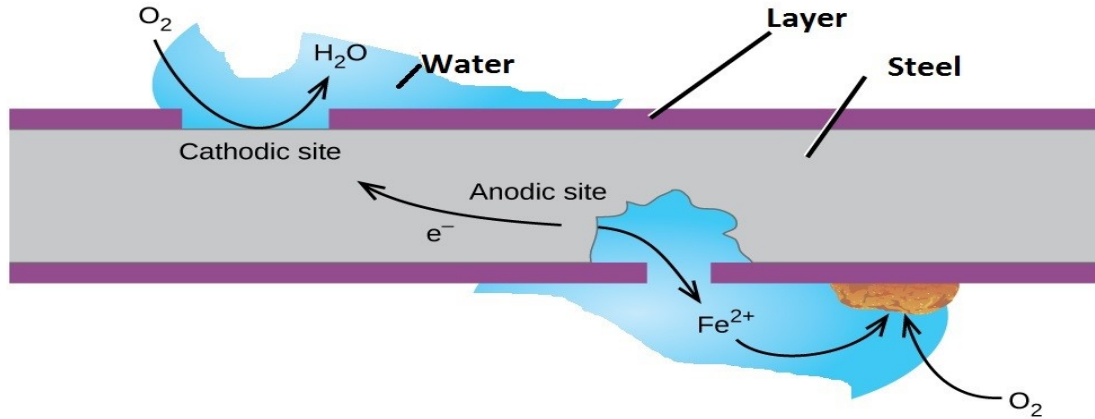
Figure 2.2: Natural corrosion process of reinforcement steel bar.

In figure given above; water is scratched on reinforcement steel, chemical reaction starts as seen bottom right of the figure. The reaction elapsed time depends on the corrosion inhibitors amount. There are some other destructive effects such as chemical composition of aggregates, concrete mix proportion, cure effect and environmental conditions [1].

2.1.2 Formation of Reinforcement Corrosion

Reinforcement steel corrosion is oxidation process that damages the reinforcement bar and causes the chemical reaction. Extensive corrosion process eventually causes structural weakness and many other structural destruction during the their service life. The natural corrosion of reinforcement in RC structures is an chemical reaction process that indicated below.

Natural corrosion observed in RC members mainly because of water. The chemical process of rust material initiated with oxidation of iron element to the irony cations which is shown by 2.1.

$$Fe \longrightarrow Fe^{+2} + 2e^-$$ (2.1)
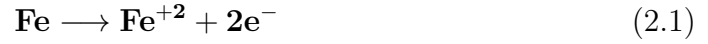
Water and air are the needs for the following stages of corrosion reaction process.

$$Fe^{+2} \longrightarrow Fe^{+3} + 1e^-$$ (2.2)

$$O_2(g) + 2H_2O + 4e^- \longrightarrow 4OH^-$$ (2.3)
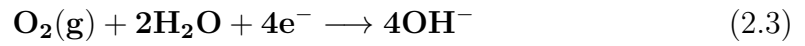
The ferric ions then combine with oxygen to form ferric oxide which is then hydrated with varying amounts of water with known chemical process. The overall equation for the rust formation at the end of the corrosion chemical process may be written as Eq.2.4 below :

$$Fe^{+2} + O_2(g) + H_2O \longrightarrow Fe_2O_3.H_2O + H^+ "rust"$$ (2.4)
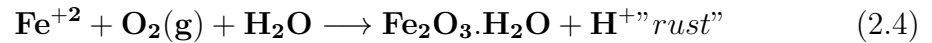
The including of water in natural environment can be taken as trigger evidence for which corrosion seems more widespread at humid environment than dry weather conditions. A lot of several destructive effects can increase the rate of chemical process of corrosion and its resultant damages on the RC structures. For example the presence of salt such as sea sand as this study focused on it, greatly enhances the rusting of reinforcement steel.

In literature, corbonation and chloride mechanism can be taken as main formation of natural corrosion process. If a reinforced concrete structures faced with chloride elements in their natural environment, it is likely possible to initiation

of corrosion reaction. The origin of chloride ions can be chemical concrete admixtures, aggregates coming from seabed, contaminants, marine environmental conditions and industrial brine or deicing salts. Carbonation types of corrosion process is the chemical reaction of carbondioxide and concrete in natural environment. This reaction process lead to decrement in pH up to lower than 8 and damage process, respectively.

The most important effects that influence the natural corrosion process: weather conditions, concrete clear cover (as shown in figure below), initial crack formation during the hyration of cement and permeability of concrete [1].

Figure 2.3: Concrete cover effect for natural corrosion attack in RC structures.

Concrete has many cracks formation and this cracks lead to start corrosion process and then reinforcements are strongly corroded, their corrosion products can expand, and deteriorate the thin concrete cover, by cracking, delamination and spalling.

2.1.3   Natural Corrosion

There are many recent study on the topic of RC corrosion which can mainly classified as accelerated and natural corrosion process of reinforcement. Natural corrosion process takes pretty time to observe corrosion results and its effects on reinforced concrete structures. On the other hand, accelerated corrosion process takes shorter time comparing to the real site natural corrosin process. But there are some problems with accelareted corrosion study process such as represantative model can not reach real corrosion process behavior due to accelaration of the chemical reaction. [3] studied on the similarities of accelerated and natural corrosion process in terms of rebar surface physical features after corrosion attack. The results pointed out that the special type of accelerated corrosion has similarity with natural reaction process. The rate of rebar corrosion that expected by Faraday's law was over than the resultant corrosion of accelerated tests.

The natural corrosion experimental program have been performed with the scope to study natural corrosion destructive effects with real time as 15 years. Chemical reaction process of natural corrosion needs to formation of electrolyte on reinforcement steel. When this chemical electrolyte occur on the steel surface as mentioned section before this section. Some researches find out the corrosion process rates under outside weather is effected from chemicals, water and weather conditions (3). Natural corrosion process formed on nature atmospheric environment without any chemical or unnatural touch. When the cracks on concrete lead to transfer oxygen and water on the surface of rebar, chemical reaction process of corrosion starts. At the end of the chemical reactions rust layer occurs on the reinforced steel bar as given above sections.

Table 2.1: Advantages and disadvantages of natural vs. accelerated corrosion behavior.

Natural Corrosion Research Study	Advantages	Disadvantages
	Real site structural behaviour	Take long time to study
	Occur partial part of structure and variable part to part	Can not control/stop the corrosion level
	Simulation of bond behavior	
	Exact material chracteristics	
Accelarated Corrosion Research Study	Take short time to study	Scenario behaviour
	Working at any corrosion level is possible	Occur whole structure and constant distribution
		Bond behavior and material characteristics are not at good agrement with real site behavior

2.1.4 Accelarated Corrosion

Accelerated corrosion process is that reinforced concrete sample specimens connected with current power with an anode and cathode side for experimental program. Reinforcement bars give electron with the current power force, increment of valency occurred on the steel, and then chemical oxidation process starts to formed. During the chemical reactions ; rebar's valency ascending with the decrement in the cathode side valency by the way. As mentioned in the section 2.1.2, reaction process accelerated and end of the process expected corrosion level reached and than test starts up.
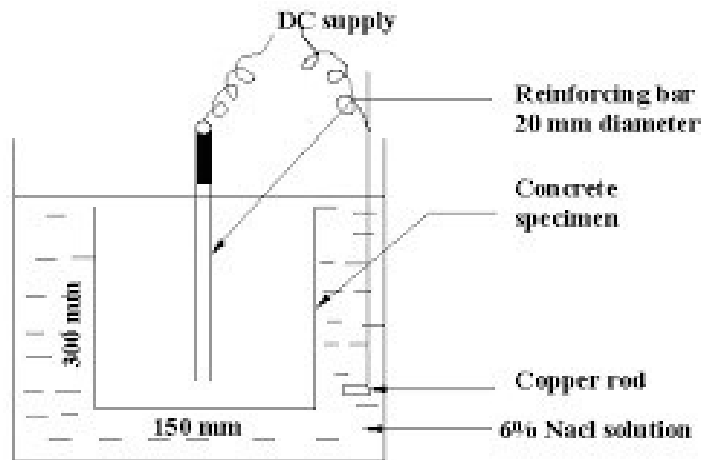
Figure 2.4: Accelarated corrosion test setup with DC power supply.

Natural corrosion experimental program needs unrestricted time such as 15 years to complete the corrosion process whereas accelerated corrosion tests needs significantly less time.

Accelarated corrosion experimental program has advantages during the design procedure and emergent corrosion process. Accelerated corrosion programs are applicaple during the construction on site. On the other hand, the results are not overlapp with real site's behavior of corrosion due to chemical touch and acceleration.

2.1.5 Literature Survey

This literature survey section is organized to collect recent corrosion related and poisson ratio related studies from the literature. There are some main group of study area on the topic of corrosion such as accelerated corrosion, RC member specimen such as only beam specimens or columns. Consequently, there is a gap over there to study earthquake behavior of corroded RC system specimens such as scaled or unscaled RC frames or site structures. Time effect and earthquake behavior does not consider in many studies on the topic of RC corrosion. This

master thesis study focused on natural corrosion effects on the one bay one story specimen with sea sand included low quality concrete, mild steel and substandard detailing under lateral cyclic-vertical axial loading.

Works are focused on destructive effects of corrosion process on mechanical properties of rebars and concrete with the base of accelerated corrosion rate. The structural behavior of RC sections with corroded steel carried out by some researchers but system specimen studies are limited. Also, corrosion effects the bond between the reinforcement and concrete as mentioned previous section negatively. There are some limited study with bond modelling for corroded RC members in literature. Consideration of corrosion in shear strength degradation with displacement ductility is another important part of the corrosion research. Poisson ratio of confined and unconfined concrete related literature survey also introduced in the section below.

2.2 Studies on the Effects of Corrosion on Concrete

Recent studies on the effects of natural corrosion on the mechanical properties of concrete are submitted below. [4] studied on evolution of the corrosion patterns based on two fully scaled RC beams which are corroded 14 and 23 years at chloride environment condition. The experimental results of the study shows that, at the cracking initiation stage (beginning of the corrosion reaction) localize the RC corrosion because of the localization of the cracks on concrete. Local pitting corrosion is the basic corrosion pattern and it has crucial impact that influence the structural deteriation process and bond behavior.

[5] studied on the structural performance of RC structure which has damaged concrete clear cover and confined using CFRP sheets. His experimental study covers exposing a RC beam specimen to an accelerated corrosion reaction through by DC power connection to the beam specimen. The rate of corrosion is a variable during the experimental study. This study pointed out that the strength and stiffness values of the corroded RC beam element is further more than reference

beam that indicate the CFRP jacketing improve the performance of RC structures from corrosion process.

[6] pointed out that building owners are faced with the cost of repearing of concrete cover that swelling with the corrosion of the reinforcement bars, generally due to chloride induced formation. Corrosion of the reinforcement bars and related strength reduction of concrete (concrete cover lost) lead this repearing and maintanance cost. He also pointed out that reinforcement corrosion lead to the loss in cross sectional area of RC members and decrement in the flexural strength capacity of them.

When reinforcement steel corrodes, its volume increase rapidly and exert a extra tensile forces on the surrounding conrcrete zone. This extra tensile force causes damage on the concrete and reducing the service life of the RC structures.

[7] studied on the structural corrosion effects on the concrete mechanical behavior. He pointed out that reinforcement corrosion is a main cause of deterioration that lead to formation of cracking on members concrete cover zone. These cracks conduce the increment of corrosion rate and then lead crucial ductility and capacity problems on RC structures.

[8] studied on the effects of natural corrosion damage on an existing RC structure. In this site study, corrosion defined as the predominant causal factor in the premature deteriation of concrete and reinforcement structure. Corrosion of reinforcement can lead structural problems because of bond loss among the concrete and rebar. Also, reduction of the concrete compressive strength is a another structural problems for RC structures. The presented study indicatesthat structure's life is restricted due to corrosion attack with the decrement in concrete strength, rising in porosity, cracking on surface and decreasing of effective cross sectional area of rebar.

[9] Present the results on a model that evaluation of the axial load capacity of reinforcement columns with different corrosion rate. The model considers strength

reduction in RC members due to cover damages and loss of confinement pressure. Concrete cover damages, buckling of corroded bars and decreasing of effective cross sectional area of rebars are the most destructive impact on RC structures because of corrosion process.

[10] studied on the modelling of bond behavior in reinforced concrete structures effected by reinforcement corrosion process. Modeling of such behavior needs effective nonlinear aproach able to cover main aspect of the corrosion such as cocnrete cracking, reduction in bond strength due to rust fand cracks formation, decreasing of steel cross section area and concrete strength reduction. The expansion of corrosion products causes concrete cracking and spalling of cover concrete. These crucial structural effects lead to reduction in contribution of concrete to the load bearing capacity of RC structures.

2.3 Studies on the Effects of Corrosion on Mechanical Properties of Reinforcing Bars

[11] work on the corrosion characteristics of reinforcement in naturally corroded RC 4 years old beam with corrosion accelerated inhibitors. The results of this study show that transverse cracks in the tension surface of reinforced concrete beam are occur due to the volume expansion of cross-sectional area of rebar. The authors mentioned that there is no huge similarities among the cracks open width and decrement of effective diameter of corroded reinforcement bar at various part of RC structures. Another result of this study is that the expansive rust formation initializes the longitudinal crack formation mostly at the mortar paste aggregate interface for the studied concrete specimens. As a result of this study, cracks that on the structures due to corrosion effect the RC structure's features. In the study of [12], effect of corrosion on the mechanical properties of reinforcement and the residual structural performance of the corroded beams are introduced. The study covers the topic of corrosion effects on the strength/capacity of reinforcing steel bars and related corresponding structural members.

[13] study on corrosion of reinforcement steel. Corrosion of rebar is the most wider form of degradation of RC structure's capacity through loss of rebar cross section, loss of bond between reinforcement steel and concrete. The decreasing in concrete strength is also another crucial effect of corrosion on reinforcement concrete structures. Corrosion attack effects on mechanical parameters of reinforcement steel is investigated through physical tests during the study of [13]. Reinforcement steels subjected to different accelerated corrosion scenario to obtain loss of strength and change in ductility along the bar. The result of the study are that ; for the plain mild steel reinforcement bars which subjected to small amounts of accelerated corrosion, the reduction in yield strength is not much greater than reduction in the cross sectional area of reinforcement steel bars. For heavily corroded rebars, the reduction in yield strength is less than the maximum reduction in cross sectional area of reinforcement steel. The decrement in ductility is greater than the decrement in yield strength for heavily and small corrosion cases. As an example for this result, reduction in cross sectional area of rebar 8%, lead to reduction in ductility 20% in reinforcement steel. In summary, this study claim that the loss of ductility insignificantly more than the loss in yield strength with increasing corrosion rate from the experimental and theoretical results.

[14] studied on the effect of corrosion on cross section loss of rebar, low and high cycle fatigue properties of Bst500s types of reinforcement steel which is widely used in Greece from 1990 to 2005 code update. During the experimental work; $\phi 12$ reinforcement steel bars were subjected to accelerated corrosion process and tested with both low and high cycle fatigue levels. The test results indicated that as the corrosion rate increases the yield strength, fracture(maximum) strength and the ductility of the reinforcement steel decreases.

In the study of the [15], effect of corrosion on mechanical properties of steel in twenty seven years old natural corroded RC beams was tested. Reinforcement rebars with dissimilar corrosion rate and consentrated pit deepness were used for tension based experimental program. It is mentioned that rate of corrosion influence the mechanical features of rebars and maximum stress-strain values. Also,

exact yield stress of corroded type of reinforcement steels kept same when their maximum stress was rising. A decrement of maximum elongation occurred to be the main impact of corrosion and effected overlapping with related standards. Also it is mentioned that the resultant corrosion behavior observed to be non-homogneous both throughout longiditional and perimeter's and cross section of reinforcement steel. Important result of the study are that; exact yield strength with effective diameter kept same with increasing corrosion rate. The proportion between yield strength and ultimate strength decrease with the decreasing corrosion rate. Another conclusion is that if the mean loss of diameter value is used in the computations, the modulus of elasticity is not effected by corrosion rate.

2.4 Studies on the Effects of Natural Corrosion on RC Structure Behavior

[16] studied on the effects of length and location of reinforcement steel corrosion on the behavior and load capacity of RC column members. Results of the accelerated corrosion formation process and eccentric load tests carried out. It is mentioned that the mechanical behavior and load carrying capacity of corroded reinforced concrete columns are affected by the location of the partial length, the corrosion level and the asymmetrical deterioration of the concrete section. Also another important point for the corroded RC columns with large eccentricity, higher corrosion rate in the tensile corroded length and a greater asymmetrical deterioration of the concrete cross section can result in less ductile structural behavior. Special failure modes are observed due to corrosion such as the splitting failure along the longitudinal corrosion cracks within the partially corroded length.

Study of [17] covers the predicting moment capacity of RC sections with accelerated corroded reinforcement steel. It is mentioned that, RC structure's deteriorated due to corrosion has raised a crucial level that effect its moment capacities.

Corrosion of the reinforcement lead to decrease in cross sectional area and debonding mechanism. This would reduct moment capacities of the RC structural sections. The results of the experimental and theoretical study find out that; reinforcement steel with natural corrosion effects had lost cross sectional area with compared unnatural corrosion procedure and because of the heavy corroded rebar $\phi 10$ had bear more loads wth huge mid section displacement. Also, non-corrosive reinforcement steel bars gave maximum moment capacities at early age of corrosion process while its behavior changed at later ages. In summary, the moment capacity of reinforced concrete decreasing based on the parameters such as loss of mass and decreasing of bond strength because of corrosion process.

[18] studied on the load carrying capacity of RC structure with corroded reinforcement. This study summarizes the results of research work carried out with corroded concrete beams. Reinforcement used in tests was corroded by added calcium chloride to the mixing water and accelerated corrosion process applied. It is mentioned that corrosion effect the type of failure in concrete beam with usual ratio of reinforcement. Corrosion of reinforcement affect the structural performance of concrete beam, increasing both the deflections and the crack widths at the service load and reducing the strength at the ultimate load. Besides, deterioration of concrete cover, due to cracking and spalling which produced by corrosion of compression bars, has also shown as important relevant.

[19] studied on the reinforcement corrosion in RC structures, its prediction and corrosion level monitoring. It is mentioned in the study that; corrosion is the one of the major durability problems. There are many parameters, some associated with the concrete quality, such as water cement ratio, cement chemical composition, concrete admixtures, initial surface cracks, humidity, air, temperature and organic bacterial effect which influence the steel corrosion process of RC structures. Prediction of the remaining service life of corroded structure is achieved by the help of numerical models and experimental procedures. Also, it is include that; generally in a well designed and constructed RC structure have

19

the contribution of reinforcement corrosion from the existing codes and design standards.

2.5 Studies on the Effects of Natural Corrosion on Bond Behavior

There are many study in literature about the influence of corrosion on bond behavior in RC structures. The most crucial conclusion in literature survey is that; bond strength rising up with increasing corrosion rate from the beginning to the 1 percent corrosion level but for the further corrosion rate bond strength decreases rapily. [20] studied on monitoring of the bond features as a function of corrosion level. They say that whereas the specimens which are unconfined show brittle failure behavior with increasing of surface cracks because of volume expansion, the specimens which are confined were reached damage limit because of confinement impact. There are some differences and similarities between the findings related to the ultimate bond strength of specimens with non-ribbed and ribbed reinforcement steels. Some part of the important researchers say that the maximum bond strength of specimens with deformed reinforcement steel is 3.5 6.9 times as high as for the bond strength of the specimen with non-ribbed reinforcement steel which is used in this thesis study (Fang et al., 2004). Moreover, the other researchers say that the maximum bond strength of specimens with non-ribbed reinforcement steel is 28.6% of deformed (ribbed) bars (Mo and Chan, 1996).

[21], Karin Lundgren et all.(2005) and Mario Plos et all.(2005) studied on the destructive effect of corrosion attack on bond in corroded reinforced RC structures. [22] focused on that the impact of rebar corrosion damages on bond behavior. Tests were achieved with four dissimilar corrosion rate. Pull out experiments and FE analysis were utilized and outputs from two stages were compared each other. For confined part, a medium level (4 percent) of corrosion has no crucial effect on the bond strength, but substantial reduction in bond strength took place when corrosion increased up to level of 6 percent. It is mentioned that the confinement

supplied an effective way to counteract bond loss for corroded steel bars of a medium (around 4 percent to 6 percent) corrosion rate. Also the results of analytical work which is finite element analysis show a reasonably good agreement with the experiments regarding bond strength and bond stiffness parameters.

[21] also work same bond parameters with Karin Lundgren et all.(2005). In this study pull-out tests were carried out to observe the effects of reinforcement corrosion on the bond strength, however important decrement in bond strength observed when corrosion rate rising up to degree of 6 percent. It is mentioned that lateral confinement provides an efficient techniques to avoid bond strength degredation. Also the results of analytical work which is finite element analysis show a overlap with the tests result's parameter of bond strength and stiffness. In this study pull-out experiments achieved to observe the degredation of bond strength because of destructive reinforcement corrosion process. A lot of specimens with different specific corrosion rate, specimens with and without stirrups were tested to observe confinment effect. Specimens that both ribbed and non-ribbed reinforcement steel bars were tested to supply the numerical information need to establish the bond properties with the maximum bond strength and end slip for different amount of accelerated corrosion level under pull out forces. The result from this study, corrosion support the increasing of bond strength for non ribbed reinforcement steel bar without any confinement at lower degree corrosion.

In the study of Mario Plos et all.(2005), effect of corrosion on bond slip behavior investigated under cyclic loading aspect. It is saying that, cyclic loading effect the bond between reinforcing steel bar and the surrounding concrete, especially when the reinforcement is corroded as same as our thesis experimental work. In Mario Plos et all.(2005) corrosion study, tests were carried out to observe bond strength slip behavior of corroded reinforcement. Accelerated corrosion level, confinement effect, bar size and type and loading history are the parameters of the study. The results mentioned that bond strength was reduced under cyclic loading. The bond strength decrement is more substantial for unconfined reinforcement steel bars than for confined ones. Besides to mentioned that the cyclic bond stress–slip

curves depended on loading history of the test programs that coming from the experimental results.

Karin Lundgren (2002) also studied on the modelling the effect of corrosion on bond in reinforced concrete. It is mentioned in this study that, corrosion leads to a volume increase on the reinforcement bars and then as a result of this increment, splitting stresses are induced in the structural concrete. By the way the bond mechanism between the reinforcement bars and concrete is influenced. Mechanical behavior of the corrosion products should be known to modelling the splitting stresses of the corrosion which is effect the structural behavior of RC sections. Author assume that the corrosion products behave like a granular material. The results of the study show that modelling method can predict the loss of bond when splitting of concrete occurs, because of the combined action effect of corrosion and bond slip mechanism.

In earlier work by researchers, a general model for the bond mechanism was developed to understand bond strength degredation during the corrosion process. In this bond model mechanism, the splitting stresses of bond relation are induced and bond stress depends on not only the slip, it also depends on the radial deformation between the concrete and reinforcement steel bars. This bond model can be simulated when the reinforcement steel is yielding during the loading. This bond model combined with the modelling of corrosion rust product behavior which is crucial to model and to reach the exact behavior of the corroded bond mechanism.

A bond mechanism model; This model includes bond relationship between the concrete and reinforcement is presented by Lundgren and Gtlltoft (2005). The bond behavior model is a frictional based theory covers nonlinearity to investigate the relationship between the deformations and the stresses occurs in the RC sections. The relationship among the tractions $\boldsymbol{t}$ and the relative displacements $\boldsymbol{u}$ are given below where D_{12} normally is negative. Also, for the hardening part

of the reinforcement is concern and a hardening parameter established in this model.

$$\begin{bmatrix} t_n \\ t_t \end{bmatrix} = \begin{bmatrix} D_{11} & \dfrac{|u_{tbond}|}{u_{tbond}} D_{12} \\ 0 & D_{22} \end{bmatrix} \begin{bmatrix} u_{nbond} \\ u_{tbond} \end{bmatrix}$$

$t = \begin{cases} t_n = \text{normal stress} \\ t_t = \text{bond stress} \end{cases}$

$u = \begin{cases} u_n = \text{relative normal displacement in the layer} \\ u_t = \text{slip} \end{cases}$
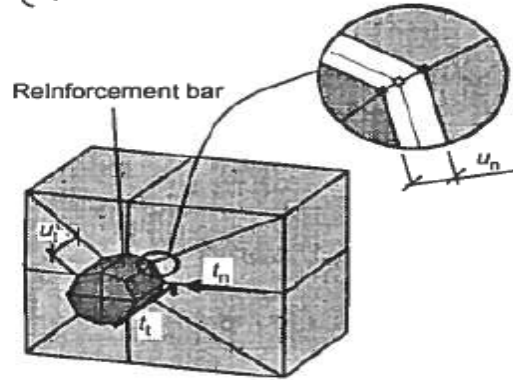
Figure 2.5: Variables of bond model interpretation t_n, t_t, u_n and u_t.

This model is valid for pull-out experiments with different section properties and loading types. In the bond mechanism, it was used in 3D finite element analysis of different anchorage situations. As a result that the theoretical bond model can describe the behavior good agreement with experimental results. In earlier analysis, slip among the concrete and reinforcement bars occurred firs and normal stresses are usually because of the suggested bond mechanism model. Also, for the modelling of the corrosion layer the mechanical behavior of the corrosion formation products(rust) should be known. Molina et all. assume that the corrosion formation product shows elastic behavior. Also some researchers assume that corrosion rust is behave like a material which cohesionless assemblage of incompressible crystals.

Table 2.2: The volume of the corrosion product rust relative to original volume of the rebar.

Corrosion Product	Volume increase
Fe_3O_4	2.2
$Fe(OH)_2$	3.8
$Fe(OH)_3$	4.2
$Fe(OH)_3, 3H_2O$	6.4

Mechanical behavior and volume expansion of rust compared with original reinforcement and modelled by this bond mechanism. The model included splitting stresses of bond and strength of the surrounding concrete. This model behavior in shortly is that the loss of bond during the splitting of concrete observed because of combined impact of bond mechanism and corrosion formation. But the most important point of this method is not concerned the creep, shrinkage of concrete and strength increasing during the life time of natural corrosion reaction process.

As a result; mechanical behavior and the volume change of the reinforcement should be known to model the bond behavior according to the Karin Lundgren (2002). Corrosion pressures before and after corrosion cracking, corrosion effect on concrete cover, frictional contact force between the bar-concrete interface should be considered during the modelling of bond behavior for corroded reinforcement according to the study of Xiaohoi Wang and Xila Liu (2006). In the study of Luisa Berto et all.(2008) assume similar statement with other researchers. Specially, they state that nonlinear behavior enough to cover the destructive impact of corrosion such as crack formation, bond loss and diameter loss of rebar. In these studies frictional type law and damage type law approaches used.

Pull-out experimental program and analytical works supports that submitted method effectively simulate the destructive impact of corrosion on bond behavior mechanism between the concrete and rebar, mainly for the damage type law approach.

2.6 Studies on the Effects of Sea Sand on Natural Corrosion

Sea effected corrosion is an main issue for marine ambiance corrosion research. Xıutong Wang et all.(2005) studied on the topic of effect of seabed sediment on RC structures corrosion. Seabed sediment type of aggregates were widely used in construction industry and the seabed soil sediment effects the RC structures to start up corrosion reactions.

Marine corrosion's environment can be examined in several parts such as splash area, atmospheric area, immersed area, tidal area and sediment area. Sea or ocean bed sediment area has lowest corrosiveness impat in a lot of reserach such as Hou (1998). On the other hand, there are some uniqueness between the studies because of the partially unknown behavior of corrosion products. [23]argue that the reinforcement corrosion process change in dissimilar areas having dissimilar natural environment such as marine site and desert site.

The sea effected corrosion process depends on many factors according to the research done by Hou et all. (2001). The electrochemical and microbial can be taken as two types of sea effected corrosion in practical site works. Electrochemical related types of corrosion directly has link with particle size, temperature, salinity, electrical resistance, dissolved oxygen and pH degree of RC structures. Microbial type of corrosion factors that include the sulphate bacteria substance, redox, organic and sulphate content. Sea water's pH value varying from 8–8.2 according to the [24] and the pH value in sea marine soil area tends to be close to that of the surrounding sea water.

Oxidation of sulphur that causes the reaction of hydrogen and sulphur elements with oxidation reaction with decrement in pH according to the Rajasekar et al.'s study. Within this pH reduction, corrosion process starts to formation and effect the steel mechanical properties in this types of sea marine environment RC structures.

Keisaburo Katona et all. study include the properties and application of concrete made with sea water and un-washed aggregates coming from sea bed. They made a lot of concrete specimens using sea water and un-washed aggregates coming from sea bed. The study mentioned that RC constructions that include non-corrosive reinforcement steel are durable with respect to other's in service life whatever the environmental condition is. In this study; to prevent concrete damages because of reinforcement bar accelerated corrosion, the applied current define the ultimate chloride at the beginning.

Using of sea water and unwashed sea sand in mix proportion of structural concrete were studied by researchers and they found that early strength of the concrete is high, and long-term strength is also retained at a high level. On the other hand, the permeability coefficient of sea or ocean water induced types structural concrete becomes small with respect to the concrete made using tap water as given below Fig[2.6].
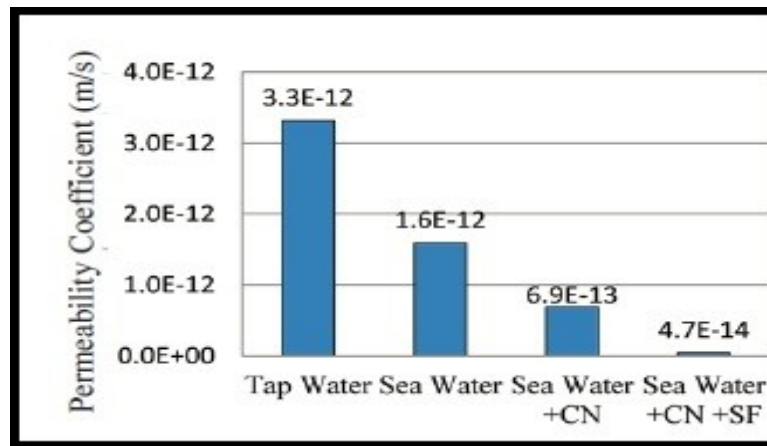
Figure 2.6: Permeability coefficient of concrete with using sea water.

Lastly, corrosion effects of sea water on RC structures and mechanical properties of structural concrete mentioned in this submitted study. Deterioration process of epoxy-coated steel reinforcement, carbon fiber rods and standard steel reinforcement were studied to understand corrosion effect on rebar after cyclic acceleration tests between autoclave conditions and ordinary environment conditions. At the end of 33 cycles tests process which corresponds to about 100 years in a marine

environment, the surraunding of reinforcement standard steel bars were corroded, but no corrosion product or chance in mechanical material features of the standard bars with the carbon fiber rods. It is easy to understand marine environment effect the mechanical properties of the standard reinforcement steel bars without any protection and coating.
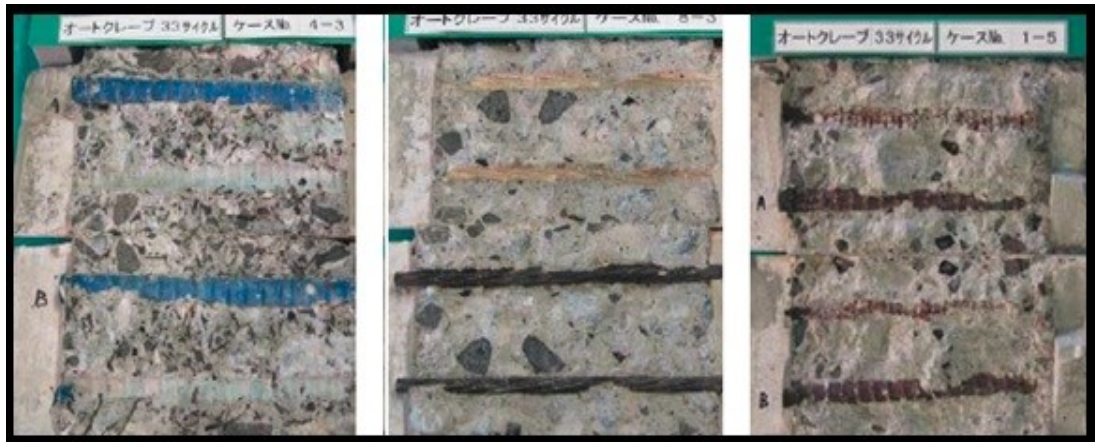
Figure 2.7: Epoxy Coated Steel, carbon fiber rod and standard reinforcement steel .

2.7 Studies on Real Site Natural Corrosion and Prediction

Prediction of corrosion rate in real site is crucial issue to comprehend the structural behavior in site practice for RC structures. To prepare a plan which for maintenance of corroded RC structures need to predict the rate and deteriotion level of corrosion.

Rapid monitoring or constant estimated corrosion level without any time effect increment models are used in damage estimated models for r corroded RC structures. Ignored parameters which influence the corrosion level in RC structures such as concrete cover loss are not considered with the modelling procedure.

to monitoring the existing corrosion level of structural RC section. A corrosion rate monitoring model is include numerical analysis of accelerated corrosion procedure. The another model that suggested by Ergün and Yalçın (1196) include

the contribution of acetate and chloride elements on corrosion rate. Existing corrosion rate is monitoring by LPR and half cell potential in this suggested procedure. The model covers the results that evaluated from accelerated corrosion experimental program with chemical touch.

Katwan et all.'s model (1996) include a numerical modelling which based on electrochemical noise technique which based on the foundation of electrochemical noise technique for the prediction of corrosion rate in RC structures for real site application. This model developed with testing of full-scale RC beams under dynamic(earthquake load/live load) and static loading (dead load) and exposed to a corrosive environment conditions such as marine environment.

[25] suggested an theoretical model based on mainly experimental test results included in a five year accelerated experiment stage on initially non-cracked RC bridge deck slabs with different parameters that height of concrete clear covers and w/b ratios. Cement contents of mix proportion was also another parameters to define a model with different accelerated corrosion rates.

Vu and Stewart's model (2000) is defined as an corrosion real statement monitoring model include that the enough air content at the reinforcement steel surrounding. This modelling does not consider the change in concrete mechanical features with variation of binder materials. This modelling narrowed to corrosion formation process where the chemical reaction is the dominant.

One of the other developed model that the Duracete corrosion bond model (1998) is an attempt to development on Alonso et all.(1988) suggested with other corrosion rate effected parameters. Model of Scott's(2004) cover the results of the testing programme which covers cracked beam specimens with different crack width, different concrete cover and different binder type as a test parameters. This model was developed by the testing of cracked specimens due to corrosion But this model not include the crack geometry as an governing factors. In the model similar to the others corrosion prediction models given above. It is not visible in the model of Scott that corrosion rate is a constant or not.

[26] studied on aexperimental methods for real site corrosion monitoring of rebar base don method of polarization resitance. The test methods that described in the [26]'s study can be used for on real site condition assessment of RC structures. This methods proper to use at any time during the service life of the reinforced concrete structures, and every climate conditions, except the temperature is lower than 0^oC. The conclusions of the study are pointed out that identification of effective corroded zones, evaluation of the effectiveness of repair techniques such as coating and implementation into structural calculations (damage functions) can be done with use of the corrosion rate determination tests and numerical results.

Accelerated test has become wide spread methodology to predict destructive effect of corrosion in RC structures within a short time of period comparing to the natural corrosion testing process. But, this methodology has some disadvantages to represent the exact behavior of natural corrosion of real site RC structures. There is a gap over there to predict the naturally corroded reinforced concrete structures earthquake behavior in site practice. As summary, factors effected the corrosion such as cover such as concrete cover spalling, concrete strength and time effect should be considered in corrosion in corrosion level monitoring models. Also, natural corrosion process is a crucial stage in prediction models which is not concerned generally. Most of the prediction models using data from accelerated corrosion tests. Therefore, real site natural corrosion process and other studies's results should be combined with modelling to develop reliable corrosion rate prediction models to obtain real site corrosion prediction for RC structures.

H. Yalciner et al.(2012) work on the effect of corrosion deteriotion on the performance level of an old RC structures. Evaluation of the serviceability of a corroded RC structure take a vital place to prevent serious effects on structures and indirectly on people actually during an unpredicted earthquake. In the study of the researchers ; 25 years old and naturally corroded RC building analysed and

theoretically researched with parameters that function of corrosion rate. Bond-slip relationships between the corroded reinforcement bar and existing concrete strength were cover the nonlinear structural analysis which based on corrosion rate function.

When the reinforcement corrosion process begins, expected load bearing capacity of a reinforced concrete structure decrease because of the different effects of corrosion on mechanical properties of reinforcement and concrete. It is vital to predict that what kind of corrosion effects are needed to be taken into account when the nonlinear seismic performance analyses reached for RC structures.

Cross sectional area loss of reinforcement steel bars can lead the reinforcement bars buckling before the reaching the point that their yield strength capacity. Also energy dissipation capacity of RC structures decreases which also causes to have less ductile behavior during an real earthquake. It is common known and mentioned in the study that corrosion can lead unexpected structural damage because of the decreasing of bond strength between surraunding concrete and reinforcement steel bars. Corrosion rate which obtained from experiment was used to taken into account the reduction in cross sectional area of reinforcement steel bars, and the decreasing in concrete strength as a function of time with increasing corrosion.
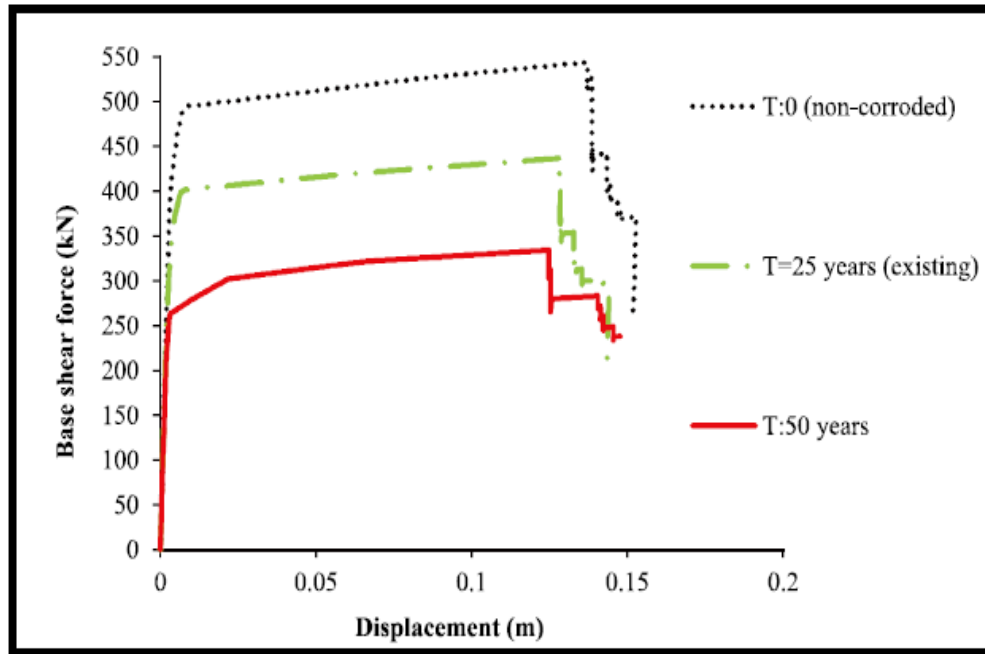
Figure 2.8: Capacity curves for non-corroded and corroded building with time dependency.

There is an important reduction of the load bearing capacity curve as shown above Fig.2.8 for the corroded reinforced concrete structure with respect to non-corroded RC structure. It is clear that when RC structures corroded, load bearing capacity will decrease due to the corrosion damages on structures. It is also clear that for the same amount of base shear force displacement increases as a function of time due to corrosion. Besides it can be observed from the graph that the mechanism of failure are affected by corrosion formation process. This study show that expected service life of RC structures is effected by reinforcement steel corrosion formation process where the quality of concrete, permeability or initial cracks on structures, and the concrete cover depth and environmental factors effect the expected service life of reinforced concrete structures.

Chapter 3

Literature Survey On Poisson Ratio

3.1 Poisson Ratio of Concrete

Poison's ratio of the concrete is the ratio between lateral (horizontal) strains and vertical strains. Poisson's ratio, mathematically can be calculated as below formulation 3.1.

$$\vartheta = -\frac{\epsilon_D}{\epsilon_L} \tag{3.1}$$

Where

ϑ = Poisson's ration

$\epsilon_{\mathbf{D}}$ = Strain along the horizontal axis

$\epsilon_{\mathbf{L}}$ = Strain along the vertical axis
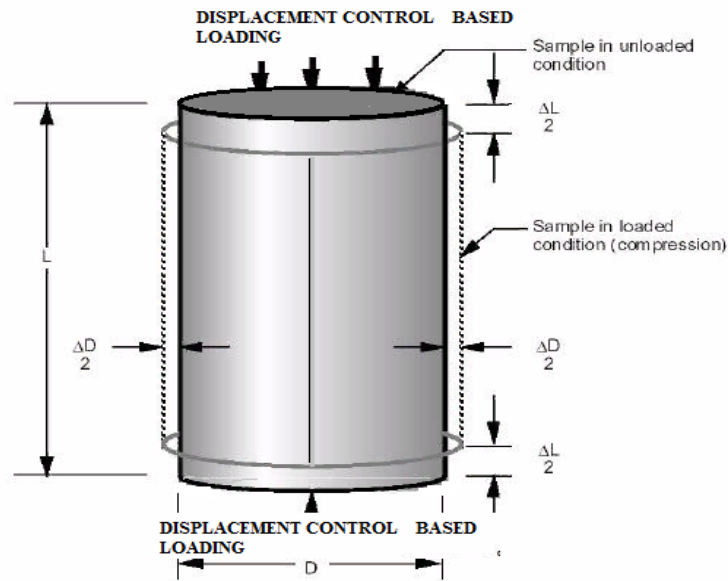
Figure 3.1: Poisson's ratio of a concrete specimen example.

When compressive force acts on a concrete specimen with the increase in loading force, two types of strains that will crop in the specimen of concrete at plastic region. Both strains are opposite in direction, one is along longitudinal axis and second is in vertical direction, that is due to reduction in volume at vertical direction.

The Poisson ratio of concrete in lowering load branch has generated research interest because of the lack of research in this topic and hardness of experimental works. The possibility of collecting deformation data of concrete with increasing load branch have been investigated unless to lowering load branch by many researchers, but to date, the information available on the Poisson ratio of concrete under axial loading at lowering branch is limited. In the literature there are some related recent works introduced on the below sections.

3.2 Studies on the Poisson Ratio of Concrete

Ata et al (2005) pointed out that Poisson's ratio of laterized special type of structural concrete with change the ratio range between 0.25 and 0.3. This study

pointed out that, if the age of concrete increase, poisson ratio of structural concrete will increase. In addition to this important point, it was noted that curing method and time, compaction level and water/cement ratio have effect on Poisson's ratio of structural concrete. In the study of M. Anson and K. Newman (2016), they work on the relation between the mix proportions and Poisson's ratio for structural mortars and concretes. This study mention that, it is visible that Poisson's ratio is affected by the method of testing, the mix proportions, environment moisture condition and temperature of the specimens. Static and dynamic properties of Poisson's ratios studied for saturated structural mortars and concretes during the experimental part of the M. Anson and K. Newman's study.

K. Sideris et all. (2004) studied on the modulus of elasticity and Poisson ratio of structural concrete. The relationship between compressive stress and Poisson's ratio of structural concrete was investigated by using the cement hydration equation in this study. Hydration criteria of structural concrete is established and hydration process used for computing the numerical outputs up to last hydration in terms of Poisson's ratio. Poisson's ratio and compressive strength have linear relationship between them according to the this and previous studies.

This study mention about that, Poisson ratio is measured from concrete strength which develop with increasing time. Also increment in Poisson's ratio is depends on the concrete strength. As a result, there is a direct correlation among the compressive stress of concrete and Poisson's ratio given below figure by the proportion methodology of two different points.
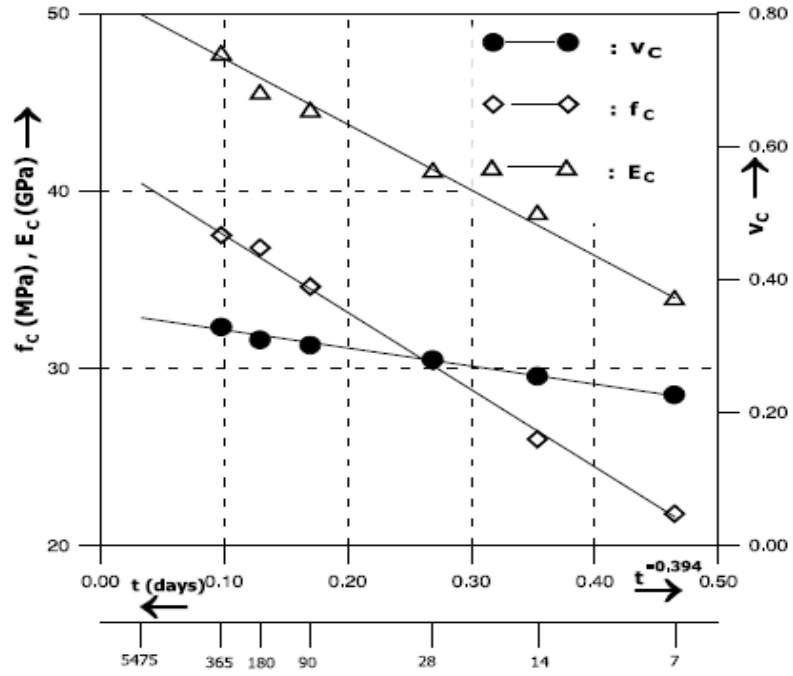
Figure 3.2: Mechanical features of concrete as a function of hydration time.

[27] studied on the monitoring of Poisson's ratio and elasticity modulus character-istics for special type of structural concrete which is unsaturated concrete. Many types of RC structures such as dome, viaduct and tunnel are located in water induced environment. In this types of water faced region ; concrete is usually unsaturated because of it is in the water with whole structure or partially along the time. Some researches have showed that the mechanical properties of concrete such as Poisson's ratio and modulus of elasticity are affected by the saturation degree of the concrete and aspect ratio of pores on the surface and body of the structural concrete.

$$\upsilon_{\mathbf{unsat}} = \frac{1}{2}(1 - \frac{1}{\frac{1}{3} + \frac{K_{unsat}}{G_{unsat}}}) \tag{3.2}$$

In this study it is also mentioned that ; fluid in wet pores limits the concrete deformation movement more than air induced (dry) pores, because of this reason Poisson's ratio value of wet concrete decrease with the decreasing of saturation

35

degree. Poisson's ratio of unsaturated concrete $mathbfv_{unsat}$ given as above formulation and relationships that given below figure.
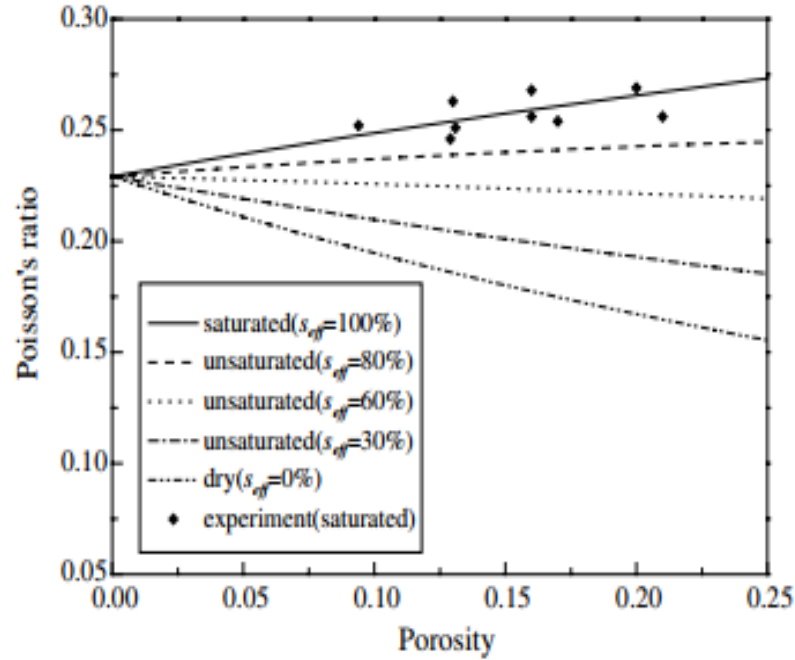
Figure 3.3: Relationship between Poisson's ratio and porosity ofunslaked concrete.

As seen in figure above, Poisson's ratio of unslaked structural concrete is gain with the rising of existing saturation level and porosity. This research conclude that; Poisson's ratio properties of moist concrete increase according to the dry specimens with same conclusion in Metha and Nonterio (1997).

3.3 Studies on the Confinement Effect on Poisson Ratio of concrete

In today's world, outer confinement of structural concrete by fibre materials has become highly popular for structural applications on site. Fibre wrapping of existing structural members and encasement of structural concrete in a FRP, CFRP and other types of confinement shells. Each type of confinement(inner or outer) effects the mechanical properties of the structural concrete.

There are limitted studies in the literature on the topic of Poissons's ratio and confinement effect. [28] studied on the confinement of concrete effects on its strength and ductility features. There is a concrete confinement model depends on capturing criteria in this study. During the this experimental study, fifty-four structural concrete specimens were tested with uniaxial compression loading based on displacement controlled.
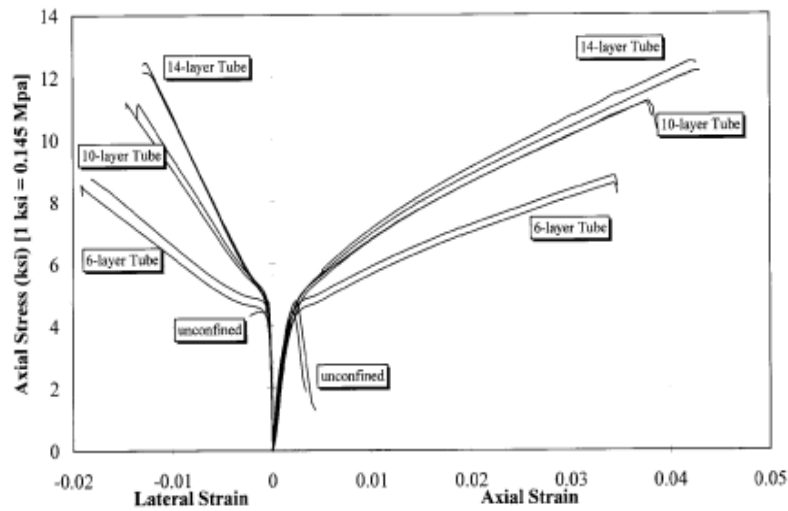
Figure 3.4: Stress-strain response for FRP confined specimens (*source: [28]

Above figure shows clearly that confinement with FRP types of materials improve the structural concrete's strength and ductility significantly. Unlike encased with steel structural concrete, behavior of encased with FRP is bilinear with no descending loading branch as shown on the figure above.
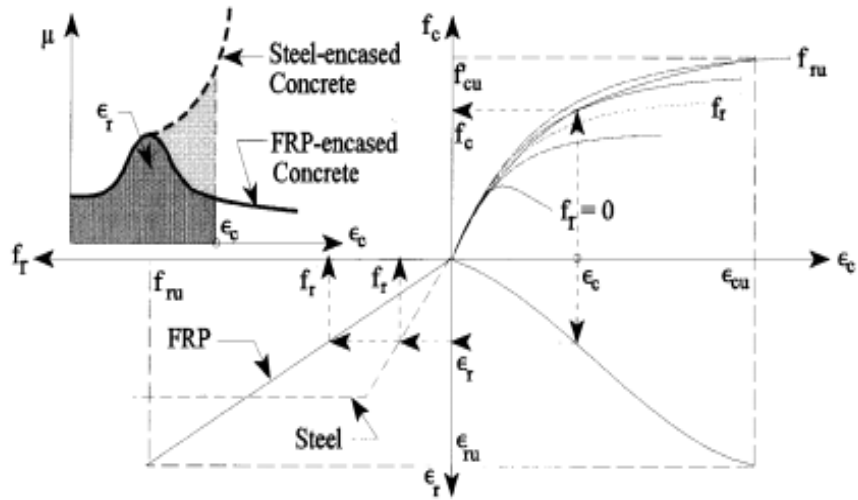
Figure 3.5: Schematic confinement modelling for FRP confined concrete (*source: [28]

Poisson's ratio of encased with FRP jacketing concrete reaches a ultimate value by the effect of confinement lateral and veritcal strain response. If the confinement increase, it limits the lateral strain and leads to change in Poissons's ratio characteristics of structural concrete.

3.4   Studies on the Stress-Strain relatonship of concrete in terms of Poisson's ratio

Studies on the stress-strain relationship and Poisson's ratio of structural concrete are introduced in this section. The focused finding concerns the vertical and horizontal strain with in terms of Poisson's ratio of concrete. As shown in figure below, large decrement of total amount of effective cross-sectional area occur in a concrete member during the ultimate axial loading.

The cracking process forms at the outer part of the concrete specimens with the micro cracks through the cylindrical type of specimen from the start of the compression test. The specimens that used for Poisson's ratio tests, these micro-macro cracks isolate a central core that is formed as biconic shape which is given

below Fig 3.6. Due to this type of shape and cracks formation, it is hard to achieve a full test during the descending loading branches. During the increasing loading branches, tests were achieved and results are given at section after this chapter.
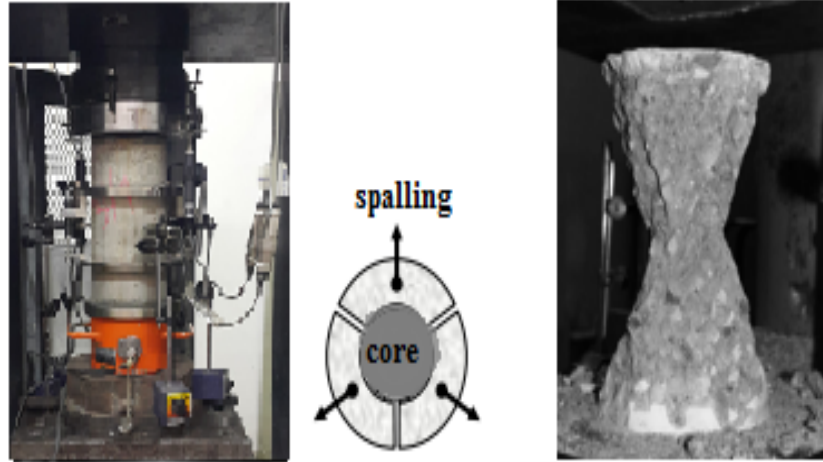
Figure 3.6: Concrete specimens during the compression and after test

[29] studied on the mechanical properties of high strength concrete. The slump test for fresh concrete, compressive strength test, flexural strength test, modulus of elasticity and Poisson's ratio tests are achieved during the experimental part of the this study. Strain-stress relationships were and used for non-linear theoretical analysis work.

The design stages and performance analysis stages of reinforced concrete structures need to cover the information on Poisson's ratio behavior during the both increasing load branches and lowering load branches. According to the AASHTO and Eurocode, if the Poisson's ratio of concrete is not determined by experiment, Poisson ratio can be taken as 0.2 for concrete.
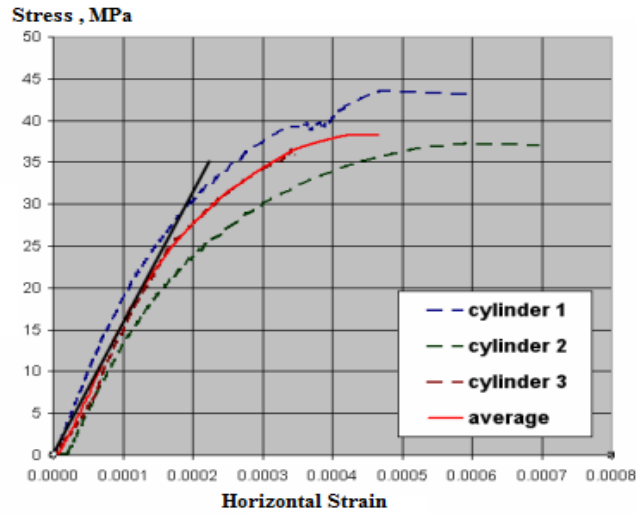
Figure 3.7: Horizontal strain versus vertical stress for Poisson ratio test

Based on the test result obtained during the study of [29], the relationship between the stress and lateral strain on the increasing load branches can be seen in Figure 3.7. From the graph of relationship, Poisson's ratio value can be calculated easily as 0.26. On th other hand, there was no experimental focus on the lowering load branches at the stress-strain relationship to obtain the Poisson's ratio at that region. So, there is a gap over there to find out the Poisson's ratio of the concrete during the descending loading branches. The experimental and theoretical work that achieved with 16 concrete specimens, focused on the this part of the studies to obtain these specific knowledge.

3.5 Studies on the Loading and Mix Proportion Effects of Concrete on Poisson Ratio

Poisson's ratio is the ratio between the lateral and vertical strain occurred on the concrete. Physical tests and other scientific methods are used to define the ratio. During the this test, some parameters effects the Poisson's ratio values such as loading speed, porosity, test setup, mix proportion of the concrete, chemical composition of the aggregates, shape of the aggregates, water cement ratio

and micro-atomic structure. These parameters should be taken into consideration during the physical experimental work on Poisson's ratio. In literature, there are some studies to cover the knowledge about these parameters effects on the Poisson's ratio. [30] studied on the effect of applied stresses on the mechanical properties especially elasticity modulus of concrete types of material. There are some methods to define the mechanical properties of concrete such as the resonance frequency method.

This method covers use of the relationship between the mechanical properties of the concrete body's and natural frequency of its vibration. If density of a concrete specimen is known, it is possible to evaluate the Poisson's ratio and each modulus by measuring the resonance frequency. Natural (resonance) frequency method and its application on nondestructive testing of concrete are described in many references such as Malhotra and Sivasundaram, 2004, Jones, 1962 and Pohl, 1966.

Simmons (1955) and some researchers studied on the resonance frequency method to obtain the dynamic Poisson's ratio of concrete at ages that beginning of casting and late age. Obtained results of these method's measurements of Poisson's ratio have a significant difference from obtained pulse velocity test which is another method to define the mechanical properties of concrete. The Poisson's ratio evaluated from the method of natural frequency where lower than the compared method. Mix proportion and other mechanical features of concrete has important role on this difference as introduced many studies in literature. The effects of concrete age, water/cement ratio, aggregate chemical content with amount and early age curing conditions on the Poisson's ratio should be recovered during the Poisson's ratio experimental and theoretical works.

Chapter 4

Experimental Works

This chapter describes the experimental study of seismic bahavior of 15 years old RC frame. Three reinforced concrete one story-one bay frames were tested to understand seicmic behavior and compare the results with reference frame that was tested before 15 years ago at main campus of Istanbul Technical University SteeLab by a team.

Description of the specimens which covers mechanical properties of used structural materials, mix proportion of casted concrete and geometrical properties are submitted fallowing section. This chapter also includes testing programme of corroded RC frame specimens, testing-setup, instrumentation, crack patterns and width measurements, data acquisition from LVDTs, material mechanical properties and measuring corrosion products distribution.

All RC structure frame and the materials tests were carried out at Istanbul Technical University Structural & Earthquake Engineering Laboratory and Material Laboratory.

4.1   Fifteen Years Old RC Frame Specimens

The tested RC frames are prepared before 15 years ago and released at natural outside environment to observe natural corrosion behavior and effects on RC structures. Three of them were tested during this experimental study to compare

the results with reference frame and to observe natural corrosion effects on seismic behavior of RC structure. The RC frames represent the existing and common building stock in Turkey which are weak column/strong beam types of structures. The specimens have sea originated aggregates and sand that coming from sea bed in mix design of the structural concrete.

Another special characteristics of the reinforced concrete frame specimens are using of non-ribbed mild reinforcement bars that was widely used before the existing design codes and standards in Turkey. The RC frame specimens have non seismic design details such as large spacing of stirrups without densification at specific levels, no confinement at beam-column node connection section and use of small diameter stirrups that was 6 mm.

Figure 4.1: General view of preparation of the RC frame specimens at I.T.U. Laboratory.

A structure is actually connected with members of 3 dimensional frame, which are connected to each other with different types of connections solutions such as precast, site cast etc. To understand the whole structural behavior of RC

structure it is quite enough to understand structure behavior by the obtaining of single frame result. In this study, reinforcement concrete frames has been constructed with rigid foundation, piece of slab, two column, one main beam and secondary beams in the laboratory at the time that 15 years ago.

The tested specimens are nearly half scale comparing to the existing apartment type of building stock in Turkey. The cross sectional geometry of columns are 200 mm by 250 mm and beams with 200 mm by 325 mm. The minimum column size is 250 mm in Turkish Earthquake Code which not satisfies for tested frames. The total story height and the gross width of the reinforced concrete frame are 1525 mm and 2200 m in order of given parameters.
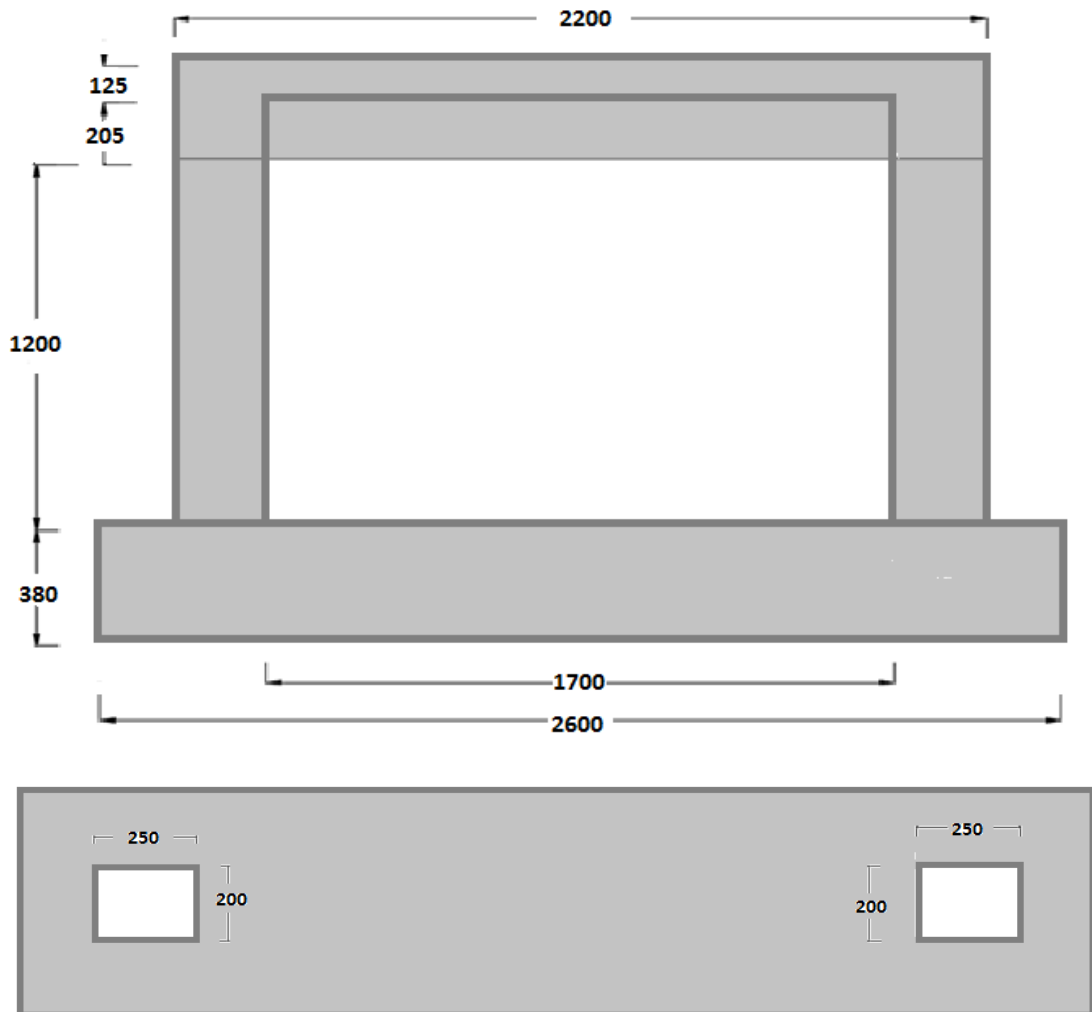
Figure 4.2: Geometry of the specimens.

The studied one bay-one story reinforced concrete frames consist of horizontal element (beam) and vertical elements (two columns) connected by a rigid foundation as shown above Fig.4.3. The beams, slab and columns members has been casted monolithically after the casting of foundation. The foundation of the studied specimen has 50 mm holes in order to fix the specimen to the ground adapter foundation during the cycling test. The aim of the this fixing is that to reduce the foundation displacement about zero during the cyclic loading. The dimensions detail, top view of the foundation and front profile of the studied RC frame are given in Fig.4.2.
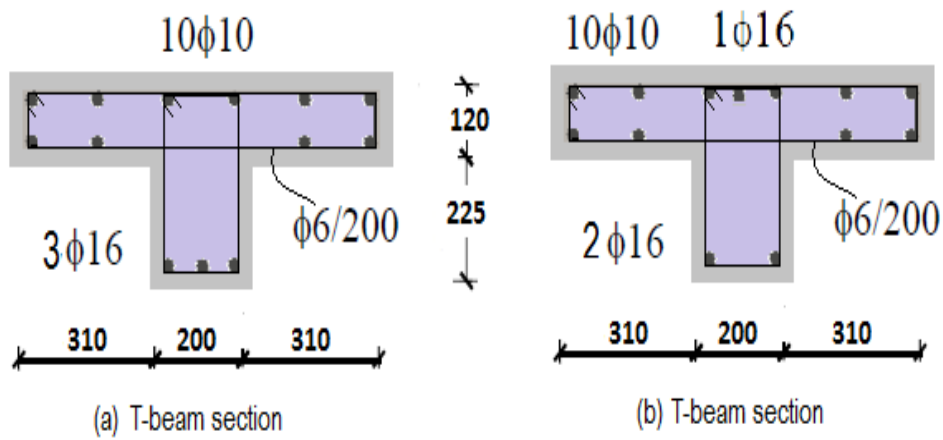
Figure 4.3: (a) Node section, (b) Mid span section of the T-beam.
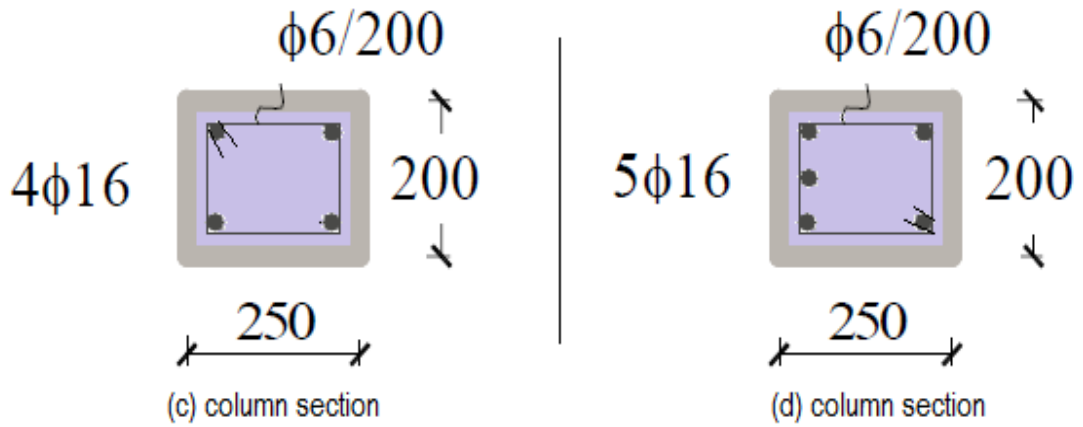
Figure 4.4: (c) Bottom section, (b) Upper section of the columns.

Columns longitudinal reinforcement continues to the bottom of the foundations as seen Fig.4.6 without lap-splice at the foundation connection level. The columns of the RC frame have longitudinal reinforcement of $4\phi16$ which have yield stress of 286 N/mm^2 and rupture stress of 409 N/mm^2 which are evaluated by the testing of the reinforcement after crashing of specimen. Also T-beam has $3\phi16$ steel bars with $10\phi10$ steel bars in the flange part. The concrete (cylinder core specimens) compressive strength is 16.38 Mpa according to the relationship between schmidt hammer number and achieved core specimen of concrete compressive strength tests that taken from the RC frame. The material test details are submitted at the section of material test results.

Figure 4.5: Beam cross section and beam-column connection reinforcement detail.

Figure 4.6: Column, beam- column upper section and slab reinforcement detail.

4.1.1 Specimens Features

4.1.2 Test Setup

The RC frame specimens were tested at main campus of ITU in SteeLab. The RC frames were tested with constant axial forces on the top of the both columns and reversed cyclic lateral increasing loads. An axial load of 282 kN (≈ 20 % of column axial load carrying capacity)was performed through a hydraulic jack at the head of the column members. The yellow rigid steel beam under the static jack used to distribute the axial load to the top of the columns as an uniformly reaction of used steel beam. During the tests, the axial load was changing in high top displacement steps due to the secondary effects. To do it constant, hydraulic jack controlled manually in both pushing and pulling cycles during the last part of the experiment. The foundations of the frame specimens were fixed to the adapter strong foundations using the $16\phi28$ screw bars without any slippage. During the test, screw bars loosen and then they were tightened again at several steps to make the foundation motion negligible small enough with respect to top displacement.

Before the anchorage of the frame specimen on the adaptor foundation, vertical and horizontal mark lines were drawn on the white painted surface of the RC specimens to observe the crack formation during the loading. Then the LVDT's holes were reamed and mirror were placed to get smooth surface for data collection. The corrosion cracks occurs due to natural process was marked on the frame as named A1, A2, A3, A4 and A5. Other specific features of the test setup and experimental program are submitted below parts, respectively.

Figure 4.7: Preparation of RC Frame specimen for the test: (left) Mirror and holes for LVDTs (right) Mirror for foundation slippage measurement surface (bottom) Anchorage of the specimens to the adaptor ground.

The applied axial load was measured by a connected load cell to the system, which was located top of the hydraulic jack as seen Figure 4.7. The experimental test setup of the reinforced concrete frame specimens is shown in Figure 4.8. After the initial preparation step of the experiment the main experimental setup were established as below. One actuator for cyclic loading ($^+_-$250 kN) capacity, load cell, hydraulic jack with manual control oil pomp apparatus, rigid steel beam to axial load distribution and LVDTs with data logger were placed for test setup. This experiment is displacement control test with introducing loading protocol. In other words controlling of actuators are displacement-based to control (stop-start) the every stage of test when needed. The data collection started with the test from actuators, jack and the each linear variable displacement transducers (LVDT) attached to the several section of columns, beams and foundations of the RC frame specimen.

Figure 4.8: Test setup of the experimental works.

In this test setup ; it is designed that the axial loading system and the lateral cyclic loading system works independent from each other during the experiment. The total vertical loads acting on the frame columns are coming from the rigid yellow steel I-beam established on the RC frame and uniform self weight of upper part of the specimen.

Beside to this axial load enough axial load intensity is controlled by a non-automatic hydraulic jack with a circular load cell established on rigid yellow steel I-beam. The amount of the vertical (axial) load kept same level during the whole

test which is calculated 20 % of the axial load carrying capacity of rectangular columns without considering any corrosion decrement effect.

4.1.3 Instrumentation and LVDT's

In this test setup ; the data collection from tested specimens have been achieved by the linear variable displacement transducers (LVDT) connected to various section of the columns, beams and foundations of the RC frame specimen which are shown on below table in detail with location. Numbers, types and measurement purpose of LVDT's are given in Table 3.2.

Table 4.1: LVDTs established frame and measurements purpose.

Name	LVDT Type	Measurement Purpose	Attached to
T1	CDP100	Top displacement	Frame
T2	CDP10	Right column upper rotation	Frame
T3	CDP10	Right column upper rotation	Frame
T4	CDP10	Left column upper rotation	Frame
T5	CDP10	Left column upper rotation	Frame
T6	CDP10	Right column lower rotation	Frame
T7	CDP10	Right column lower rotation	Frame
T8	CDP10	Left column lower rotation	Frame
T9	CDP10	Left column lower rotation	Frame
T10	CDP25	Displacement of the whole system (foundation sliding)	Frame
T11	CDP50	Out of plane	Frame
T12	CDP50	Out of plane	Frame

Total 12 unit LVDTs are established on important locations to measure the displacements and rotations of the members and whole structure. The rotation of the columns and beam, the relative displacement of the RC frame specimen, the foundation slippage, the target top displacement and the out of plane motion of

the frame are measured by placed LVDTs. The applied load on hydraulic jack and displacement of hydraulic load tools are measured and saved by test setup system. The all LVDTs are attached to a switch box tool and data logger apparutes.

Figure 4.9: LVDTs connected and $2^{n}d$ step (+0.07 mm) of the experiment achieved.
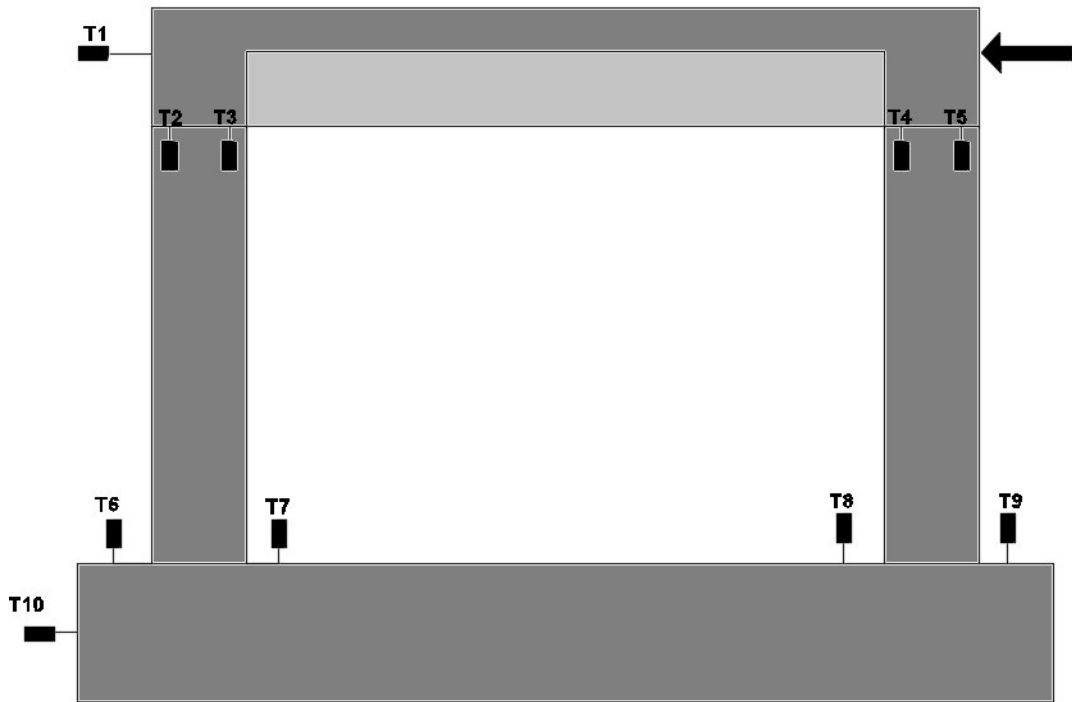
Figure 4.10: LVDTs used in test setup-view of specimen front side.
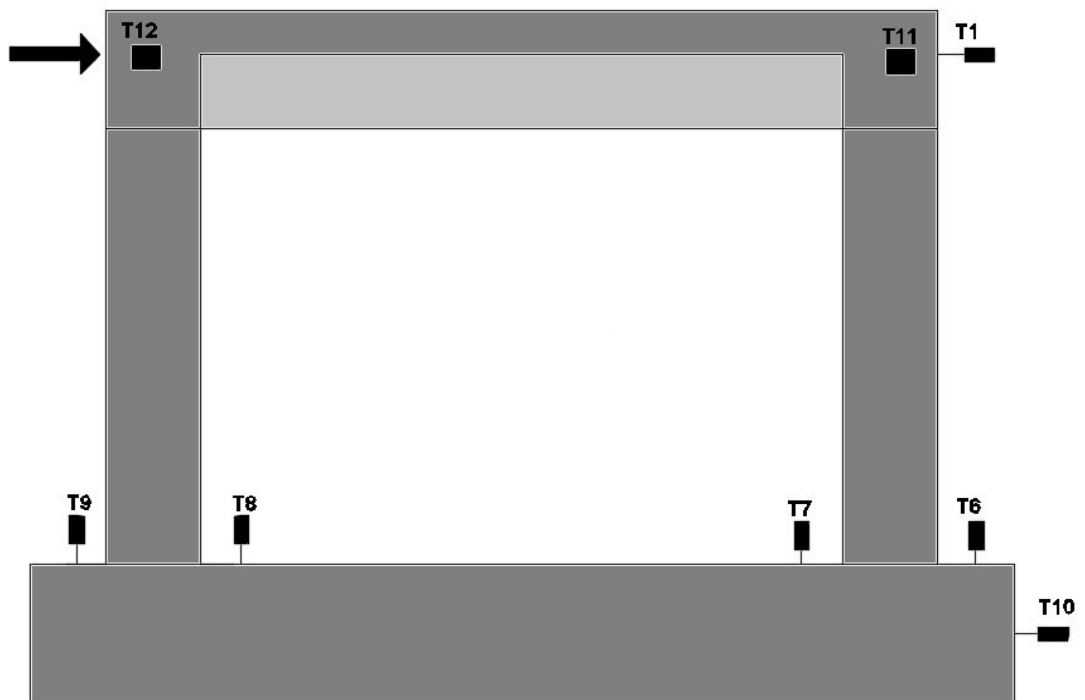
Figure 4.11: LVDTs used in test setup-view of specimen back side.

4.1.4   Induced Displacement Protocol

There are a lot of different loading protocols are applied to the structural systems to obtain expected structural response. For testing program it is essential to use well-defined standardized displacement pattern for exact response.

Loading history has an important effect on the induced damage on buildings in seismic events. It is crucial to use appropriate loading protocols in experiments due to establishing the good agreement with real structural behavior. The crucial point is to suggest displacement protocols which could be representative of the actual behavior imposed by a earthquake effects. In this presented study, the type of external cyclic load which represents the earthquake effects is induced during the testing of reinforced concrete specimens. The displacement protocol used in researches is either to represent far field or near field earthquakes effects on the structures. Cyclic loading tests are useful to provide reliable information on structural behavior, including data sets on strength parameters and stiffness characteristics, deterioration behavior at large deformations level, cyclic hardening or softening effects and deformation capacities of members.

Displacement control base cylic experiments define the seismic behavior of RC structures more better than force control tests. The most common protocols that have been used in literature research are the sequential phased displacement (SPD) protocol, [31], Ficcadenti et al. (1998), the Forintek Canada Corporation protocol (Karacabeyli 1998) and the International Standards Organization ISO (1998) protocols.

The SPD (sequential phased displacement) protocol involves a large number of loading cycles steps with the amplitude of each loading cycle based on the yield displacement as given Fig.4.12. On the other hand, the ISO protocol has a smaller number of loading cycles with the cyclic amplitude based on the displacement at ultimate load applied. In presented study below quasi-static loading protocol applied to the RC frame specimens to represent the earthquake effects on structure during the experimental test program.
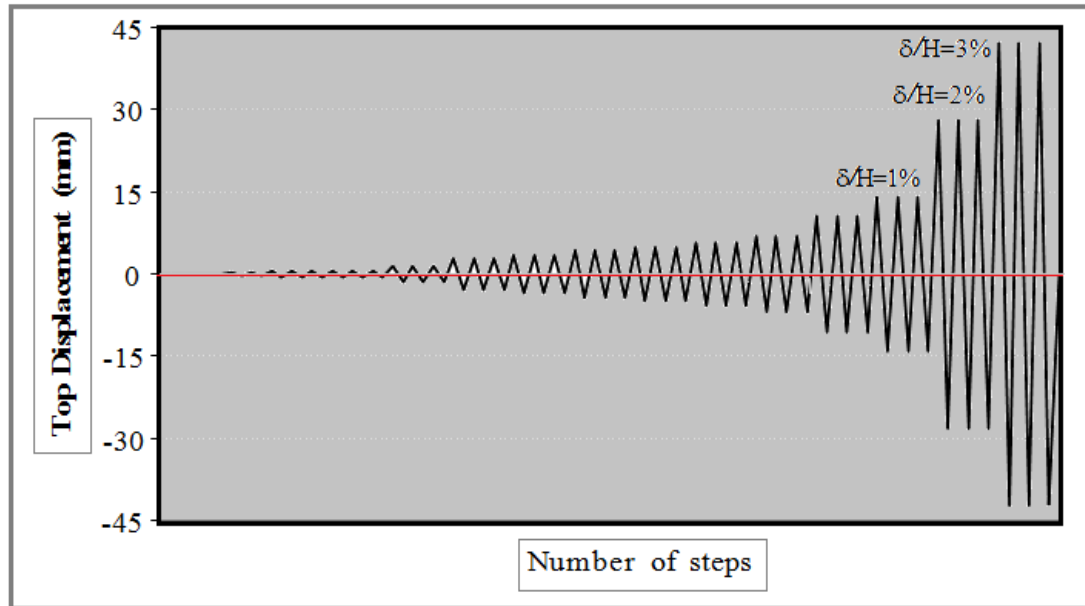
Figure 4.12: Loading protocol applied on the frame specimen.

In this presented study, displacement loop with rising intensity are applied to the RC frame by actuator according to the displacement protocol. In the elastic and inelastic region of test, each displacement loop is continued three times for both backward and forward loading cycles.

The occurred cracks were marked and other structural features was observing at the end of each displacement target by given displacement protocol. The highest drift introduced to the RC frame structure was 3%. According to the Turkish Earthquake Code v.2007, the acceptable drift is 2% of the total story height. This induced loading protocol include step by step cyclic application of displacement with a early described loading protocol to the structural system. The target lowest deformation of the loading history that must be safely smaller than the value at which the lowest damage state is first observed on the structural system(FEMA-461). It is taken 0.035 mm for this test and applied.

The targeted maximum displacement which achieved at level of ultimate story drift ratio of the loading protocol that is an predicted range of applied deformation at which most destructive damage stage is estimate to begin for structure

according to the FEMA-461.

Table 4.2: Step of the displacement protocol.

Load Step	Target Displacement[mm]	Relative Story Drift
1	0.035	0.000025
2	0.070	0.000050
3	0.140	0.000100
4	0.280	0.000200
5	0.350	0.000250
6	0.467	0.000300
7	0.700	0.000500
8	1.400	0.001000
9	2.800	0.002000
10	3.500	0.002500
11	4.200	0.003000
12	4.900	0.003500
13	5.600	0.004000
14	7.000	0.005000
15	10.500	0.007500
16	14.000	0.010000
17	28.000	0.020000
18	42.000	0.030000

In this study, a displacement based cyclic loading protocol was used to test reinforced concrete corroded frame specimens. To simulate the earthquake effects on structure, reversed lateral displacements were applied for both pulling and pushing cycles as a target to the corroded RC frame. Drift ratios (Δ/H) were calculated as the ratio of the lateral displacement of the top of the corroded RC frame (Δ) which is measured by T1 LVDTs, to the story height (H) which is 140 cm.

4.2 Test Results

4.2.1 Test Results of Materials

Three cylindrical concrete specimens tested with Instron 5000 kN capacity instrument and eight core specimens tested Besmak 200 kN compression capacity test equipment that taken from RC frame. These tests were performed to determine the mechanical properties of the concrete to success of the numerical modelling of the RC frame specimen. It is known that compressive strength of concrete increases with time, the concrete tests performed to show this strength increment respectively. Besides to these tests, reinforcement steel bars were tested to determine their mechanical properties.

4.2.2 15 years old Concrete Test Results

The important point to achieving a durable concrete mix proportion depends on the each material characteristics used. Cement type, water chemical composition such as sea water or waste water, aggregates features such as aggregates coming from sea bed and other factors effect the concrete quality, durability and other features.

Concrete used for construction of the RC frame specimens is given in below Table 4.3. 300 kg portland cement, 140 kg water, 690 kg sand and 1070 kg No:1 aggregate with sea sand used for specimens of RC frame's concrete. Concrete quality were obtained from compressive strength tests on standard cylinders specimens taken at stages of the construction of foundation and upper part. Minimum of three standard cylinders were tested at 28th days and 5420th days to comparing the strength development with time. The graphs of results are given below respectively. The concrete strength properties that used in the theoretical works, obtained from the material test achieved. Eight core specimens taken from the RC frame were evaluated with schmidt hummer reading. Results obtained from

core specimens and standard specimens are submitted in below Table 4.3 for the RC frame specimens concrete.

All standard cylinders (15/30) and core specimens were tested at the Construction Materials Laboratory of ITU using a 5000 kN Instron Displacement control press machine and 200 kN capacity Besmak compression press machine respectively. Core concrete 1. cylindrical specimens were tested in compression with a loading rate of 0.03 mm/min in Besmak special type of machine. Standard cylindrical concrete specimens were tested by using the technique of displacement control based material test.

Table 4.3: Mix composition of RC frame concrete.

Metarial	Weight ratio
Portlan Cement	300 kg (32.5 R)
Water	140 kg
Sand	690 kg
Gravel	1070 Kg (1 No aggregate)

Compressive strength of standard cylinder specimens of concrete were obtained from press tests on standard (150/300 mm) specimens taken at stages of the construction of foundation and upper part of the RC frame. Three standard cylinders R-29-1, R-29-2 and R-29-3 were tested at 28th days before 15 years ago. At the day of 5420th, three standard cylinders T-29-1, T-29-2 and T-29-3 were tested to comparing the strength development and modulus of elasticity increment with time and results are given below Table 4.4.

Table 4.4: The compressive strength of standard cylinder specimens for 28th days and 5420th days.

Specimen Name	Test Time [day]	Compressive Strength [Mpa]	Modulus of Elasticity [Mpa]
R-29-1	28	12.41	25449.04
R-29-2	28	12.51	25495.08
R-29-3	28	12.45	25467.48
T-29-1	5420	18.62	28024.04
T-29-2	5420	20.83	28832.96
T-29-3	5420	22.31	29350.87

Figure 4.13: Standard cylinder specimen tests 28th days and 5420th days.

M. Abd elaty (2013) and many other researchers study on the concrete strength gain with time. M. Abd elaty (2013) study on the existing experimental data for

concrete strength of different concrete proportion mixes and a related statistical analysis. Concrete is a cement based materials that after the mixing and hydration process takes place and continue strength gain with time. CSH is the type of compound resulting from hydration process of concrete formation and it gives the concrete its compressive strength. Ages strength assumption is an important point in civil engineering for design and service life of RC structure. There are some studies and related work to find the concrete compressive strength with related their age. In many standard and codes, the relationship between the 28th day strength f_{c_28} and the 7 th day strength, f_{c_7} is given below formula 4.1.

$$\mathbf{f_{c_2 8} = 1.4 f_{c_7} + 150 psi} \tag{4.1}$$
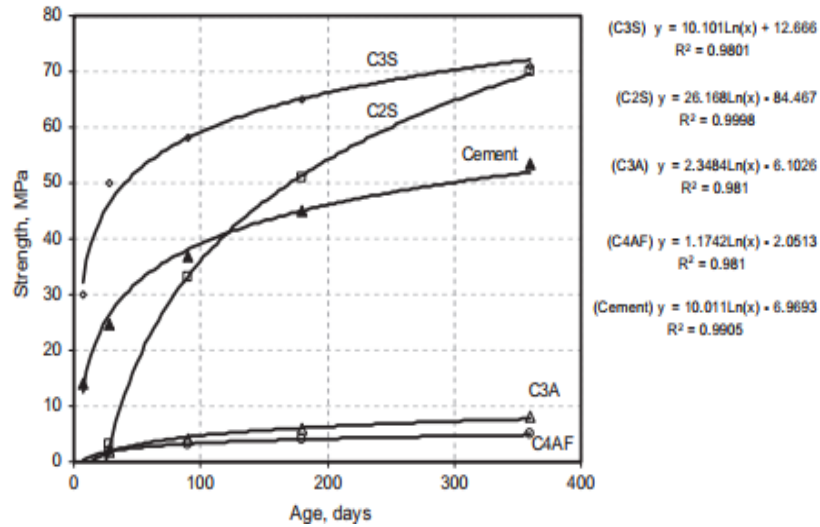
Figure 4.14: Relationship between compressive strength and age for clinker minerals and cement [14].

It is seen in the above figure that strength gain of concrete mixing type of hydration material such as cement with age at normal temperature are increase with time a reasonable accuracy. To support these known theory, we carried out some concrete standard cylindrical specimen tests which are 15 years old. There was total 9 (nine) set of cylinder specimens which are T-29, T-30 and T-32 series of specimens for testing. Here T-29 series of specimens results are conducted with

28th day and 5420th day combined displacement based control test result and given below figure. In the figure, R-29-1 specimen has 12.41 Mpa compressive strength at 28th day. At the end of the 15 years, same concrete mix design specimen which named T-29-1 has 18.62 Mpa compressive strength at 5420th day which is about 50% strength gain of concrete after 28th day respectively. This is very valuable result for late age experiment for concrete in literature. The other specimens (29-2 and 29-3) are also have 66.5% and 79.2 % compressive strength increment with age at natural environment conditions.
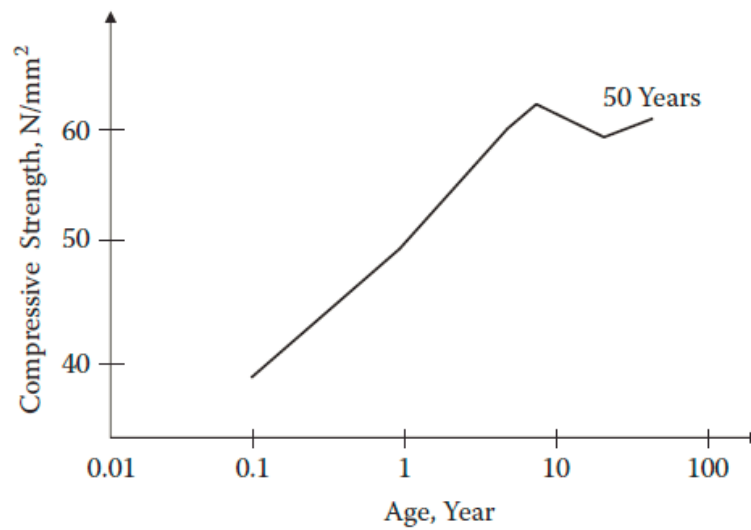
Figure 4.15: Concrete strength variation with age.

Washa et all. (1989) find out that the compressive strength of concrete which has low contentC_2S and stored natural conditions for 50 years generally increased as a logarithm of the age for about 100 years. In this graph after representative 10th age point, the compressive strength of late age concrete decreased small can taken constant as seen easily above.

In the study of MacGregor (1983), used same method as Washa et all. (1989) and formulated the relation between compressive strength of concrete and age factor as given below formula 4.2 and 4.3.

$$\mathbf{fc(t) = 15,85 + 40,4In(t) \ N/cm^2 \quad for \ t < 10 years} \tag{4.2}$$

61

$$\mathbf{fc(t) = constant\ N/cm^2 \quad for\ t < 10years} \qquad (4.3)$$

where $\mathbf{fc(t)}$ is the concrete compressive strength for late age and early age as given function of time and t represents the age of concrete in terms of days.

The compressive strength of late age concrete is affected with age and increase with the relation given above. In Turkish Earthquake code, the RC member capacity such as beam and column is usually calculated as a function of RC cross-section dimensions, the total reinforcement area, the compressive strength of concrete and the reinforcement mechanical strength properties, but there is a change in concrete mechanical properties due to corrosion, strength gain with age etc. Most of the literature tests were conducted at concrete age of 28th day, when its strength is considerably lower than its long-term strength expected. It is important to know long term strength for design stages of RC structures.

To achieve the late age mechanical properties of concrete some concrete tests was carried out at ITU Material Laboratory during this master study. This study cover up standard cylinders concrete test based on displacement control. One set of the results (R, T-29 SERIES) are given below in Stress (Mpa) and Strain in measured vertical direction from top and mid part of the specimens.

In Turkish Earthquake Code ([32]) ; stress-strain relationship of confined and unconfined concrete defined as below figure 4.16. The strain limit at ultimate stress level for unconfined concrete defined as 0.002. Then, the ultimate strain defined 0.005 respectively. On the other hand, these values increasing if the confinement of the concrete increase as given TEC-2007 [32] and 2018 [33].
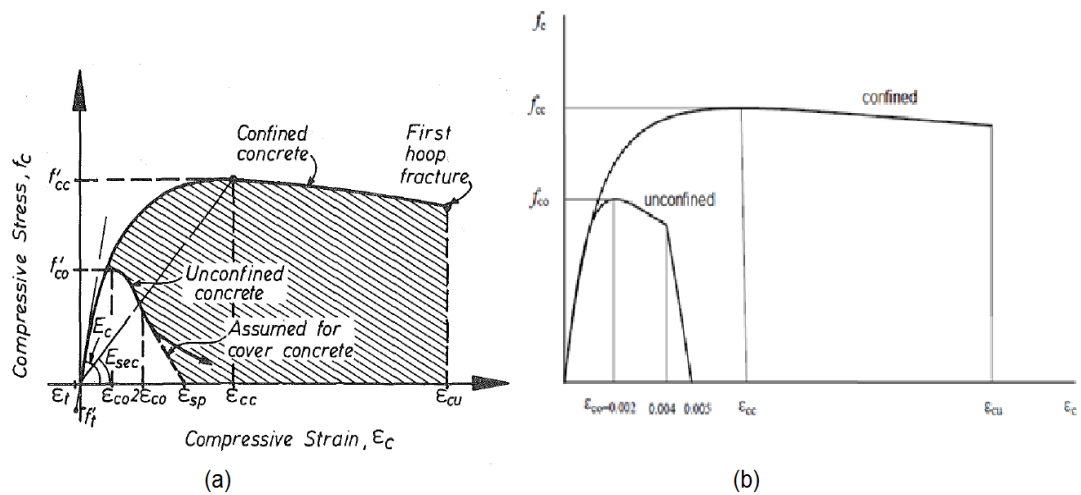
Figure 4.16: Stress-Strain relationship of confined and unconfined concrete (a) Mander Model (b) TEC-2007.

[34] ; the aim of study was determine the effect of confiniment on the concrete compressive strrength and strain. [34] conclude that RC members under axial compression loading may be confined by using stirrups to increase the RC member strength (capacity) and ductility. In our study, we try to point out the confinement effect on some special specimens which are casted 15 years ago at ITU SteeLab. Initial results of this study are given below graph and tables in terms of stress and strain values.
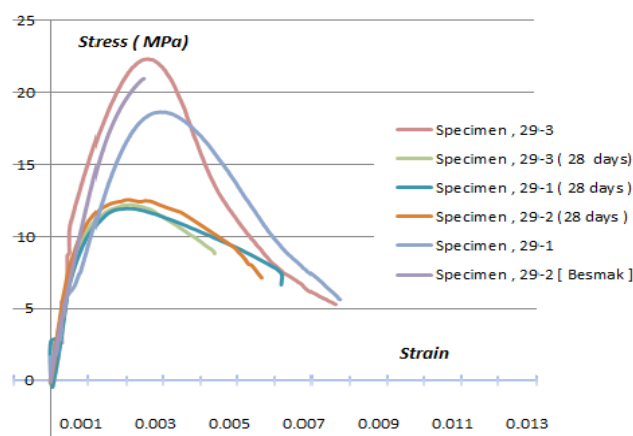
Figure 4.17: Relationship between compressive strength -strain with age for concrete cylinder specimens.

63
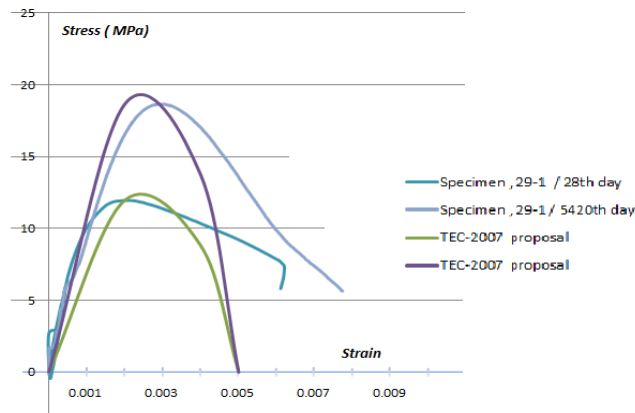
Figure 4.18: Relationship between compressive strength -strain with age for concrete cylinder specimens and TEC-2007 [32] proposal for unconfined concrete.

It is seen above figure that compressive strength of standard cylinder specimens of concrete with increased in each of three specimens higher than 50 percent. The results include three standard cylinders R-29-1, R-29-2 and R-29-3 were tested at 28th day and 5420 days after three standard cylinders T-29-1, T-29-2 and T-29-3.

Total 6 (six) standard cylindrical specimens were tested to comparing the stress-strain development for early age (28th day) and late age (5420th day) concrete with age factor. Press tests which is displacement control based on standard cylinder (Diameter =150 mm and Height = 300 mm) specimens taken at stages of the construction of foundation and upper part of the main specimen of this study which is one bay one story RC frame. Results show that concrete strength increase with time higher than 50 % and strain at same level will also increase respectively. Each type of specimen sets results overlap with this increment theory which is well known in literature.

Concrete cores specimens are used for define the actual strength properties of concrete in tested RC corroded one bay-one story frame. With the schmidt hummer reading, sampling of concrete cores and testing of its compressive strength of concrete is described with 92 % R value. The eight core specimens were taken but some of them are far away from the average so they eliminated to get more convenient result as given below graph and tables.

Figure 4.19: Taken of core specimens from tested RC frame with core holes.

The concrete cores specimens were cut by help of the rotary cutting tool with diamond bits as seen in Figure 4.19. The cylindrical specimens were obtained from left-right column, beam and slab. The cores specimens were measured, described and photographed before the load control press test. The concrete specimen cores tested and evaluated with standards TS EN 12504-1, TS EN 12390-3 and TS EN 13791.

If the values of *Height/Diameter* (H/D) ratio less than one, correlation factor applied to the results with code requesting. In this study, concrete core specimens results with H/D ratio less than 1 evaluated with BS 1881 value as 0.95.

Figure 4.20: Core specimens and testing equipment of press tool.

The relationship between Schmidt hammer test and concrete compression test of core specimens is determined in this part. The calibrated Schmidt hammer (UTEST-HT 225 A) is used to determine surface hardness to determine relationship between the strength of core concrete and the rebound number of the Schmidt hammer readings.

RELATIONSHIP BETWEEN SCHMIDT HAMMER NUMBER AND SMALL SPECIMEN OF CONCRETE COMPRESSIVE STRENGTH FOR RC FRAME				
Specimen Name	Schmidt number	cube (15x15x15) c.strength [MPa]	cube (15x15x15) c.strength [MPa]	cylinder (15x30) compressive strength [MPa]
R-column-1		16.77	19.47	16.55
L-column-2	26.96	19.32	19.32	16.42
slab-1	40.46	20.59	20.59	17.50
slab-2	40.46	20.59	20.59	17.50
slab-3	40.46	20.59	20.59	17.50
	avarage	19.57	20.11	17.10
	St.dev.	1.66	0.66	0.56
	$f_{c,du,cube}$		19.27	
	$f_{c,du,cylinder}$			16.38

Figure 4.21: Eliminated core specimens results and schmidt hummer readings relationships.

Correlation applied to data obtained from 5420th days RC frame surface and core specimens surface before taken it. This correlation used for 15 years old corroded RC frame concrete strength and Schmidt hummer reading tests. First, Schmidt hammer reading test on RC frame specimen surface was completed, the concrete cores specimens were cut by help of the rotary cutting tool and after the preparation, press was applied up to ultimate strength.

The results were obtained and plotted in below Figure 4.22. Also, the 15 years old corroded frame core specimens R^2 value is found to be 0.7451 and its equation given above figure where is the compressive strength obtained and x is the rebound number obtained from hummer reading. Schmidt hammer reading test results can be effected from some factors which are the characteristics of the mixture design used to construct, surface carbonation of concrete, moisture condition of existing environment, hardening rate and curing type. So, the correlation should be consider these effects. In this study, some records were far away from the avarage value due to this reason. Some of the data were eliminated to obtain R^2 value is 0.7451 as much as closer to the 1.00. If we eliminate the Slab-1 core specimen result, R^2 is more closer to the one which is 0.9297. This value gives us

concrete compressive strength of RC frame specimen as 19.10 for cube and 16.24 for cylinder strength which will used for analytical future work during the study.
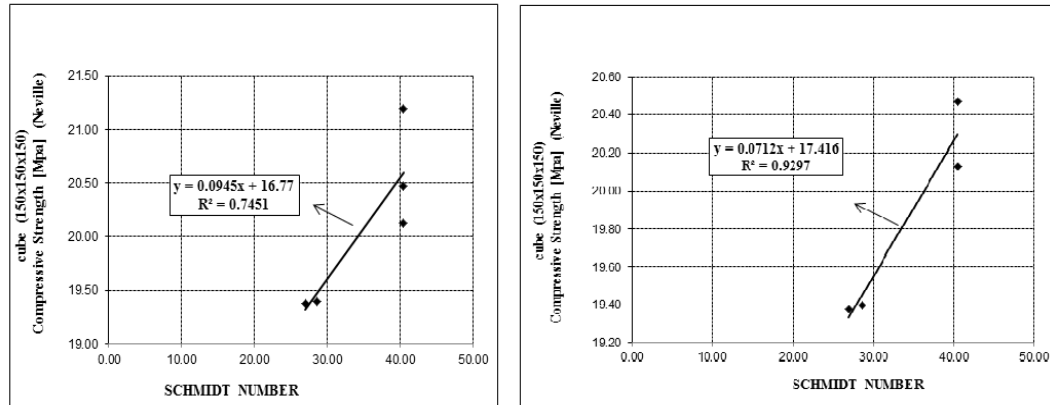

Figure 4.22: Core specimens results and schmidt hummer readings relationships.

There was many station of core specimens from different section of RC frame such as left and right column, beam and slab. Some data (R-column-1, Slab-1) was not correlate with average values so then they were eliminated from data sets to get more accuracy result for concrete mechanical properties.

4.2.3   Natutally Corroded RC Bars Test Results

Reinforcement steel corrosion due to chloride induced or other effects can cause of the degradation of reinforced steel cross section area and relatively effect the concrete structures capacity and ductility. To understand the mechanical properties of 15 years naturally corroded reinforcement tensile tests and corrosion cleaning were carried out during this part of the study. In literature, there were no significant differences of corrosion behavior observed between smooth- mild steel (S220) bars and ribbed bars (S420). Corrosion behavior can differ only due to surface finishing of reinforcement bars and chemical composition of steel.

Tensile tests and corrosion cleaning were carried out during this study to get the mechanical properties of 15 years naturally corroded reinforcement in a RC structure. After the testing of the one bay-one story RC frame, the specimens

demolished to observe the corrosion formation on the steel bars and to get out the reinforcement bar for tensile test. Total $4\phi16$ longidutional non ribbed S220 type of reinforcement bars samples were tested at the I.T.U. Material Laboratory using tensile testing machine.
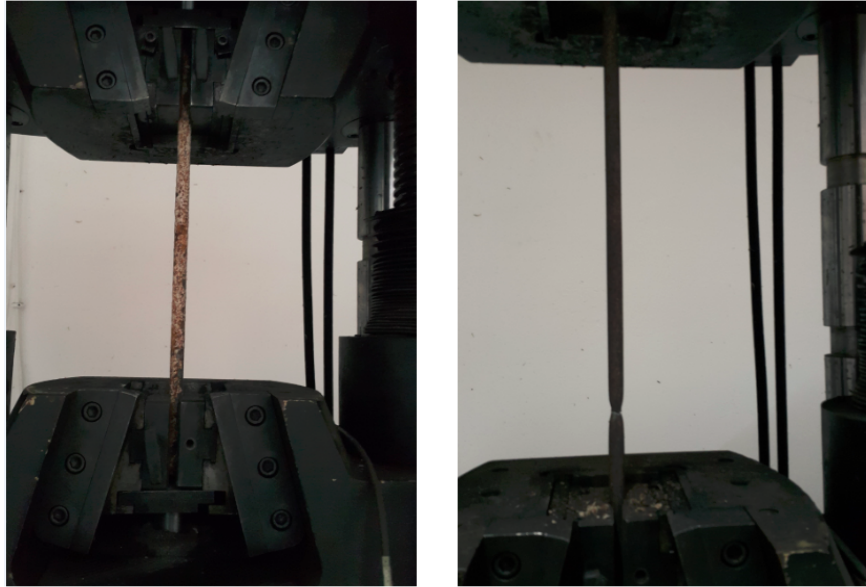
Figure 4.23: Tensile test of corroded reinforcement bars.

Four $\phi16$ bar specimens were taken from column longidutional reinforcement after the testing of RC frame. Initial mechanical properties of used steel bars given at P. Teymür thesis in Table 5.1 [SOURCE *thesis of PT]. Results after 15 years later are given Table 5.2 below respectively.

Diameter [mm]	$\phi16$	$\phi10$	$\phi6$
$\sigma_y[MPa]$	270	290	325
$\sigma_{max}[MPa]$	420	450	481
$\sigma_{su}[mm/mm]$	0.25	0.30	0.35

Table 4.5: Mechanical properties of reinforcement bars 15 years ago *[P.T]

Specimen Name	Diameter [mm]	Yield Strength [MPa]	Fracture Strength [MPa]	ε_{su} [mm/mm]
R-Spec1	15.9	293	404	0.39
R-Spec2	16.1	284	416	0.39
R-Spec3	15.9	284	404	0.41
R-Spec4	16.0	283	415	0.39

Table 4.6: Mechanical properties of naturally corroded reinforcement bars

As a result of the tensile tests, some specimens volume or diameter were increased due to the corrosion rust product formation which were easily seen on the surface of the specimens and given above Table 4.6. Yield strength of bars increased with respect to the 15 years ago results but the fracture strength were decreased about 5 % due to the effective diameter of the rebar which reduced due to corrosion formation.

4.2.4 Reinforcement Bars Corrosion Cleaning and Surface Cracking Process

4.2.4.1 Reinforcement Corrosion Surface Cracking Process

In this section, the process of bond mechanism between the reinforcement steel bar and concrete is explained in terms of cracking formation stages. This procedure gives a better understanding about the relationship between cracking of concrete and bond strength in corroded RC structures. The cracking stages covers initial cracking stages, primary cracking stages and final cover cracking stages.

The initial stage of cracking is the part of crack initiation at the rebar-concrete interface and the surface due to the pressure exerted by higher volume of rusty corrosion products. Then, the influences of initial corrosion cracks on cracking

parameters, such as time to cover cracking, volume expansion forces due to additional tensional forces and loss of the diameter of rebar are investigated.

Production of corrosion formation in RC structures occupies a volume several times larger than the initial volume. This higher volume formation leads to concrete cover cracking process. The development of the visible cracks on concrete surface due to corrosion formation process is named primary cracking stages of natural corrosion.

When the naturally corroded reinforced concrete structures corrosion crack's pattern reaches a critical damage point where concrete provides no more any confinement to the longiditional bar (no bond state), this stage is the final cracking stage of natural corrosion cracking process in RC structures. This stage occurs at high-level corrosion rate and the corresponding range is 4 % corrosion rate and above this value, depending on compressive strength of concrete with cracks, reinforcement effective bar size and concrete clear cover zone which protect the reinforcement bar.
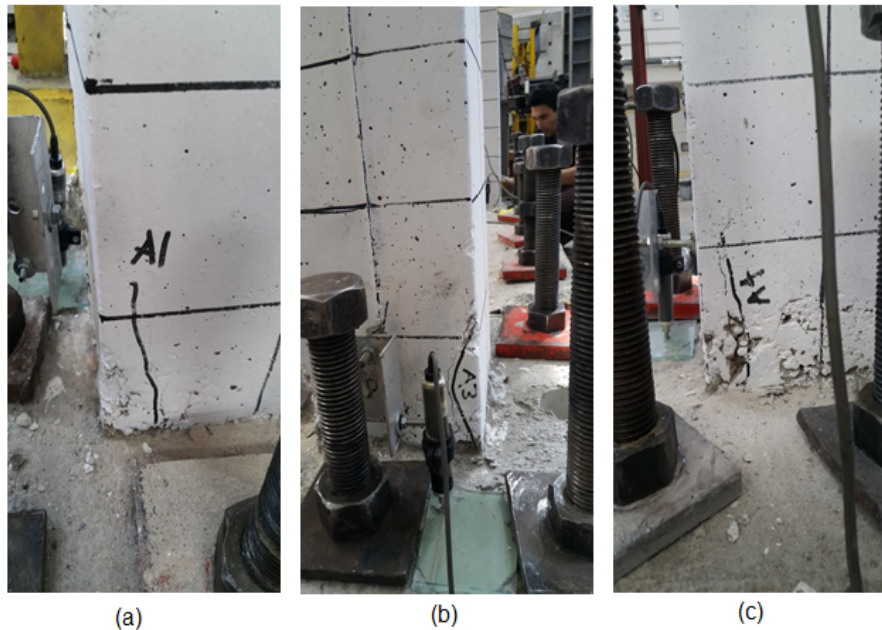

Figure 4.24: Surface cracks due to natural corrosion process (a) A1, (b) A3, (c) A4.

Reinforcement corrosion process products take huge amount of volume according to the uncorroded reinforcement bar and result in bursting stresses which can let to formation of cracks and spalling of concrete clear cover part as shown above Figure 4.24 which include the cracks before testing A1, A3 and A4 with another crack which named as A2.

The initial crack width changes from 0.1 mm to 5 mm. The cracks that appear on the surface of the concrete structures run parallel to the longidutional rebar as seen on Figure 4.24 The reinforcing steel bars closest to the concrete surface generally be affected by natural corrosion first because of the water entrance velocity. Typical occurrence of cracks due to corrosion was over shear reinforcement on the sides of the RC frames both columns in several locations.

It should be noted that reinforcement cross-section loss is determined by comparing the section losses of each taken specimen reinforcing bars. It is clear that in the bottom and outer section part cross-section loss take more important role on the behaviour in certain cases (such as fracture of the stirrups bar as given below), average cross-section loss may be more governing in some other cases (such as bond loss or buckling).

Figure 4.25: Bottom part of the corroded and buckled rebar after test.

Papadakis and Apostolopoulos (2008) study on that stress which is on surface of the reinforcement bars increases due to corrosion process and this increment in stress, lead to reduction of the safety factors taken for the mechanical design properties of the structural reinforcement bar. Also, the reduction in the cross-section of a rebar reduces the moment of inertia respectively and hence the maximum buckling load of the longidutional reinforcement bar. Because of this reduction reinforcement buckled in the loading process at the early stage as shown above Fig.4.25.

4.2.4.2 Reinforcement Bars Corrosion Cleaning

To understand the corrosion effects and rate on reinforcement steel, the reinforcing steel bars were removed out from RC frame specimens and cleaned according to the ASTM G1-03 (2003) as given procedure below.
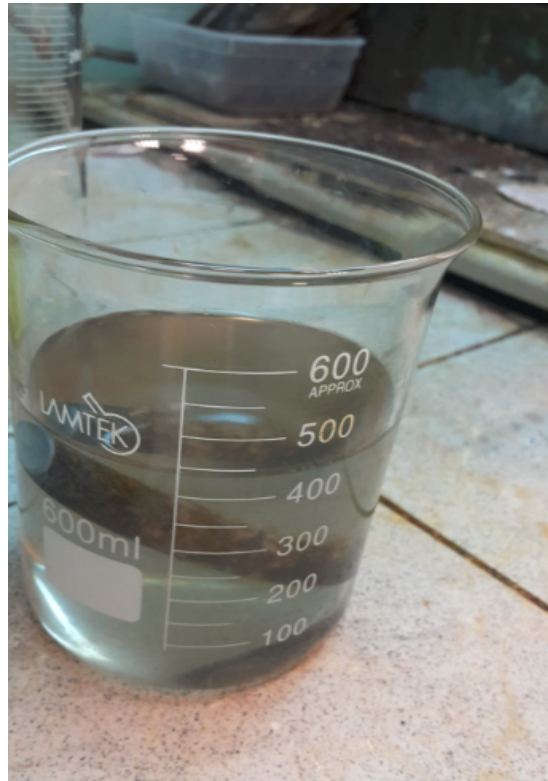
Figure 4.26: Solution for the corrosion cleaning process and corroded rabar.

Fluid solution shown in Figure above, formulated for cleaning the rust and other particle from surface of the corroded bars. The solution mixture includes 250 mL hydrochloric acid (HCl), 5 g antimony trioxide (Sb_2O_3) and 12,5 g stannous chloride (SnCl_2). After the testing of the RC frame, the reinforcing bars were removed from concrete to cleaning process and tensile test. During the cleaning process, bars were put into solution for several minutes until the reaction end time. After cleaning the rust from the surface with the special solution, the cleaned bar were washed by pure water and dried at oven to weigh.

According to the result as given below Table 5.4, corrosion effect in confinement bars is higher than the longidutional bars due to clear cover thickness. Also, the corrosion rate at lower part (1NF16) of the RC frame specimens is higher than the upper part (2NF16) of the specimens due to water induced effect from foundation. There was higher corrosion rate at the connection point of longidutional bars and

stirrups due to initial touch and continuous of corrosion mechanism from outer part to inner part of the concrete.

Figure 4.27: Corroded bars and cleaning process by special solution.

Specimen Name	Diameter [mm]	Weight Before Cleaning [g]	Weight After Cleaning [g]	Change in Weight %
1NF16	16	152,626	151,626	0.655196
2NF16	16	160,460	159,819	0.399477
3NF16	16	154,322	154,022	0.194399
4NF16	16	158,334	157,930	0.255157
5NF16	16	154,023	153,354	0.434351
6NF16	16	150,150	149,949	0.133866
7NF16	16	153,818	153,464	0.230142
8NF16	16	151,106	150,130	0.645904
9NF16	16	146,577	146,114	0.315875
10NF16	16	189,497	188,814	0.360428
1NF6	6	21,864	21,681	0.836992
2NF6	6	24,540	24,120	1.711491
3NF6	6	18,828	18,507	1.704908
4NF6	6	24,297	23,993	1.251183
5NF6	6	23,019	22,857	0.703766
6NF6	6	24,677	24,270	1.649309
7NF6	6	22,129	21,908	0.99869

Table 4.7: Corrosion cleaning specimens and corrosion rate according to the weight loss

4.2.5 Test Results of the Reference Frame

This chapter includes the experimental results of the natural corroded frames with comparing to the 15 years ago noncorroded frame reference results in terms of different parameters. The testing setup and measurements points on the specimens given in the test setup section before. Top displacement of the frame, foundation displacement (bottom slip), rotation of the columns and beams were measured

and evaluated results are presented here to understand the natural corrosion effect on the RC structures.

All results are compared with reference frame (bare frame) which were tested 15 years ago. But concrete quality and reinforcement bars diameter are changing with respect to the 15 years ago but geometry of the specimens are still same as before one. Envelope curve diagrams, hysteritic energy loops and other related results presented in this section.

The experimental and theoretical work results will compared based on their structural failure modes and their failure shapes, lateral load bearing capacity with increasing corrosion rate, initial stiffness of the each specimens, dissipated energy in linear and nonlinear part, ductility, stiffness and other related parameters.

This specimen was the reference frame used for the corrosion study to compare the results with 15 years old naturally corroded one bay one story RC frames. The test setup, measurement tools and their purpose are given in the previous chapters. The displacement protocols applied are same for both reference frame and the specimens tested at 15th year. The test is displacement control based test and the largest top displacement enforced to the RC frames was 42 mm in both pushing and pulling cycles of the displacement protocols applied. In specimen 2, there was no failure at the 42 mm because of that one more step which is 56 mm cycle applied to the tested frame specimen. The total axial load applied to the frame 330 kN at the beginning of the test which equals to about 20% of the total axial load bearing capacity of the two columns. The reference frame experiment were carried out at the ITU Structure and Earthquake Lab. fifteen years ago. The results are recorded by Civil Engineer Hakan Saruhan for using of future corrosion study.
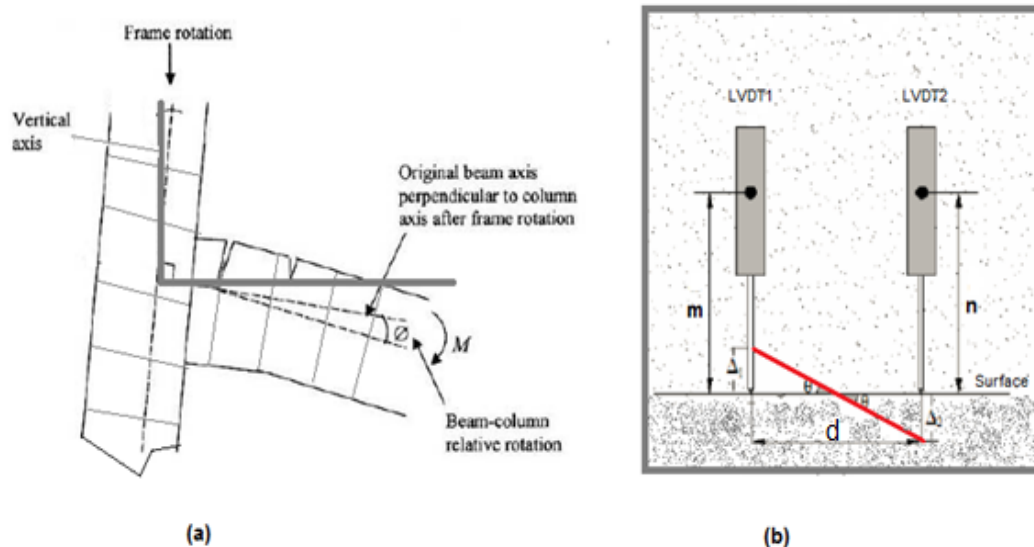
Figure 4.28: (a) Rotation of the beam column connection joint, (b) calculation of the rotation at the beam and column element

Rotation at the beam-column and column-foundation joints are calculated by the measurements of LVDTs placed at these important connection points. The total displacement values which is the sum of the measurement of LVDT1 and LVDT2 and divided by the distance between the two LVDTs as given above Figure 4.28 (b) and formula 4.4 below. Here, surface line represents the before deformation state and red line in the Figure 4.28 represents the after deformation state respectively.

$$\textbf{Rotation},\ \theta = (\boldsymbol{\Delta_1} + \boldsymbol{\Delta_2})/\textbf{d} \qquad (4.4)$$
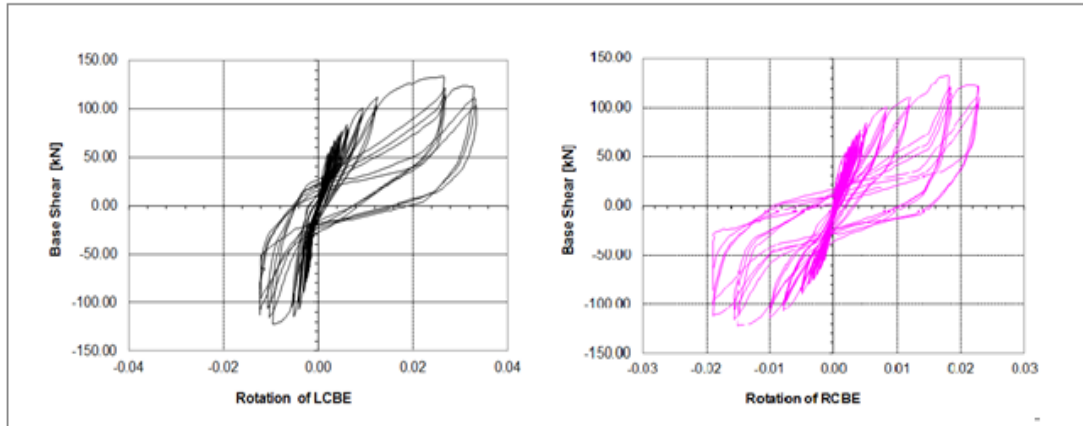
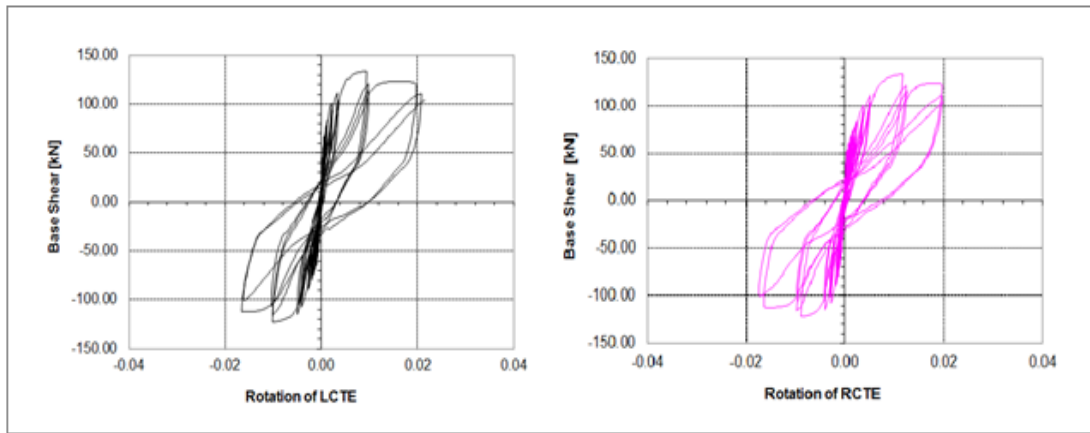Figure 4.29: Rotation of the left and right column at the bottom end

Figure 4.30: Rotation of the left and right column at the top end

In Figures 4.29, base shear versus bottom side rotation of the left and right columns and in Figure 4.30 rotation of the left and right column at the top end versus base shear are submitted here. The ultimate value of rotation measured at column elements are 0.0345 radian that obtained at left column bottom end.
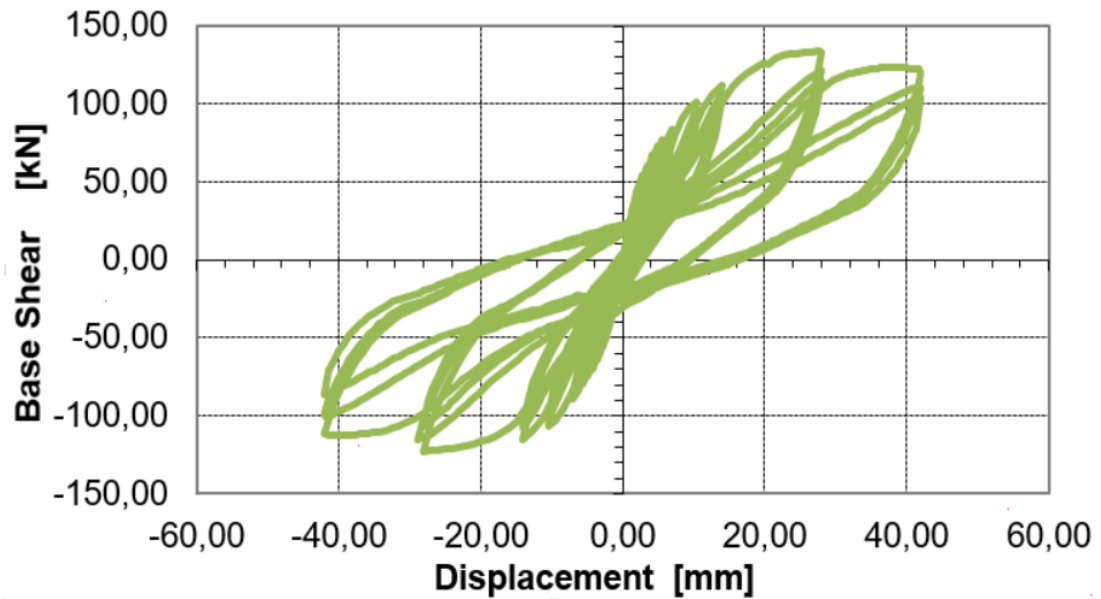
Figure 4.31: Top displacement- base shear curve of the reference RC frame

Base shear versus top displacement graph of the reference RC frame are given above Fig 4.31. The maximum top displacement in both pushing and pulling cycles is 42 mm. The maximum load applied to the structure is 134 kN in pulling zone at the 17th step of the loading protocol which is the 28.0 mm cycles. On the other hand, the maximum load carried by specimen is 122 kN in pushing zone at same step cycle at pulling zone. In this quasi static test, there are three pulling and pushing cycles for each step of displacement protocol. Because of the nonlinearities of the materials, there are some differences between the three loops of same cyles as seen above Figure 4.36. The maximum drift applied was 3% where the base shear of the frame are 86 kN in compression and 104 kN in tension. At the beginning of the test, envelope curve starts with linearity up to point about 40 kN and than goes with nonlinearity curve due to nonlinear material behavior of the RC structure as defined.
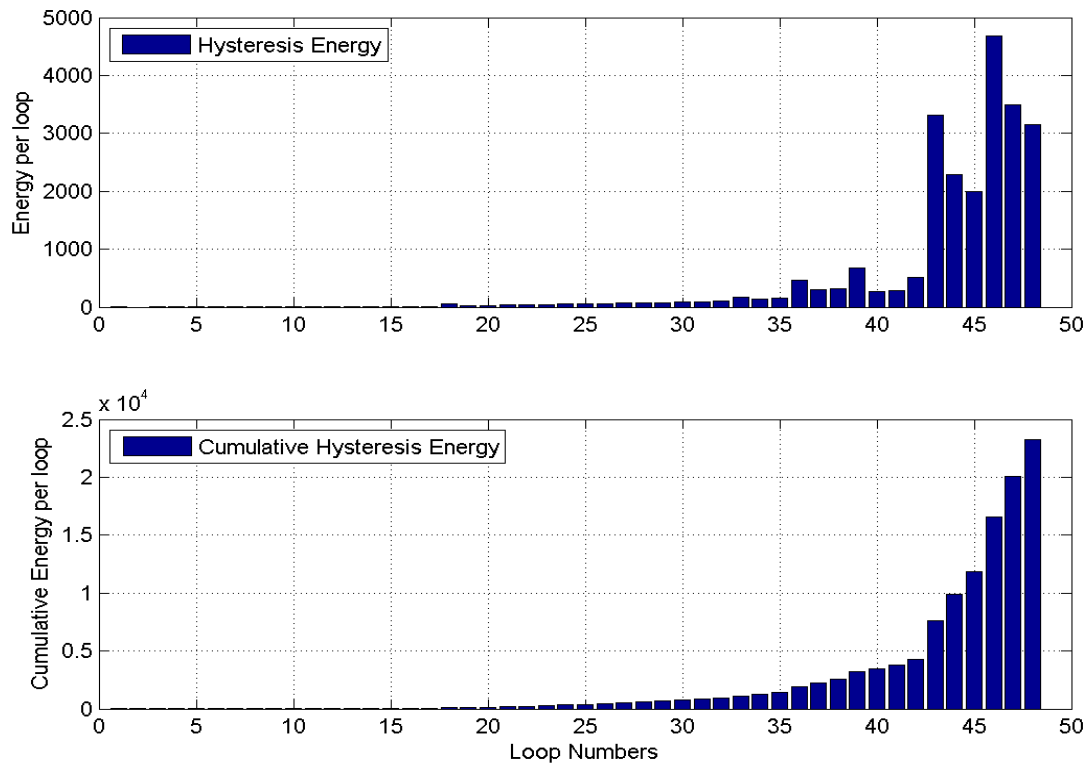
Figure 4.32: Cumulative energy dissipation capacities of reference frame at stage of all cyclic loop up to failure

During the test asymmetric cyclic behavior in positive and negative directions was observed in load-displacement pattern. The RC frame is subjected to cyclic behavior as given above Figure 4.32, than the energy dissipation capacity obtained using the real curve area in two opposite directions by using Matlab. The cumulative energy dissipation of reference specimen which is tested 15 years ago are given in Figure 4.32. There are forty eight cyclic loop at this reference frame test. The total cumulative energy dissipated by this reference frame is about 25000 [kNmm] at the end of the tests given above Figure 4.32.

Crack name and crack width drift at different stages such as 1%, 2% and 3% as given Table 4.8.

Table 4.8: Cracks width of referance frame at specific drift level

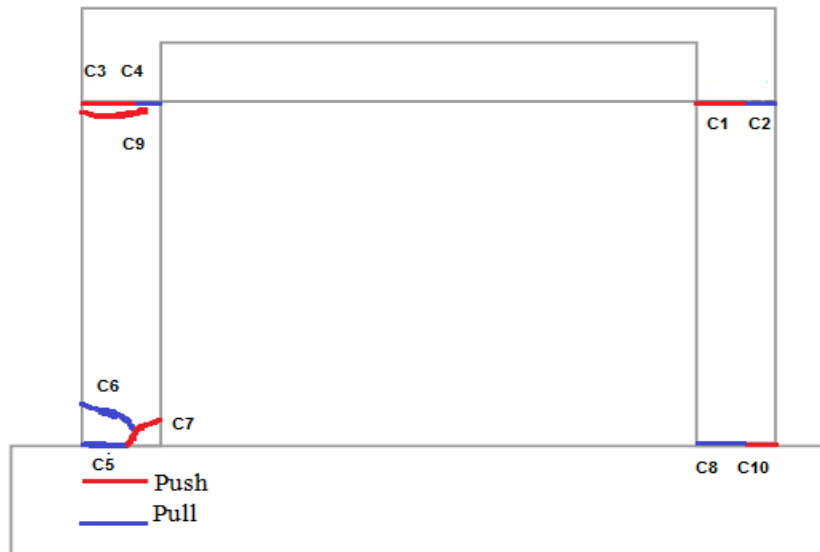| Crack Name	Drift (1%)	Drift (2%)	Drift (3%)
C1	1.6 mm	3.0 mm	-
C2	0.6 mm	1.4 mm	Bigger than 3.5 mm
C3	0.1 mm	0.1 mm	0.2 mm
C4	1.2 mm	2.5 mm	-
C5	0.5 mm	0.9 mm	0.9 mm
C6	0.2 mm	0.9 mm	-
C7	0.15 mm	1.4 mm	3.4 mm
C8	0.3 mm	1.0 mm	Bigger than 3.5 mm
C9	0.1 mm	1.4 mm	3.5 mm
C10	-	0.2 mm	0.9 mm

Figure 4.33: Crack formation of reference frame at the last stage of the experiement

Crack pattern of the reference frame specimen is presented in Table 4.8 shows the width of cracks at various drift ratios. C1, C3, C7, C9 and C10 are the cracks of push cycles according to the right edge. The other cracks occurred on columns

top and bottom edges are the pulling cycle cracks during the reference frame test. The first cracks occurred at the top of the right column as given C1 respectively. The crack named as C1 was equal to 1.6 mm at 1% story drift and 3.0 at 2 % story drift as given Table 4.1. At the end of the test this part of concrete column was crushed. The biggest crack which is C2 observed on the top of the right column as given above Figure 4.33. Inelastic behaviour has started at this top ends of the right columns while beam ends stayed elastic. In the later cycles, several micro cracks occurred parallel to the this main cracks given. There are many several shear cracks occurred in both right and left columns. The specimen after the test can be seen in Figure 4.35. Table 4.8 include the width of main cracks at several stages.

4.2.6   Test Results of Specimens RCF-2

This specimen is a RC naturally corroded frame which is tested 15 years after from casting date. The RCF-2 specimen is the frame tested for the corrosion development study for RC structure to compare the results with 15 years ago. This frame is naturally corroded one bay one story RC frames. The test setup, measurement tools and their purpose are given in the previous chapters which are same for each specimen. The displacement protocol are same for both reference frame and the specimens (RCF-2) tested at 15th year as given previous chapters. The test is displacement control based test and the largest displacement enforced to the RC frames was 56 mm in pushing and 42 mm in pulling cyles with the displacement protocols applied. During the test of RCF-2 specimen, there was no critical failure at the 42 mm so one more step which is 56 mm cyle applied to the frame specimen respectively. The total axial load applied to the frame is 330 kN at the beginning of the test which equals to 20% of the total axial load bearing capacity of the two columns. This fifteen years old corroded reinforced concrete specimen experiment was carried out at the ITU Structure and Earthquake Lab. in the year of 2017. The results are recorded by data logger and saved for analysis.
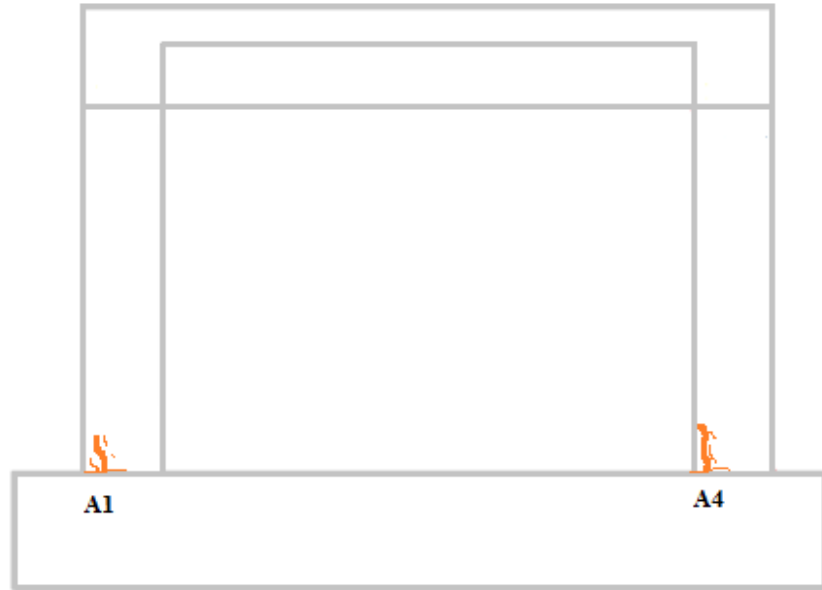
Figure 4.34: Crack pattern of RCF-2 before the experiment

Initial crack observed on the reference frame specimen is given in Fig 4.34. The cracks which are A1, A2, A3 and A4 is the initial cracks observed front and back side. The width of initial cracks are change between the range 0.1-0.4 mm. These crack's width increase with the increment of the drift ratio. These cracks formed due to the corrosion process along the longidutional reinforcement bars as given in Fig 4.34.
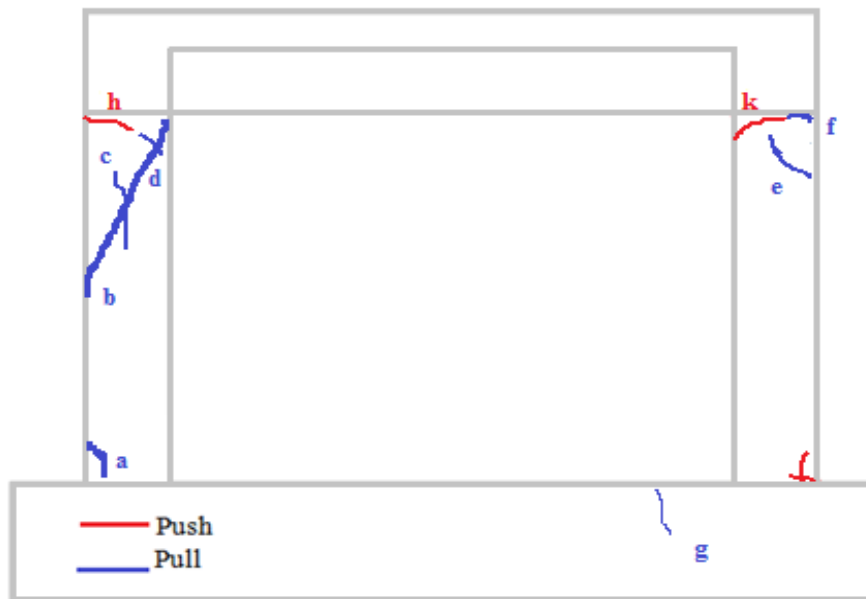
Figure 4.35: Crack scheme of RCF-2 specimen at the end of the test

Crack scheme of the specimen after the experiement is given in Fig.4.35. Total 31 cracks were observed during the test and recorded on a chart. The width of cracks start to observed at the level of 0.1 mm and checked end of the each stage of test. The RCF-2 specimen faced with shear failure at the last step from the crack b. The maximum measured crack width is 10 mm before the failure step.
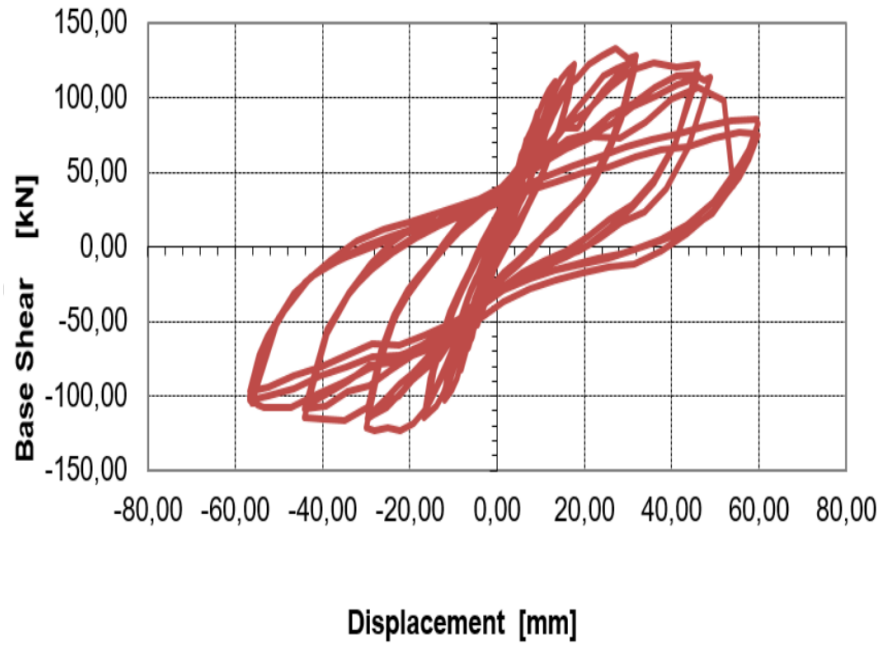
Figure 4.36: Base shear versus target displacement graph of the RCF-2

Base shear versus target displacement graph is given below Figure 4.37 with all triple cycles. The ultimate strengths in compression and tension are 122 kN and 132 kN occurred at 2% story drift. The ultimate capacities occurred at 3% and 4% story drift, respectively, compression and tension as 97 kN and 75 kN.
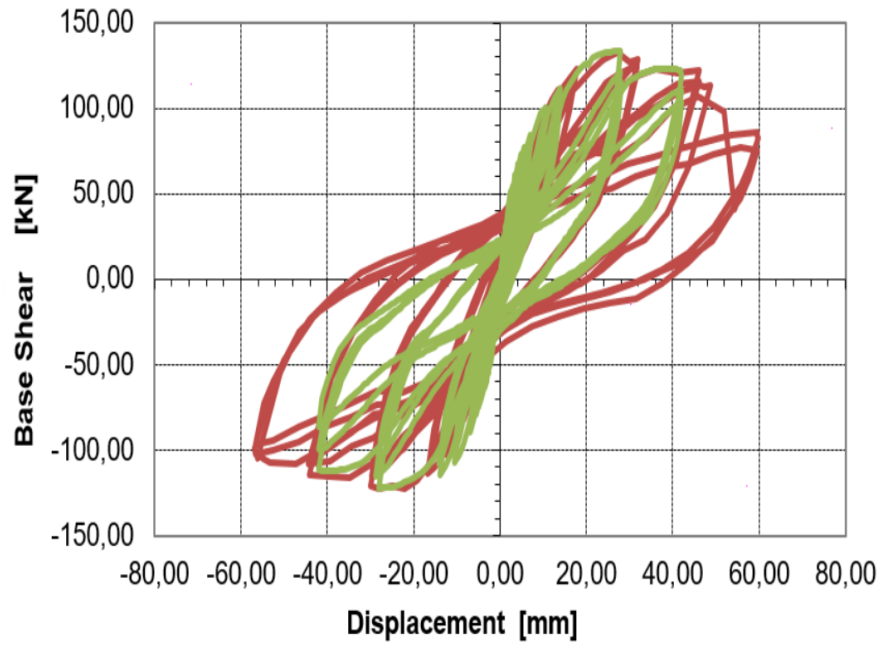
Figure 4.37: Base shear versus target displacement graph of the reference frame and RCF-2
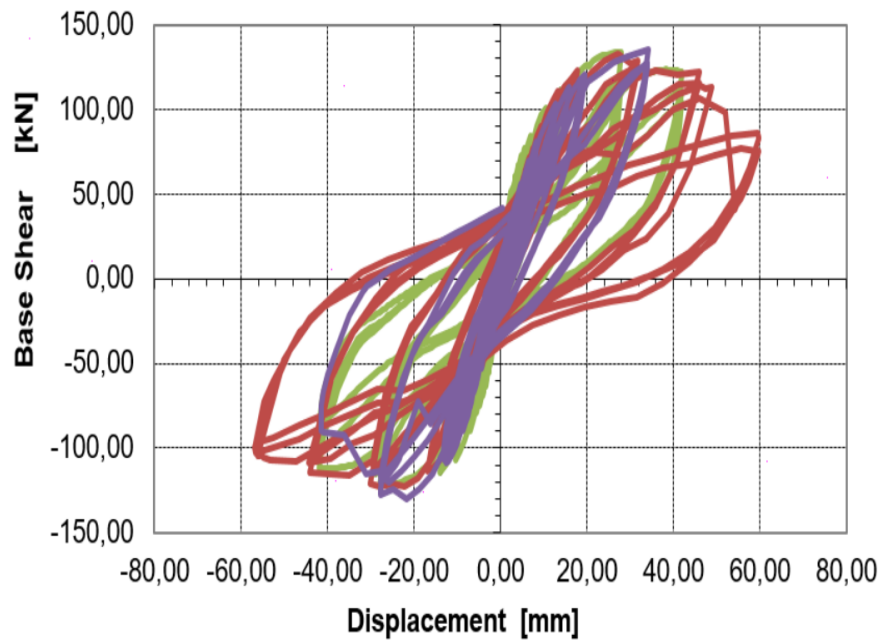

Figure 4.38: Base shear versus target displacement graph of the reference frame, RCF-1 and RCF-2
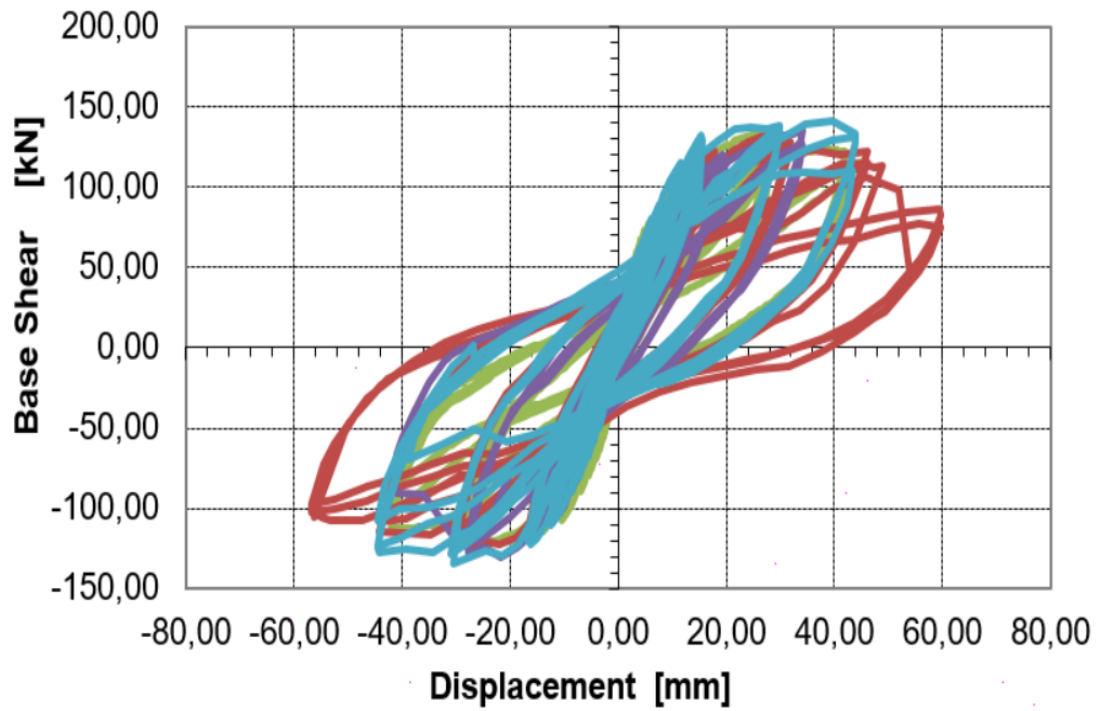
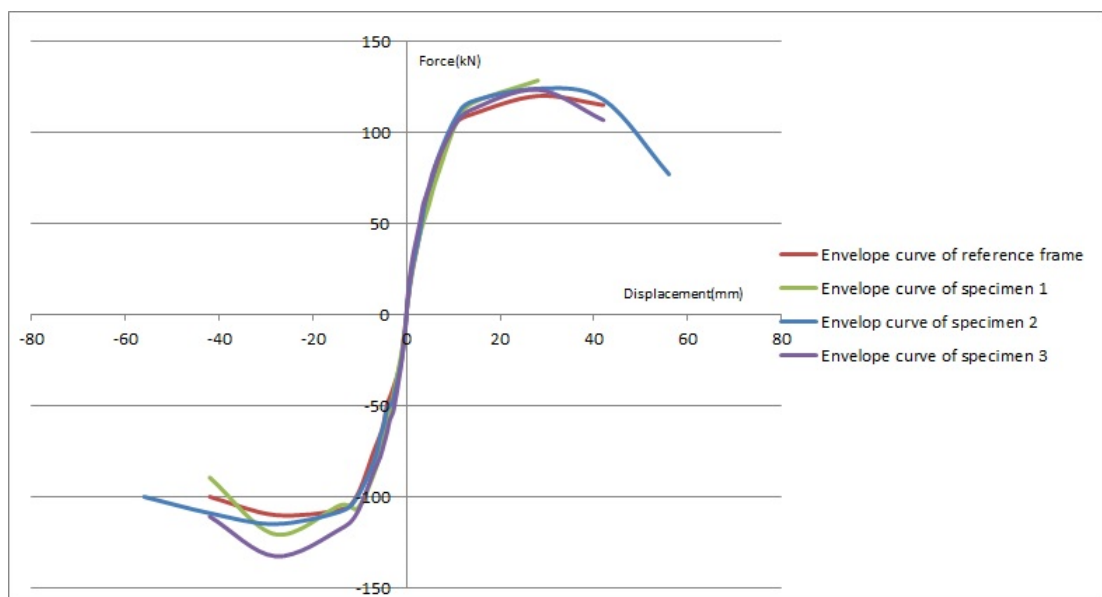Figure 4.39: Base shear versus target displacement graph of the reference and tested specimens

Figure 4.40: Envelope curve of the reference frame, RCF-1, RCF-2 and RCF-3

In Figure 4.40, top end relative displacement of frame and base shear are given for all specimen, respectively. Reference frame is represent the RC frame which was tested 15 years ago at Istanbul Technical University Laboratory by the a team. The other three specimens which are specimen 1 (RCF-1), specimen 2 (RCF-2) and specimen 3 (RCF-3) . The bare frame used as a reference frame and the effect of the different corrosion level and concrete strength are compared and discussed with this reference RC frame given in Figure 4.40. This four specimens are compared with each other according to their failure modes, load carriying capacity, dissipated energy, member ductility and their stiffness.

The target top displacement applied to the all was 42 mm as given in the displacement protocol but it reached during the test of RCF-2 as given Fig 4.37. According to the base shear- top displacement graph of all specimens; specimen RCF-2 reached the ultimate target displacement that is 56 mm. The maximum corresponding load occur during the test of the RCF-3 as given in Fig 4.36. The highest loads occurred during the pushing cyles which is 133 kN for reference specimen. It is 132.8 kN for the RCF-2 during the pushing cycles. Initial stiffness of the reference frame was equal to 22.0 [kN/mm], it is equal to 25.4 [kN/mm] for specimen RCF-2.
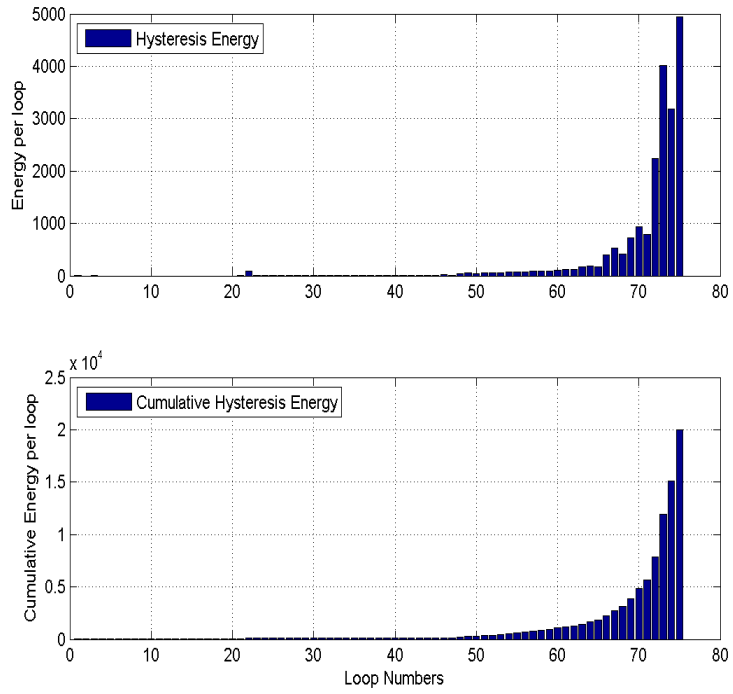
Figure 4.41: Energy dissipation capacities of RCF-1 at stage of all 75 cylic loop up to failure
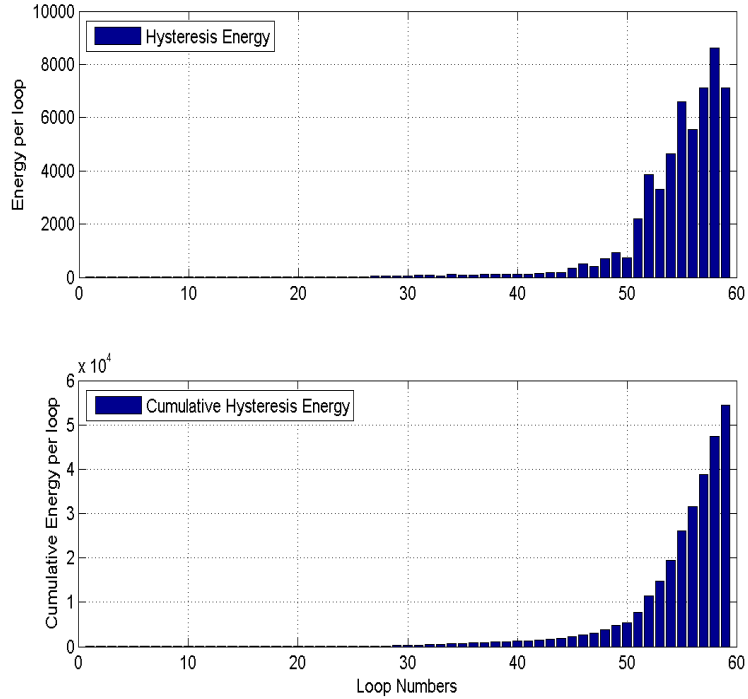
Figure 4.42: Energy dissipation capacities of RCF-2 at stage of all 59 cylic loop up to failure
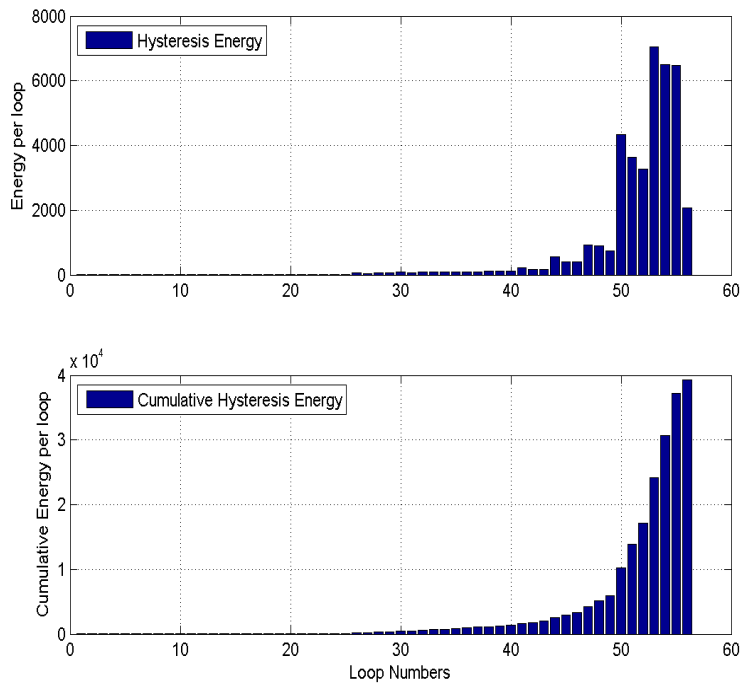
Figure 4.43: Energy dissipation capacities of RCF-3 at stage of all 56 cylic loop up to failure
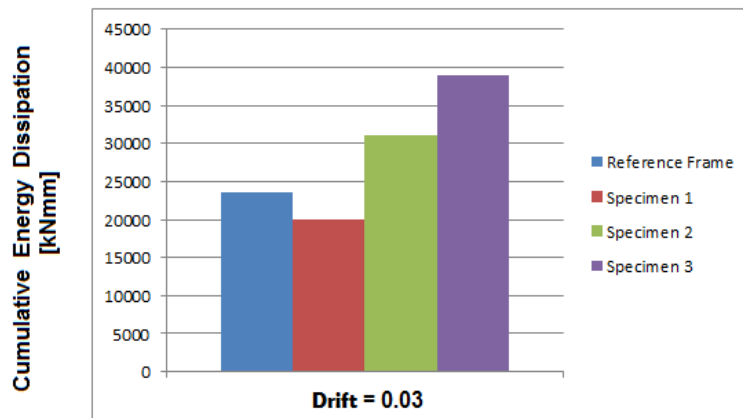
Figure 4.44: Energy dissipation capacities of reference frame, RCF-1, 2 and 3 at 0.03 story drift

The cumulative energy dissipation of the reference frame (specimen 1) at 0.03 story drift is 20.000 [kNmm]. The total energy dissipation of the RCF-2 at 3% story drift is 1.6 times bigger compared to the reference frame's shown in Fig 4.44.

4.2.7 Evaluation of the Results

Figure 4.45: Demolished part of the specimen RCF-2 at the end of the test

The results are given below:

- The initial lateral stiffness of the reinforced concrete corroded frames increased compared with the reference's RC frame.

- The base shear carrying capacity kept constant level compared with the reference's RC frame as seen in Fig 4.28.

- The cumulative energy dissipation of reference frame at 0.03 story drift is 1.6 times increased compared to the RCF-2 shown in Fig 4.44.

- The ultimate displacement capacity increased at 4 % story drif level for RCF-2 compared to the reference's RC frame.
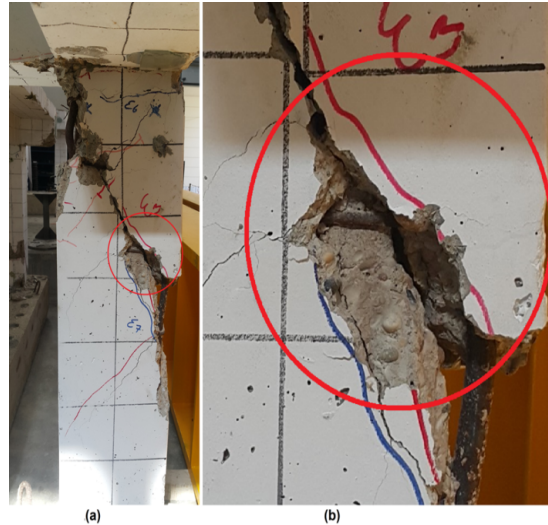
Figure 4.46: (a) Failure mode of the specimen RCF-2 at the end of the test, (b) stirrups failure due to corrosion

The comparison of corroded RC frame test results with each other are submitted below. Each of the RC frame specimen is evaluated based on the parameters given in previous section. Lateral load carrying capacity, failure mode and shape, initial stiffness and energy dissipation capacity are evaluated and submitted at this part.

• Failure modes and shapes :

During the displacement control based test, displacement protocol applied on the structure and the failure modes occurred at the stage of ultimate load level. Bending and shear failure occurred at column bottom/top ends of reference RC frame. Shear failure observed at left column ends of RCF-2 as shown Fig 4.46. The shear strength capacity of the column is low because of corrosion of the reinforcement effects the shear strength of columns as given figure above. This is because the failure occurred on the confinement reinforcement as given Fig 4.46 (b) in detailed.

• Lateral load bearing capacity :

The lateral load bearing capacity of RCF-2 kept same as compared with reference frame that tested 15 years ago. Concrete strength development and corrosion of the reinforcement (effective cross sectional area lost) balance each other during the time up to test.

• Initial stiffness :

The initial stiffness of the frames are calculated from the base shear versus displacement graph as the tangent of maximum shear occurred during the cyles. Initial stiffness of the reference frame was 21.6 [kN/mm] and 25.4 [kN/mm] for specimen RCF-2.

• Cumulative energy dissipation capacities :

The cumulative energy dissipation of the reference frame (specimen 1) at 3 percent story drift is 20.000 [kNmm]. The total energy dissipation of the RCF-2 at 3% story drift is 1.6 times bigger compared to the reference frame's as shown in Fig 4.44.

4.3 Poisson's ratio related test

This chapter describes the experimental study of stress-strain behaviour of 15 years old special concrete specimens. Total 56 concrete specimens were tested to evaluate the Poisson's ratio at descending branch and compare the results with reference specimens that was tested before 15 years at main campus of Istanbul Technical University Material Laboratory by a team.

Description of the specimens which covers mechanical properties of used structural materials, mix proportion of casted concrete and geometrical properties are submitted fallowing section. This chapter also includes testing programme of concrete specimens (150/300 mm), testing-setup, instrumentation, failure modes, data acquisition, material mechanical properties.

4.3.1 Specimens

There are 56 cylindrical specimens with standard size (150/300 mm) but some of them were tested during the this experimental work. Three standard cylinders R-29-1, R-29-2 and R-29-3 were tested at 28th days before 15 years ago to obtain the stress-strain relationship. At the day of 5420th, three standard cylinders T-29-1, T-29-2 and T-29-3 were tested to comparing the stress-strain relationships and modulus of elasticity incremental with time and results are given section 4.2 in detailed.

Figure 4.47: Typical cylindrical specimens for Poisson's ratio test.

For doing that a lot of tests on 15 years old cylindrical 15/30 cm specimens has been conducted first. The results have been compared by code proposals, the stress-strain relationships of confined/unconfined specimens have been compared paying attention on the descending branches. The poisson ratio of fifteen years old confined and unconfined concrete in descending branch of stress-strain diagrams was another topic for which only limited amount of literature is available.

All standard cylinders (15/30) were tested at the Construction Materials Laboratory of ITU using a 5000 kN Instron Displacement control press machine. Standard cylindrical concrete specimens were tested by using the technique of displacement control based material test.

Material	Weight for one unit
Portland Cement	300 kg (32.5 R)
Water	140 kg
Sand	690 kg
Gravel	1070 kg (1 No aggregate)

Table 4.9: Mix composition of specimens

4.3.2 Test Setup

Test setup and instrumentations are described for Poisson ratio related topics in this section. Detailed drawings included test setup are given in the following part. A typical test setup for cylindrical specimens are shown in below Figure 4.48 and Figure 4.47.
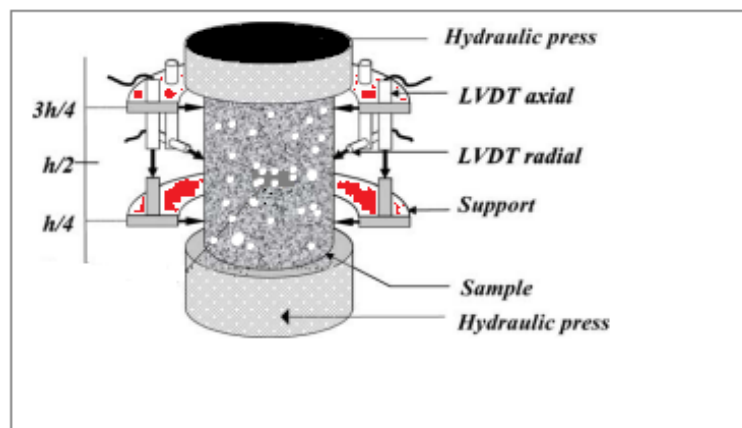

Figure 4.48: Typical test-setup for cylindrical specimens.

4.3.3 Instrumentation and LVDT's

As seen in Figure 4.48 above, axial load which is increasing throughout the test is applied on the cylindrical specimens by means of a hydraulic press machine which have 5000 kN capacity. Controlling of hydraulic press machine is displacement-based due to the Poisson's ratio precision during the lowering load branch. Data collection enforced by the axial LVDT's and radial LVDT's as given above figure. Linear variable displacement transducers connected to the mid section of the specimens and upper-lower rigid plate. These LVDT's placed on axial and radial orientation to measure the deformations of the concrete in both direction which are horizontal and vertical deformation change to get the Poisson's ratio of the specimens.

The name of LVDT's used, their measurement capacities and purpose are listed in Table 3.3 and their detail are shown above. The vertical deformation of the cylindrical specimens are watched through four channels that are the TP1, TP2, TP3 and TP4. Radial deformation of the specimens are measured by three LVDTs listed below Table 3.3.

Table 4.10: LVDT's used for cylindrical concrete specimens

Name	LVDT Type	Measurement Purpose	Attached to
TP1	CDP5	Vertical deformation	Specimen
TP2	CDP5	Vertical deformation	Specimen
TP3	CDP5	Vertical deformation	Specimen
TP4	CDP5	Vertical deformation	Specimen
TP5	CDP5	Horizantal deformation	Specimen
TP6	CDP5	Horizantal deformation	Specimen
TP7	CDP5	Horizantal deformation	Specimen
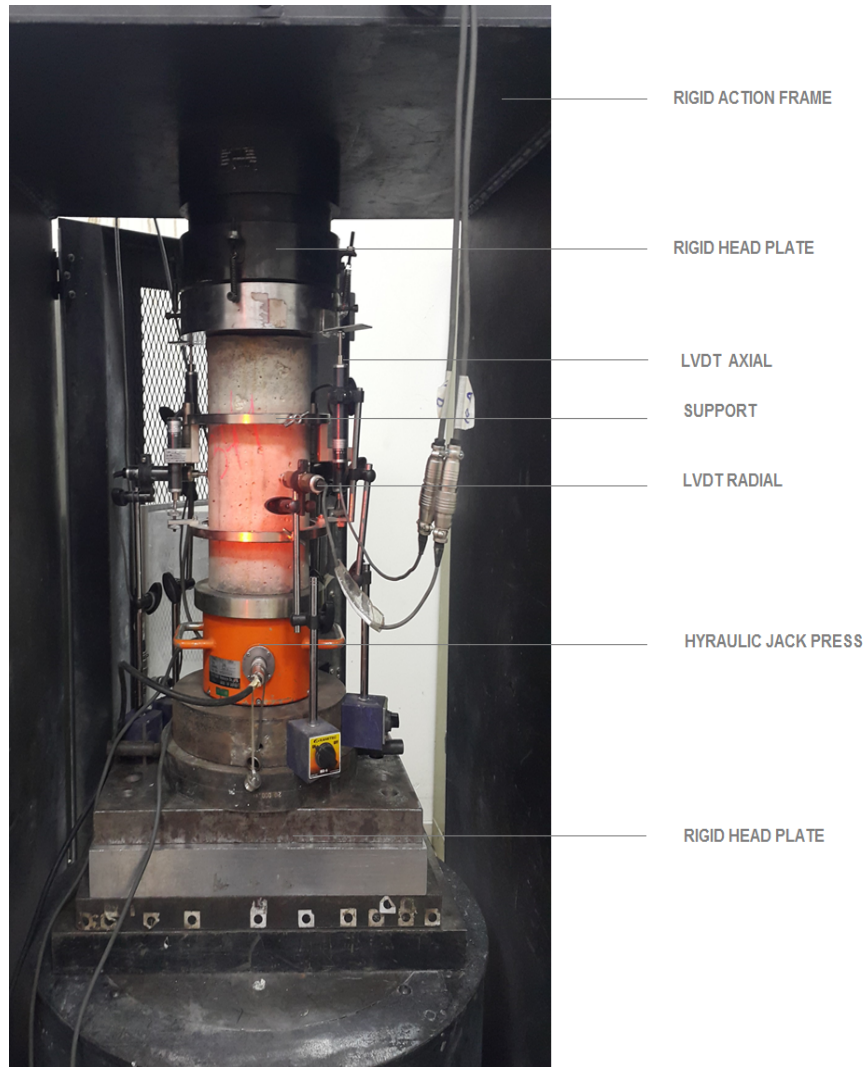
Figure 4.49: Testing instrument of the Poisson's ratio measurements.

In order to measure vertical and radial deformation accurately, calibrated testing machine were used to perform the experiment. Movement of the rigid head plate and radial deformation of the specimen were reading. Then, the recorded strain measurements for the tests were evaluated to get the Poisson's ratio both in upper loading and lower loading branch in stress-strain curves.

4.4 Test Results

During the test, eight cylindrical 15/30 cm specimens has been conducted first. The results have been compared by code proposals, the stress-strain relationships of confined/unconfined specimens have been compared paying attention on the descending branches. The Poisson ratio of fifteen years old confined and unconfined concrete in descending branch of stress-strain diagrams was another topic for which only limited amount of result is available here.
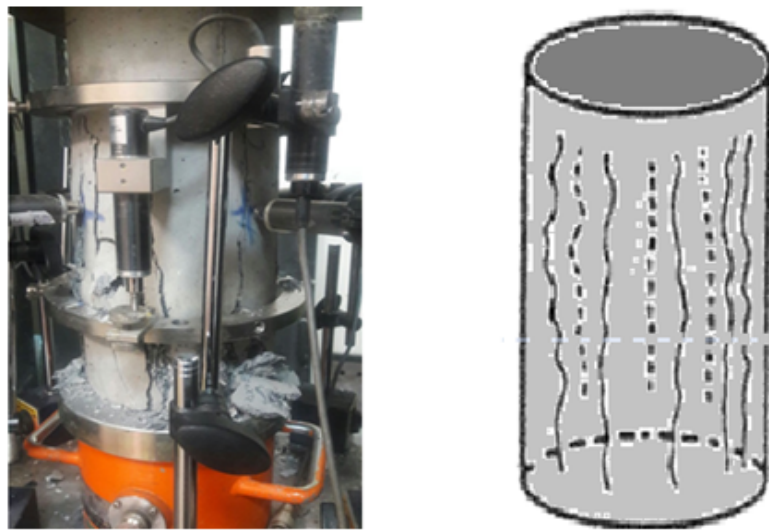
Figure 4.50: Failure mode of specimens S/30-2 under axial loading.

Features in the type of failure were recorded and photographed one by one for each concrete specimens. Examples of one of the satisfactory failures shape is shown in Figure 4.50 above. In this failure shape, there are straight cracked as seen in Figure 4.50. Although there are several measurement points on the specimens, some of the measurements are unsatisfactory due to the failure shape and huge radial deformations as seen in the Figure 4.50. This type of huge radial fracture and deformations lead to unrelated data collection to get more accurate Poisson ratio value. In descending load branch, the specimens were dispersed as

seen above. Because of this dispersion of the concrete specimen, it is hard to get available data to evaluate the Poisson's ratio of the testing specimens.

During the Poisson's ratio experiments, there are eight cylinder concrete specimens were tested and more specimens were aimed to test. But there are some problems to get the radial strain during the lowering load branch due to the expansion of the shell concrete without natural bahavior. Total eight of the specimens were tested and detailed results are given below section.

4.4.1 Test Results of the Specimens without Confinement

Totally eight cylindrical 15/30 cm specimens has been tested during the experimental work. The stress-strain relationship in both direction have been collected and saved to analyse. Especially in descending branches, there are some problems to get the radial strain during the load applied due to the expansion of the cover concrete as shown on Fig 4.50. Total eight of the specimens were tested and detailed results are given below respectively.

Figure 4.51: Vertical and horizontal strain versus stress diagram of specimen S2/29-1.
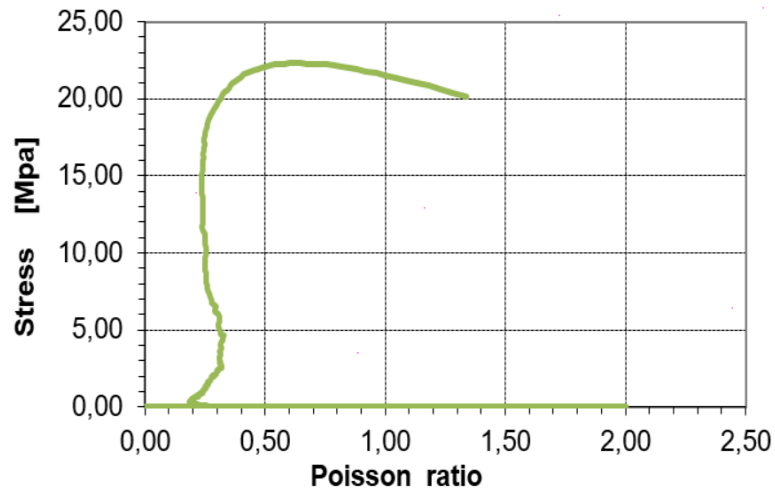
Figure 4.52: Poisson's ratio versus stress diagram of specimen S2/29-1.

Poisson's ratio of concrete is the ratio of horizontal (radial) strain to axial strain in a cylindrical specimen subjected to compression. Poisson's ratio of standard concrete varies between 0.15 and 0.35. In engineering practice, the value is taken as 0.15-0.2 for capacity design.

Figure 4.53: Vertical and horizontal strain versus stress diagram of specimen S2/29-1.
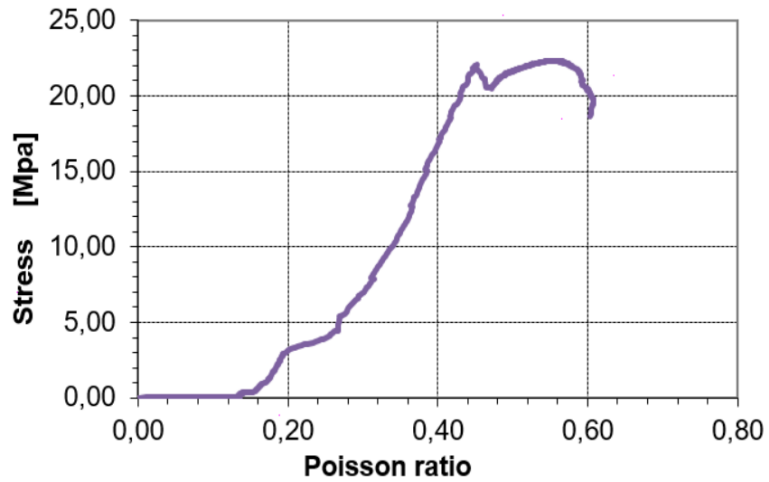
Figure 4.54: Poisson's ratio versus stress diagram of specimen S2/29-1.

Poisson's ratio of specimen S2/29-1 is calculated by ratio of horizontal strain to vertical strain that is given in Fig 4.53. The unconfined cylindrical specimen's Poisson ratio which subjected to compression starts about 0.2 and varies between 0.2 and 0.44 during the increasing load branch of test. Especially in descending branches, there is no exact radial strain values because of the expansion of cover concrete as shown on Fig 4.50.
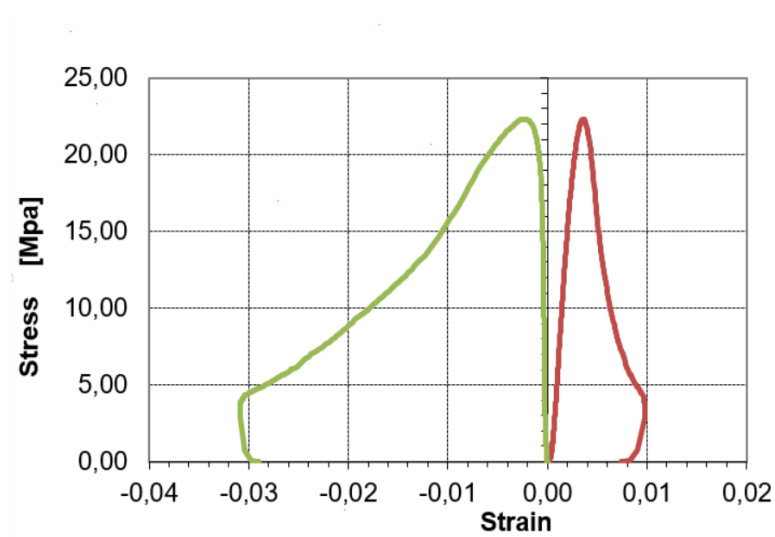

Figure 4.55: Vertical and horizontal strain versus stress diagram of specimen S2/34-1.
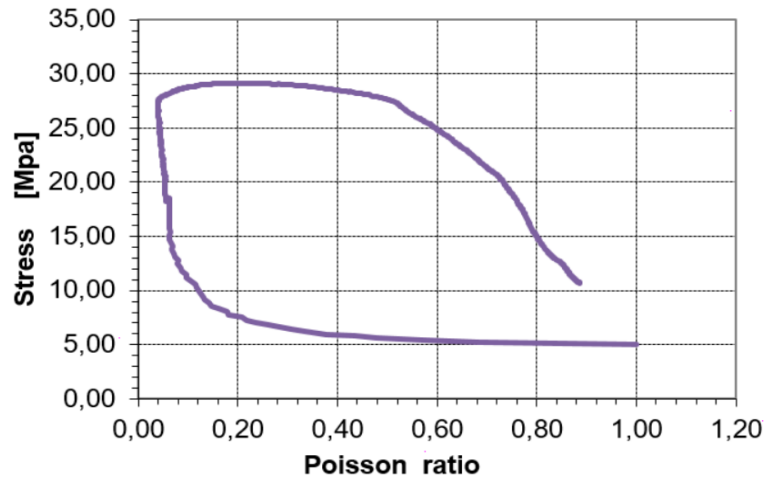
Figure 4.56: Poisson's ratio versus stress diagram of specimen S2/34-1.

Poison's ratio is continuously decreasing or increasing with the changes in loading rates and conditions because of that displacement control based test applied to the specimens to get the more convenient values. Poisson's ratio of specimen S2/34-1 is measured by ratio of horizontal strain to vertical strain. S2/34-1 specimen Poisson's ratio varies between 0.15 and 0.2 during the increasing load branch after the stress level at 7 MPa. Especially in descending branches, there is no exact radial strain values because of the spalling of specimen at radial direction.
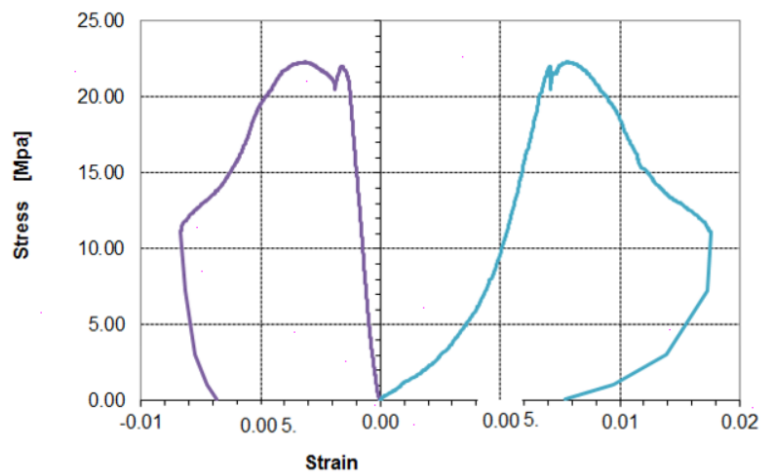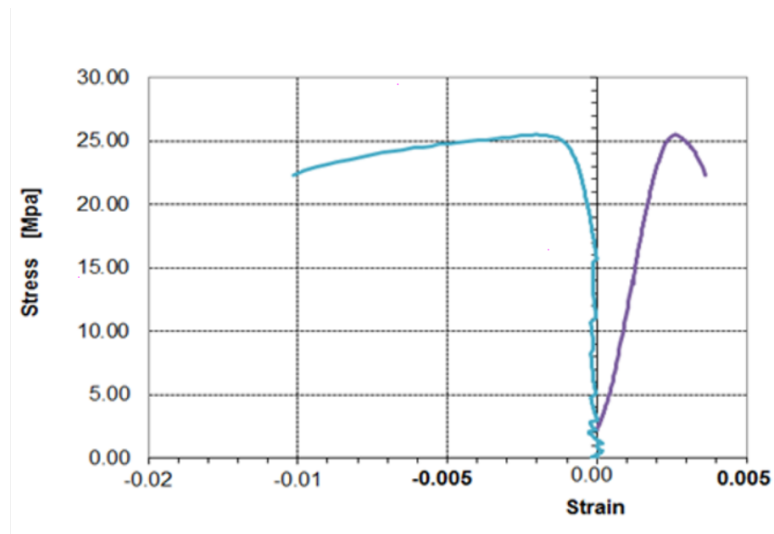

Figure 4.57: Vertical and horizontal strain versus stress diagram of specimen S2/34-3.

104

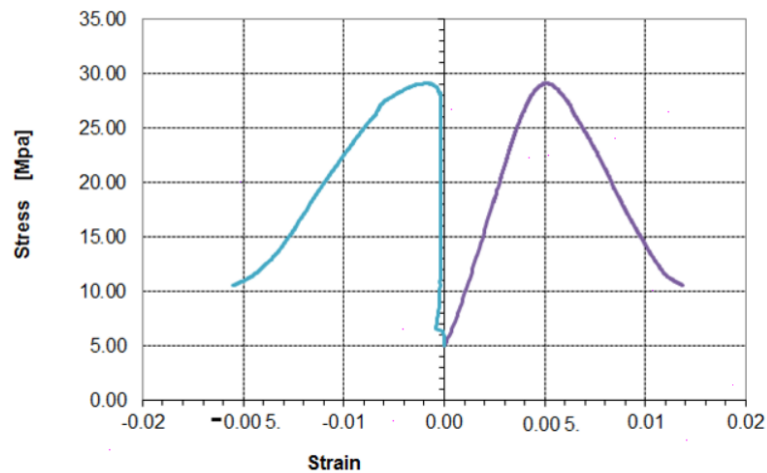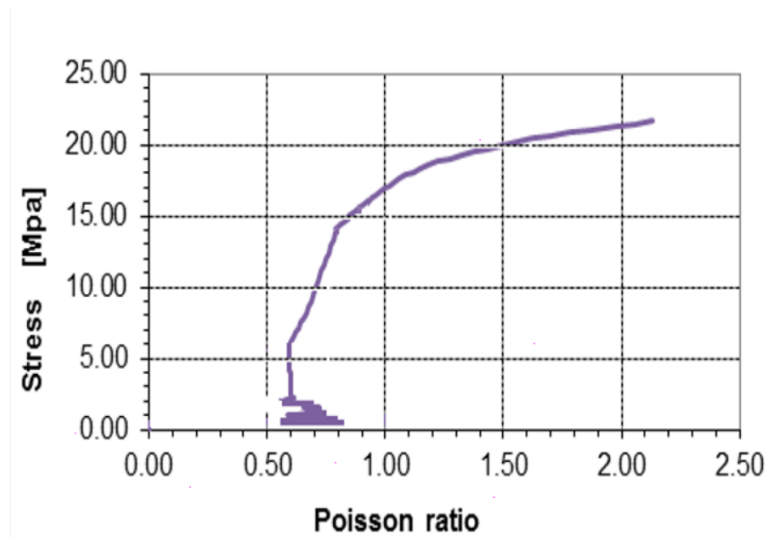Figure 4.58: Poisson's ratio versus stress diagram of specimen S2/34-3.

The applied loads, corresponding vertical and radial strains at different four points of the radial section of the cylindrical specimens were collected and saved. At the analysis stage, there is an overlap on the increasing of Poisson's ratio with the improvement in compressive strength of concrete. Specimen S2/34-3 has compressive strength 26 MPa and Poisson's ratio varies between 0.55 and 15 during the increasing load branch after the stress level at 2 MPa. There is no convenient radial strain values because of the spalling of specimen at radial direction at plastic limit initiation point.

4.4.2 Test Results of the Poisson Ratio of Confined and Unconfined Concrete

During the rest of the experimental work, confined cylindrical specimens tested with same procedure with the unconfined specimens. The poisson ratio of fifteen years old confined specimens in descending branch of stress-strain diagrams stopped due to the spalling of specimen at radial direction and time effect.

Radial expansion of the concrete is a crucial point for conducting the confinement level in reinforced concrete structures. Measuring horizontal strains in laboratory

experiments is hard because of several reasons that explained previous sections. There are some analytical models for lateral strain and axial strain behaviour. These models are based on the assumption that structural concrete shows elastic behavior in the beginning of the compression and then nonlinear behavior up to ultimate stress. The experimental programme cancelled that cover the testing of a number of RC confined concrete cylindrical specimens to find out the effect of the confinement on the stress strain relationships and especially Poisson's ratio value.

Figure 4.59: Confined cylindrical concrete specimens.

Chapter 5

Analytical Studies

This chapter presents some analytical model related different computer program such as DC2B, XTRACT, SAP2000 and SeismoStruct. DC2B and XTRRACT are used to define moment- curvature relationships of RC frame members. DC2B was also used for to analyse the one bay one story RC frame under cyclic loading and other nonlinear effect. SAP2000 and SeismoStruct are used to analyse the structure and to compare the results with experimental outputs. The analysis were carried out to predict the load versus displacement relations for each case of the study.

Many researchers ; Smyrou et al.(2006), Cattari and Lagomarsino (2006), Crowley and Pinho (2006) are studied to modelling reinforced concrete structure behaviour with SeismoStruct. Prof. Dr. Faruk Karadoğan, Prof. Dr. Sumru Pala, Prof. Dr. Ercan Yüksel and Res. Asst. Yavuz Durgun are used to analyze RC frame with spread permanent strain station. Yüksel (1998), Nanakorn (2004), Yüksel and Karadoğan (2009) have detail of these type of nonlinear static analysis for especially RC frame.

5.1   Nonlinear Static Analysis Using DC-2B

DC-2B (s2) is a basic computer program which developed by Karadogan et al (2016). Nonlinearities of the RC elements and materials behavior are used in the

program. Structural damage distribution (distributed plasticity) were considered to get more accurate analysis during the theoretical work. Material inelasticity is assumed to spread along the member of reinforced concrete structures. Geometry of the column and beams are submitted at the section 4.1 above. Columns are bended along the weak axis.
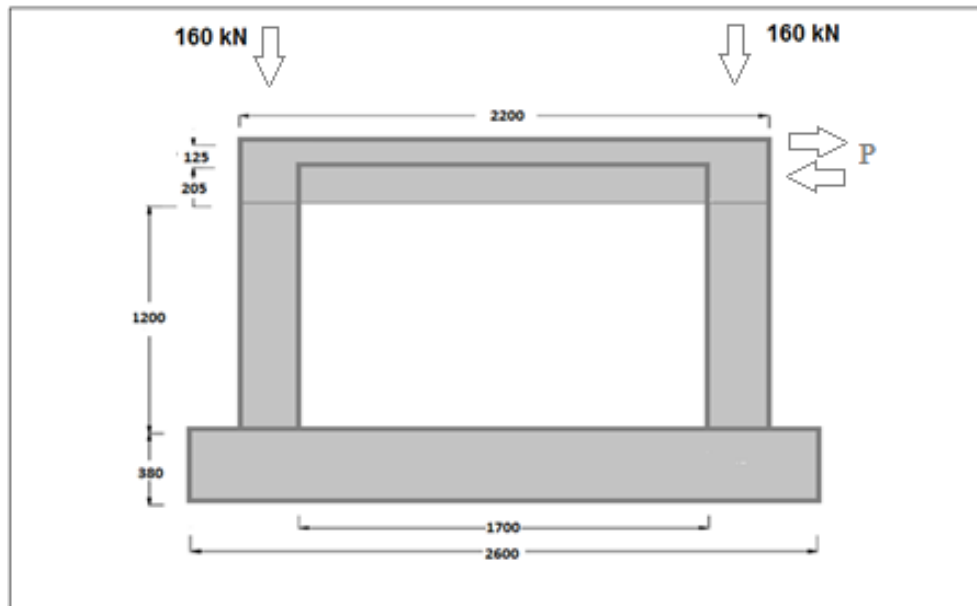
Figure 5.1: Model for analytical study in DC-2B(s2) program .

General geometric features and loads acting on the frame are given above Figure 5.1, respectively. Distributed load acting on the beam represents the self weight and experimental setup equipments load and unit loads acting on the columns are the vertical loads of the experiments which are about the 20 % axial load carrying capacity of the columns. Concrete compressive strength and yield strength of reinforcement steel are 16.3 Mpa and 286 Mpa, respectively. There is no confinement effect contribution considered coming from the stirrups. Rigidity of the elements were calculated by the help of non linear moment-curvature relations as initial and cracked during the pushover analysis.

5.1.1 Moment-Curvature Relations of Frame

Moment curvature relationships are very important to get idea about the capacity and ductility of the reinforced concrete structures. As we know, ductility is the deformation capacity of the member of RC structure after the first yield due to behavior of concrete or reinforcement under different types of loading such as snow, wind and earthquake etc. Elastic, elasto-plastic and plastic behavior stage gives us a measure of the energy dissipation capacity of a structural section as defined Fig.5.2.
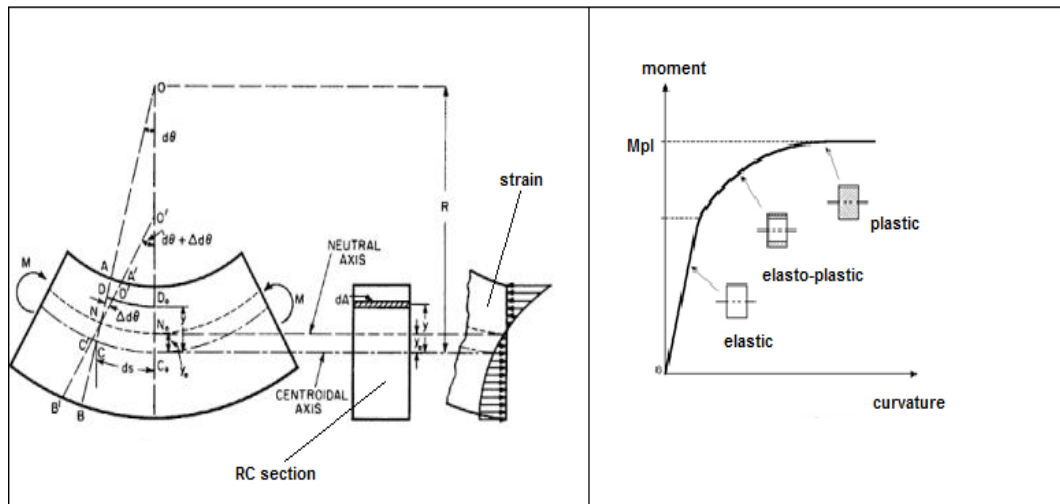
Figure 5.2: Moment-curvature relation of a RC section and strain distrubution.

In the moment-curvature analysis stage ; geometry of the sections, material characteristics, material model and loading type effects the curvature according to the research of A. İlki (2004). In this theoretical study, analytical moment-curvature relationships were obtained for RC members section by section with using three different models for confined concrete. In this chapter, theoretically obtained moment-curvature relationships are compared with literature's. The results showed that; the theoretical moment curvature relationships obtained by all of these three models were in quite good agreement with experimental outputs.

In the second part, cracked rigidity used as a parametric investigation to carried out the moment-curvature relationships.
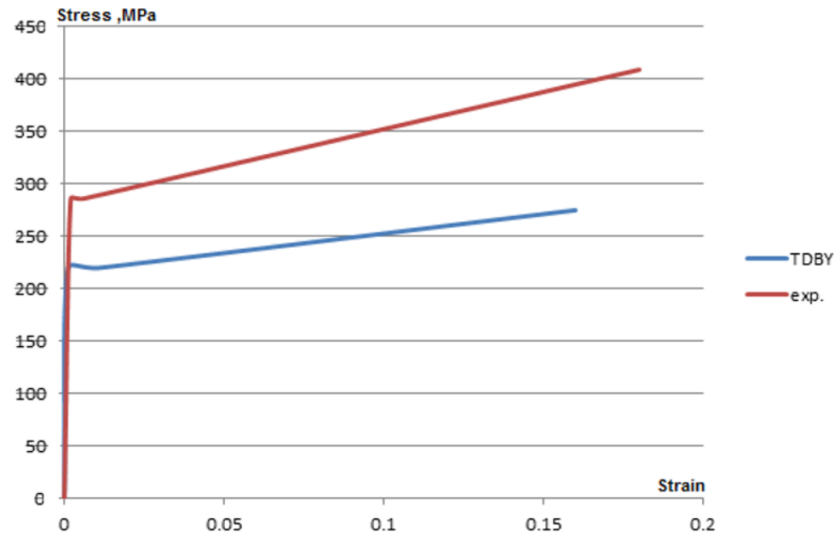
Figure 5.3: Steel material model used in analysis and TEC-2007 comparision.

Defined parameters for RC steel that are available for the material behavior are taken form the experimental tests with corroded reinforcement steel after 15 years. The evaluated properties from several experiments are used to define a material model for existing rebar. TEC-2007 rebar model is utilized to identify reinforcement mechanical behavior of tested systems.
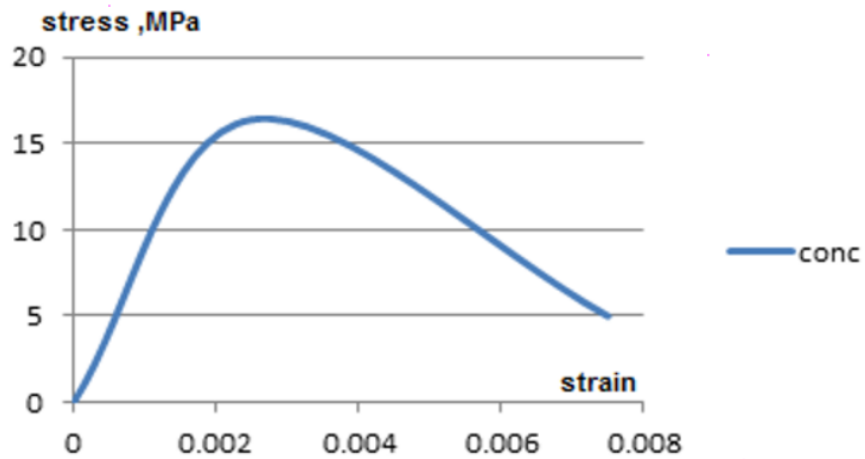
Figure 5.4: Concrete material behavior utilized in analysis.

Nonlinear constant unconfined concrete model is used to model the concrete stress-strain behavior. Compressive strength, tensile strength, strain at peak stress and specific weight are calculated by the experiment by done at ITU Material laboratory with 15 years old concrete core specimens and cylindrical specimens that given material's test results section.

Material characteristics were taken as given above and the evaluation of moment and curvature relations are utilized based on the theory that plane section kept plain after the any deformation stage.
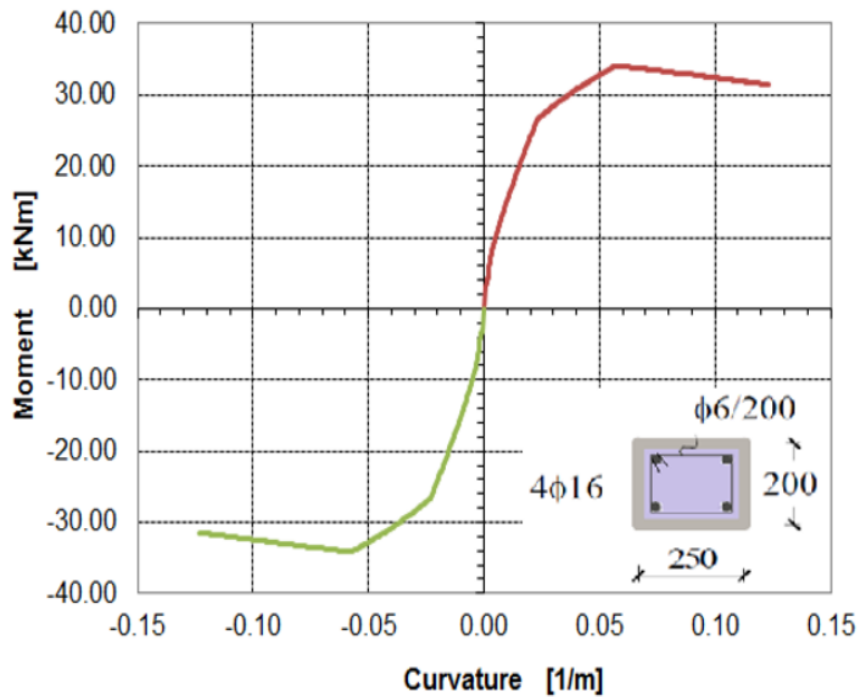
Figure 5.5: moment and curvature relationships of bottom column part of 15 years old frame.

As seen from Fig 5.5, the curvature values of the column member calculated from 0 to *(1.417-0.385) cm* height above the rigid foundation (support) that varies from 0.05 to 0.10 (1/m). According to the experimental study and literature, it is important to notice that the damage is accumulated especially along the plastic hinge area of the member from top of the base.

If the analysis results are compared with upper part of the column, yielding and ultimate moment capacities of the sections increase when reinforcement ratio increases. In other words, the more ductile behavior is observed due to increment of transverse reinforcing steel ratio of RC rectangular column section. Moreover, numerical analysis results are concluded that the increment of longitudinal reinforcing ratio effects the yielding and ultimate moment capacities of the frame's columns. Due to the this increment, plasticity starts from bottom of the column to the top as like as experiment.
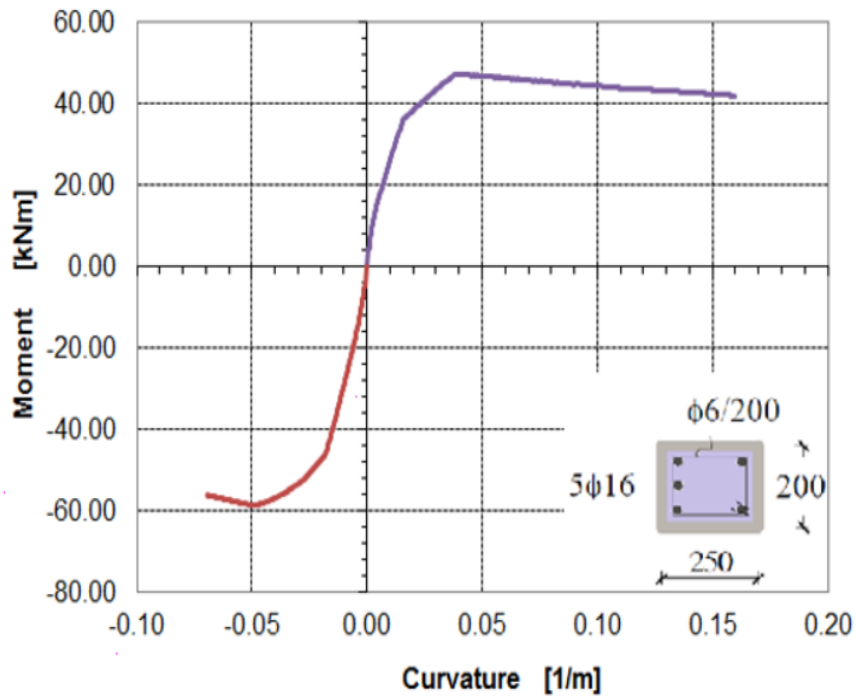
Figure 5.6: Moment and curvature relationships of upper column part of 15 years old frame.

As seen from Fig 5.6, the negative moment capacities of the T-shaped beam member calculated and it varies between 0.03 and 0.05 (1/m). According to the experimental study, positive moment capacity and negative moment capacity of the columns have difference in terms of curvature and moment capacity. The negative yield moment capacity of the section is about -44 kNm but it is about 37 kNm for positive moment side of the rectangular section. The ultimate moment

for negative side is -59 kNm and -47 kNm for positive side as given in figure just below.
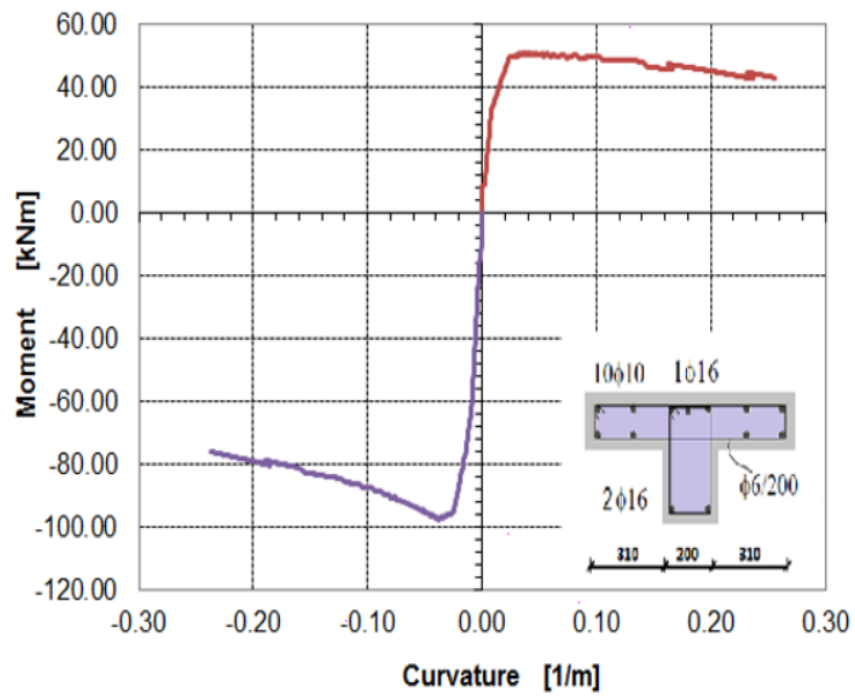
Figure 5.7: Moment and curvature relationships of T-shaped beam node part of 15 years old frame.
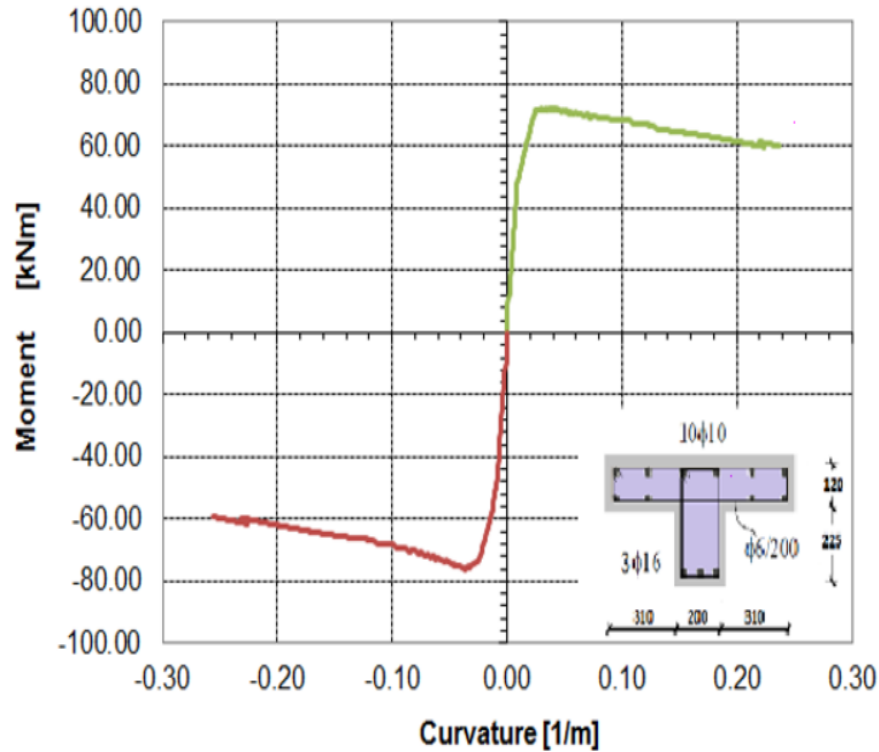
Figure 5.8: Moment and curvature relationships of T-shaped beam node part of 15 years old frame.

As seen in Figure 5.7 and Figure 5.8, the curvature values of the T-shaped beam member calculated in the order of 0.05-0.10 (1/m). The negative moment capacities of the T-shaped beam member is higher than the positive moment capacities in both cases. According to the numerical study, positive moment capacity and negative moment capacity of the columns have difference because of the longidutional bar location as lower or upper case. If the bar location is the lower case, the negative ultimate moment capacity of the section is about -78 kNm. It is about -96 kNm when the bar at upper location case as given above figures. The ultimate moment for positive side is 75 kNm and 46 kNm for lower side and upper side case given in Figure 5.7 and Figure 5.8, respectively.

If the results are compared with node and mid part of the T-shaped beam, yielding and ultimate moment capacities of the sections increase when negative moment acting on the section. In other words, the more ductile behavior for RC beams

cross sections is observed due to increment of curvature ductility on RC T-shaped section when negative moment acting on the section. Moreover, numerical results are concluded that the location of longitudinal reinforcing affect the yielding and ultimate moment capacities of the T-shaped beam types section.

Nonlinear material characteristics and linearized moment-curvature relations are used in the computer program. To get more real evaluation of structural damage distribution, material inelasticity is taken as spread along the whole member length of the RC frame and across to the RC cross section of the one bay one story RC frame.

Moment-curvature relations of the columns and beams were evaluated by the computer program DC2B(s2) and checked another program which is XTRACT section analysis program. Results of the moment-curvature relations of the different cross sections are given in detailed at section before this section. By using this moment curvature relations, member rigidity are found as initially and cracked values given below Table 5.1, respectively.

Cracking of the RC section is inherent in analysis of RC, and this cracking effects the reinforced concrete structure's durability, serviceability and its ductility. In the micro scale, cracking formation effect the rigidity parameters of the reinforced concrete sections directly. During the analytical study; changes in this micro scale paramater should be considered for more real solution. RC members frame are under the effect of bending because of that cracked bending rigidity are used during the computer analysis. At the section of 7.4.13 (TEC-2007); If there is no restricted calculation about the bending rigidity of cracked section, bending rigidity definition should be taken into consideration as given as fallows:

$$For\ beam: (EI)e = 0.40(EI)o \qquad (5.1)$$

$$For\ column: If\ \ ND/(Acfcm) \leq 0.10\ \ :\ \ (EI)e = 0.40(EI)o$$

$$If\ \ ND/(Acfcm) \geq 0.10\ \ :\ \ (EI)e = 0.80(EI)o$$

$$WhereNDistheaxialloadactingonthemembers.$$

Table 5.1: LVDT's used for cylindrical concrete specimens

Member	$\mathbf{EI}_{initial}$ [kNm$_2$]	$\mathbf{EI}_{carcked}$ [kNm$_2$]	$\mathbf{EI}_{TEC-2007}$ [kNm$_2$]
Beam (node)	3990.1	2100.2	1596.04
Beam (Mid)	5068.4	2918.9	2027.36
Column (bottom)	1149.2	572.1	459.68
Column (top)	459.68	1251.6	923.36

In literature, there are some different way to calculate the bending rigidity of the cracked section. One of them, Yongzhen Li (2010) used moment-curvature relationship of RC section to obtain a realistic determination of the stiffness of the element, the bending moment, related parameters of the element both for uncracked and cracked stage of the sections.

$$(EI)_{s,cr} = E_c I \tag{5.2}$$

The inertia modulus of cracked section as given below ;

$$I = \frac{bx^3}{12} + bx \cdot (\frac{x}{2})^2 + \alpha_e A_s (d-x)^2 \tag{5.3}$$

116

b is the cross section width

x is the compression zone depth

A_s is the reinforcement area in tension

α_e is the ratio of elastic modulus where $\frac{E_s}{E_c} = \alpha_e$

The stiffness at the cracking stage as given fallow;

$$(EI)_{s,cr} = E_c I = E_c \cdot (\frac{bx^3}{12} + bx \cdot (\frac{x}{2})^2 + \alpha_e A_s(d - x)^2) \tag{5.4}$$

By using the T-shaped and rectangular reinforced concrete cross section stress-strain balance, the compression zone depth obtained under the both axial load and bending moment effect. The bending rigidity is an important parameter related to the load-stress effect caused by plastic deformation on the section. After the compression zone depth of the section is obtained, by using the law of Tension Stiffening, the cracked elastic rigidity is calculated by the slope of the moment-curvature curve at the yielding points as given in Table 5.1 as above.

The analytical model of RC frame prepared in DC-2B(s2) is shown in Figure 5.1. Beam and columns elements are divided into 400 imaginary pieces to do analysis in more precision. The foundation of the frame was given in to the program as fixed type support for bottom ends of the columns. Three degrees of freedom are considered for each node of the RC frame by the program.

The analytical model used in program was subjected to constant vertical point loads on the center of the columns as during the experiment, distributed load on the beam and lateral push-pull load acting at the centre of the beam as shown in Figure 5.1. Lateral loads increased step by step up to the failure stage. In the analysis of the reinforced concrete one bay one story frame, 15 years old concrete properties are taken into account with corroded reinforcement material properties as a nonlinear material model given section before this part. Properties of the

reinforcement such as quantity, bar size and geometric location are introduced in the moment-curvature analysis step of the computer program DC-2B(s2).
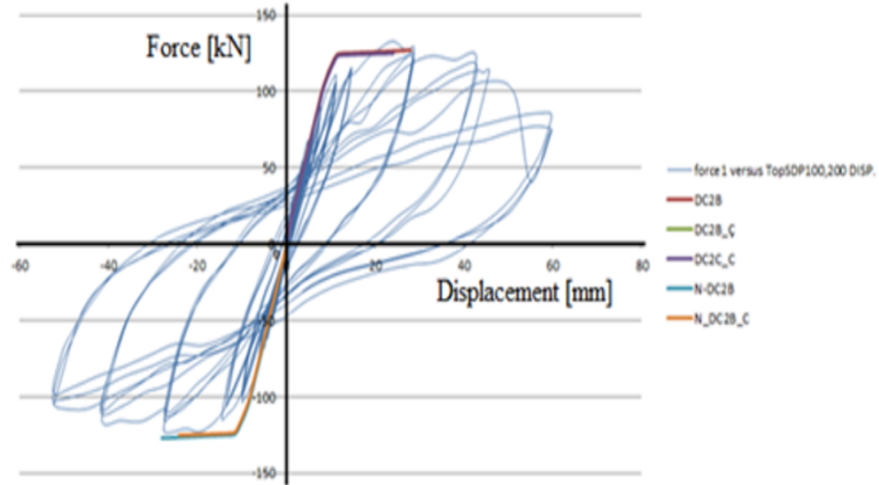
Figure 5.9: Force – Displacement curves of the computer program versus experimental.

As shown in Fig 5.9; analytical study by DC-2B(s2) overestimates strength values at the initial elastic cycles up to deformation point 18 mm. In the analytical study, reinforcement are yield at the point 10 mm top deformation and ruptured at the pint about 20 mm as seen in Fig 5.9. During the experiment, when the stirrups ruptured the cyclic analysis continue up to point that whole collapse of the system due to mechanism failure.
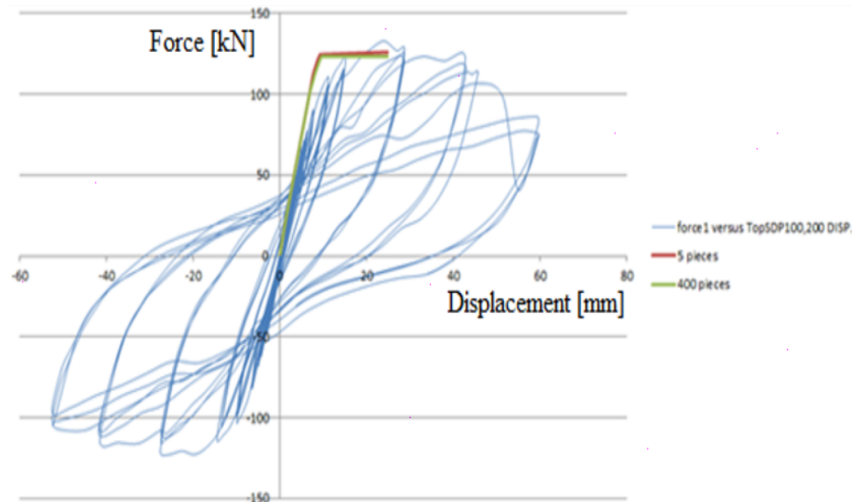
Figure 5.10: Force – Displacement curves of the computer program versus experiement with 5 and 400 pieces for RC members.

During the analysis of the RC frame with DC-2B(s2) ; there were several different parameters such as cracked sectional rigidity, material models and analytical details. Initial rigidity and cracked rigidity of the RC sections were used and compared as seen in the Fig5.9. The maximum deformation capacity of the stage of initial rigidity is higher than the cracked rigidity used stage as shown. In the Fig5.10, columns and beams were divided in to 5 pieces and 500 pieces and there was no changes observed at results of the push-over analysis.

5.2 Analytical Studies with SAP2000

In this theoretical study stage, to achieve a static pushover analysis with consideration the effect of natural corrosion on the structural behavior is investigated because of that SAP2000 used for numerical modelling. This section includes information about the computer program used to model the RC one bay one story frame. In the theoretical model created, the nonlinear behavior of RC members is represented using the distributed plasticity theorem where the plastic deformations occurs over a defined length. The rotational behavior cover the concepts of

119

bilinear hysteretic response based on the Modified Ibarra Krawinkler Deterioration Model (Ibarra et al. 2005). Cyclic deterioration were neglected and column axial loads is applied to the frame to simulate P-Delta effects for buckling safety. Material model and other parameters are same properties with section before this section.
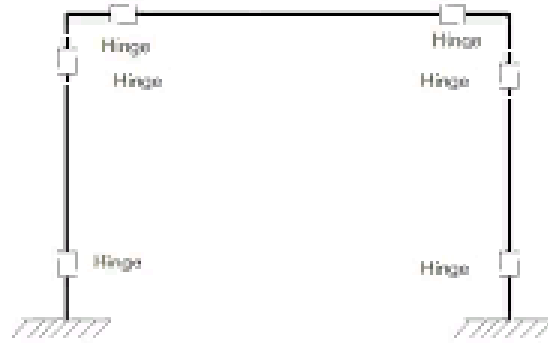
Figure 5.11: Frame model and hinges used in SAP2000.

The theoretical results of the distributed plasticity model was predict concentrated plasticity model quiet well. The results of the pushover analyses from the the SAP2000 model and experiment are shown in Fig.5.12. The experimental and SAP2000 results agree at the displacement level between 20 mm and 40 mm. The ultimate strength values agrees well for both analytical and experimental result at level 132 kN. Reinforcement reached minimum limit at top end of the first column and at the same top displacement level confined concrete has reached safety limit at the top end of the first column of frame.
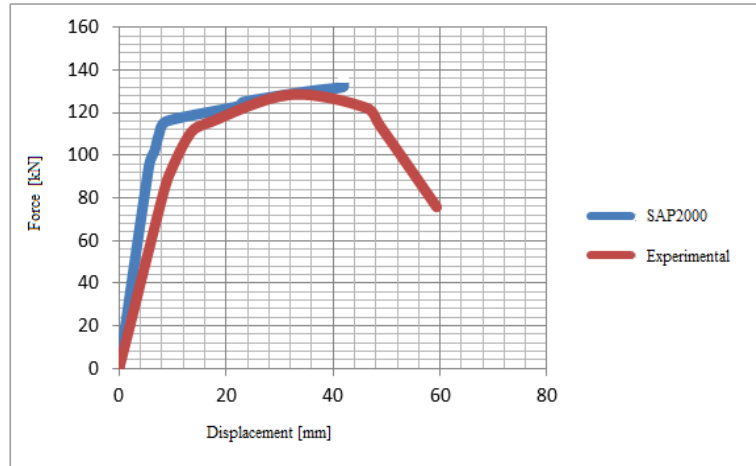
Figure 5.12: Pushover curve of the frame with SAP2000 and experimental.

The determination of natural period of the RC structures is an essential stage in earthquake based design. During the theoretical work, pushover analysis carried out with several computer programs and results compared with experimental outputs. The natural period of the RC frame calculated by hand, DC2B and SAP2000 outputs. During the nonlinear pushover analysis, period of the structure increased with the increment of the applied load and plasticity.

When the reinforcement reached damage limit at top end of the first column and concrete has reached safety limit at the top end of the first column of frame, period become bigger and bigger after that limit point as given below Fig.[5.22].
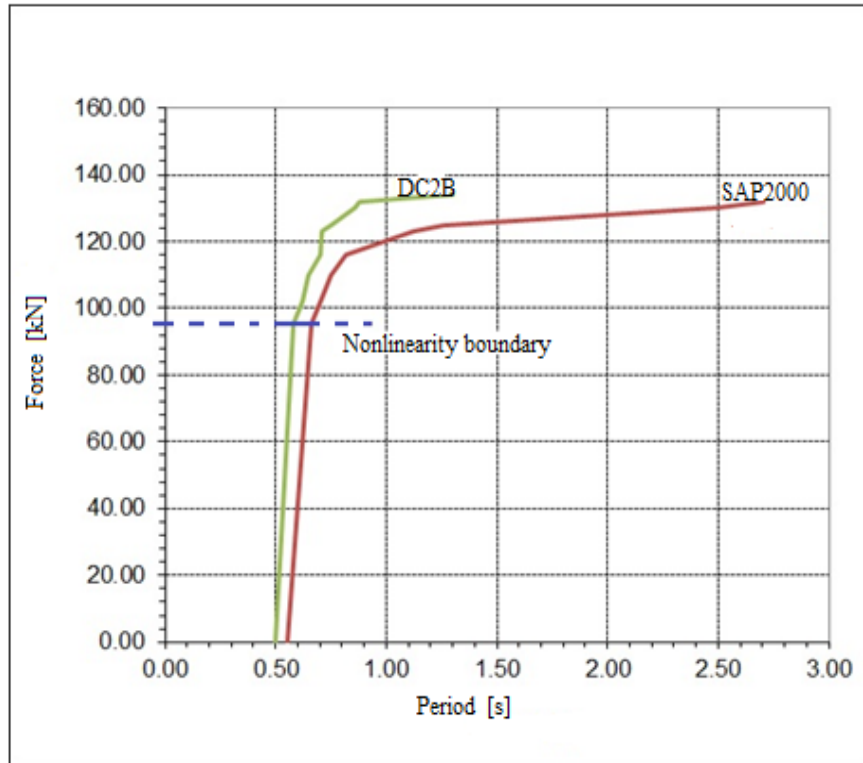
Figure 5.13: Force versus period diagram with capacity curve.

5.3   Analytical Studies with SeismoStruct

There are several computer programs to analyse the RC structures such as ABAQUS, SAP2000, OpenSess, ANSYS and SeismoStruct. In this theoretical study, the effect of the corrosion on the structural behavior is investigated because of that SeismoStruct used for numerical modelling. This chapter includes information about the computer program used to model the RC one bay one story frame.

Material nonlinearities are used in the computer program as given in the section before this section. To get more convenient result, material nonlinearity is assumed to spread along the structural sections as implemented fibre modelling.
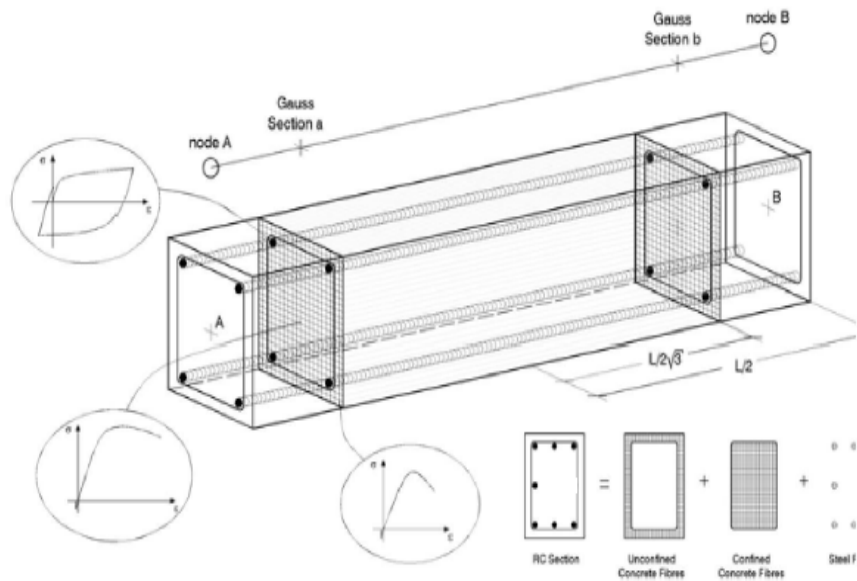
Figure 5.14: Integration points in RC frame elements and fibre modelling.
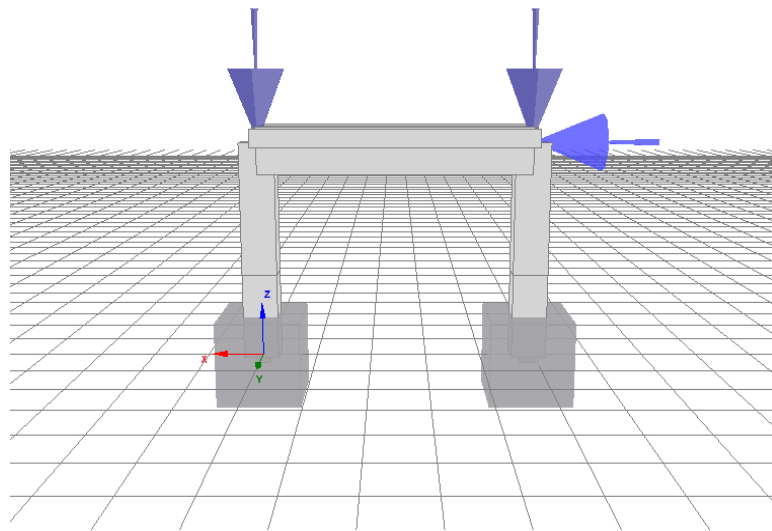
Figure 5.15: Frame model used in SeismoStruct front view.

Inelastic reinforced concrete frame elements were used, geometric and material nonlinearities were defined to the program as given Fig.5.17.
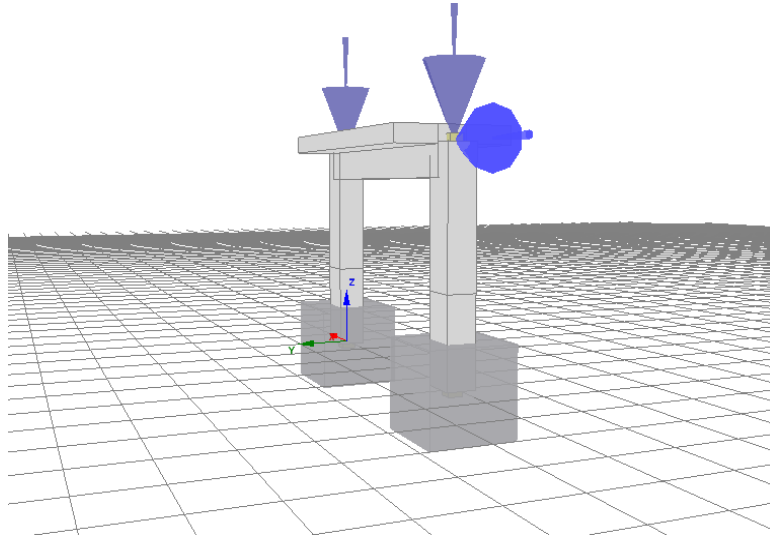
Figure 5.16: Frame model used in SeismoStruct side view.

During the definition of the material models, some of the parameters are inserted from the tests results that achieved at experiment stages. Some parameters defined to the program manually. Reinforcement model and concrete model is used given in Fig.5.17.Modulus of elasticity, yield strength, transition curve coefficients,specific weight, bar diameter, compressive strength of concrete, tensile strength of concrete and confinement factor were defined manual to the program.
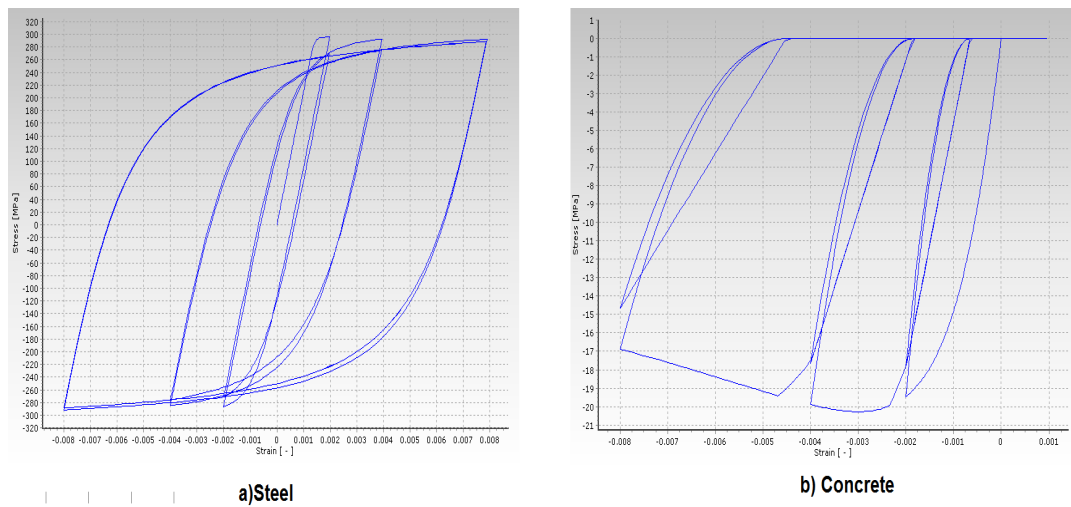
Figure 5.17: Material models used in analytical study.
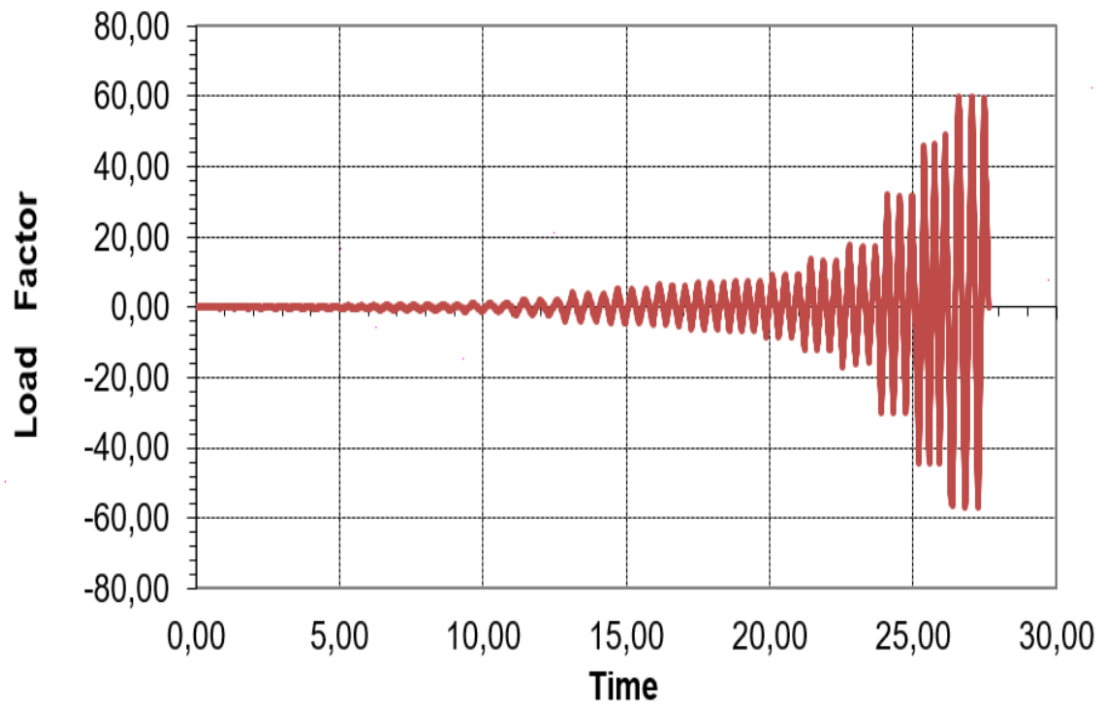
Figure 5.18: The displacement pattern applied to RC frames.

The displacement protocol applied to bare frame and RCF-2 is given in Fig.5.18 as applied experiment. Minimum damage limit, safety limit and collapse limit are defined according to the Turkish Earthquake Code proposal.
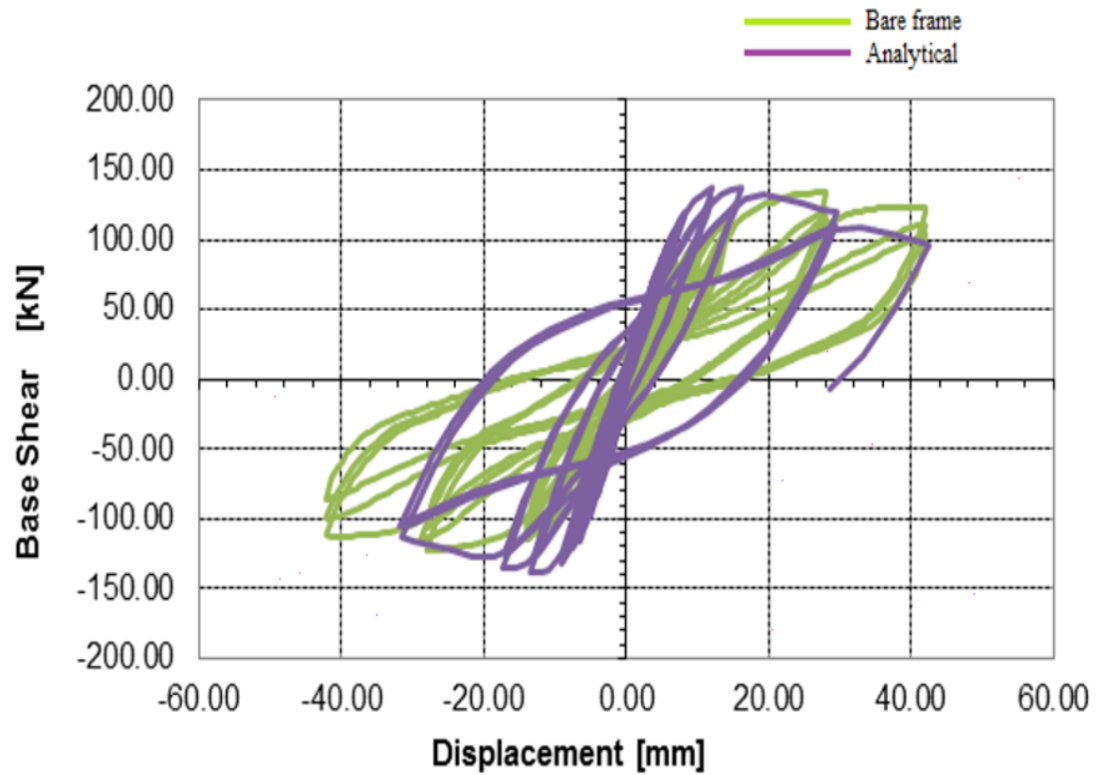
Figure 5.19: Hysteretic curves of the bare frame experimental and analytical results.

The maximum load and target displacement occurred in the structure is closer as experimental results as given in Fig.5.19. Descending load branch slope of the experimental results is lower than the analytical results obtained by nonlinear static analysis. Reinforcement bars has reached minimum damage limit at the bottom and top closer node section. At the same stage unconfined concrete has reached collapse and safety limit at the lower section of the second columns.
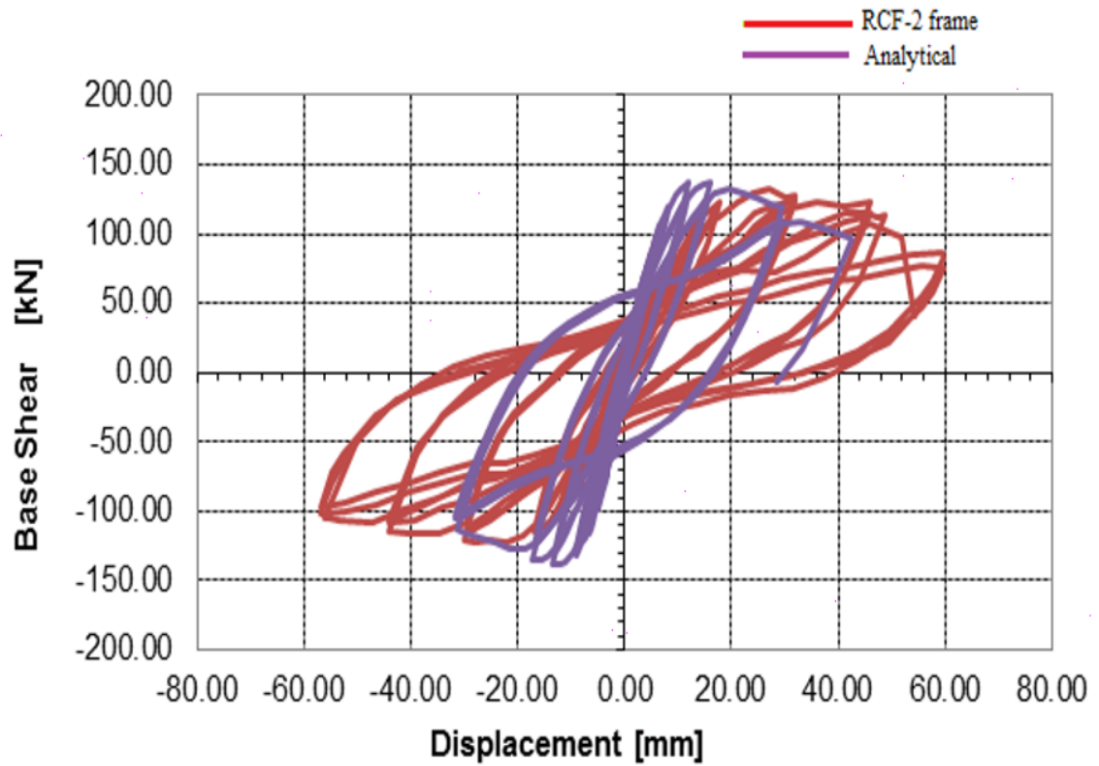
Figure 5.20: Hysteretic curves of the RCF-2 frame experimental and analytical results.

As given in Fig.5.20, experimental results overlapp with the analytical study quiet well at elastic region. The maximum load observed in the analysis as same as experimental results. Reinforcement performance level has reached damage limit at three percent drift ratio level at the bottom end of the first column. Confined concrete capacity reached the collapse damage limit as the bottom node of the first column at 3% story drift stage.
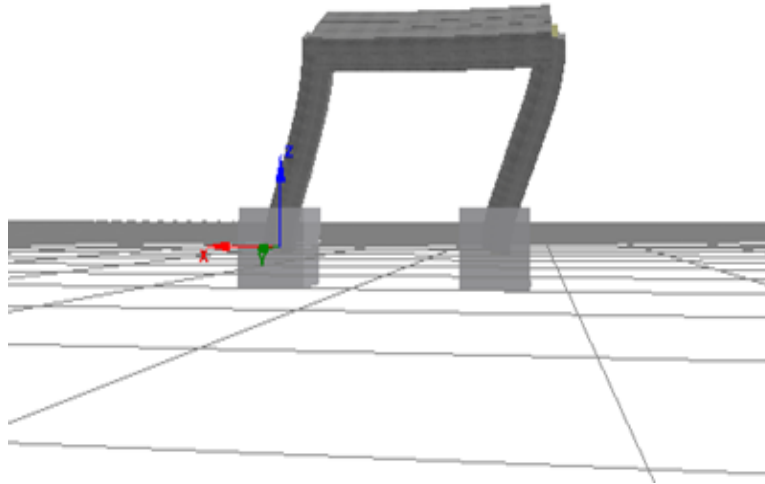
Figure 5.21: Damage shape of analytical work of RCF-2 at push cyle.

The damage model occurred in SeismoStruct is shown in Fig.5.21 and Fig 5.22, respectively. The RC frame was subjected to constant axial loads on the columns and horizontal cyclic displacement protocol applied to the frame to represents the seismic behavior. Analytical works achieved for reference bare frame and other tested RC frame to comparison them between each other. Hysteretic curves, failure modes and shapes, failure reason and damage limit results were given at this section, respectively.
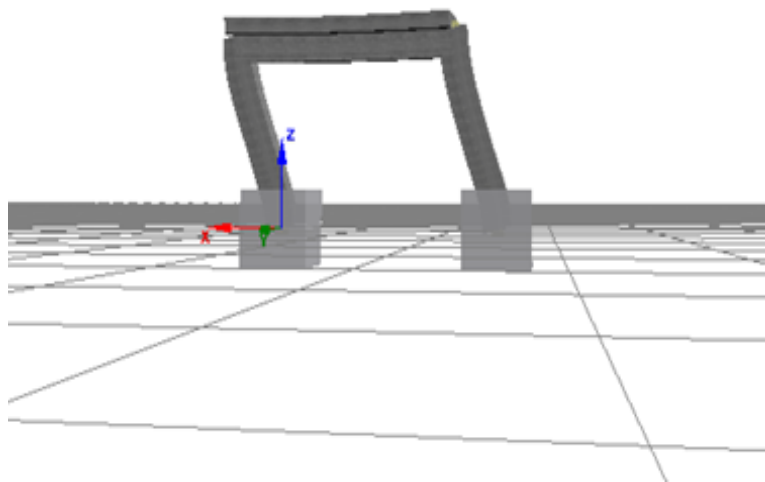
Figure 5.22: Damage shape of analiytical work of RCF-2 at pull cyle.

5.4 Design of a computer program for buckling load parameter

Several computer programs such as SAP2000, SeismoStruct and DC2B(v2) were used to analytical works of modelling the corroded RC frame and a special purpose computer program has been developed for finding the buckling load parameters of a frame with and without plastic hinges. NetBeans IDE 8.2 and DC2B computer programs were combined to find the buckling load parameter when the nonlinear static analysis applied on the defined structure. Computer program flow chart is given below and code is given at appendix A.
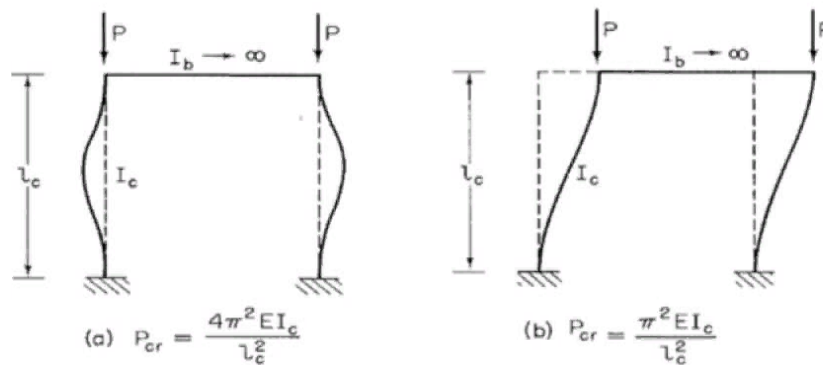
Figure 5.23: Modes of buckling for the RC frame.
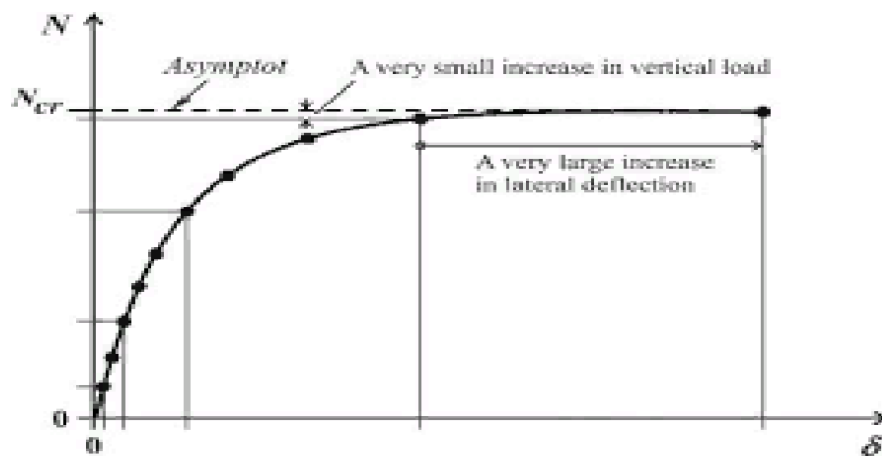
Figure 5.24: P-Delta curve assesment for buckling load.

Global or local bukling is a curial problem for several types of members and structures. It should be controlled during the each step of the loading. It is known that plastic hinge formation starts with the materials nonlinearitiy limits and this formation effects the members and structures safety factor against buckling. Push over analysis starts with the zero load- zero deformation state and it goes on to the target/limit displacement. Sectional rigidity, member rigidity and system rigidity change at every step of the analysis. By the way structures going to be more closer to the buckling than before state. By the help of the this computer programs, bucking safety factor checked at each new state by the matrix stability method as defined in the outline chart. NetBeans IDE 8.2 and DC2B computer programs were combined to find the buckling load parameter when the nonlinear static analysis applied on the defined structure. Computer program flow chart is given below and code is given at appendix A.

At the first stage, DC2B package computer based program calculate the rigidity values according to the structural features and it gives the output values for matrix evaluation part. The developed computer program construct the rigidity matrix according to the output values.

The first case calculate the determination of matrix A according to the Gauss elimination method and it checks the stability of the matrix. If the cases satisfies the condition, program gives the buckling load accordingly. But if the condition not satisfies the given case, the computer programs continue to the other loops. At the end of the loop analysis, computer program gives the buckling load to draw the P-Delta curve that is given above.

Where;

$$\mathbf{N_{ij}} : axial\ force$$
$$\varphi_{\mathbf{ij}} : a\ constant$$
$$\mathbf{L_{ij}} : member's\ length$$
$$\mathbf{EI_{ij}} : bending\ rigidity$$

DEFINE THE STRUCTURAL SYSTEM

M a b

$$\varphi_{ij} = L_{ij} \sqrt{\frac{N_{ij}}{EI_{ij}}}$$

Find B_{11} B_{12} B_{14} B_{44}

k_{11} k_{12} k_{14} k_{44}

$$[\ ]*[\ ]=[\ ]$$

CHECK   CHECK

Case must ;) If det(A)=0

Give Result. ....▶

Case a ;) If det(A)>0

loop

Increase N_{ij} to $(N_{ij} + x)$

Case must ;) If det(A)=0

Give Result. ....▶

Case b ;) If det(A)<0

loop

Decrease N_{ij} to $(N_{ij} - x)$

Case must ;) If det(A)=0

Give Result. ....▶

END

131
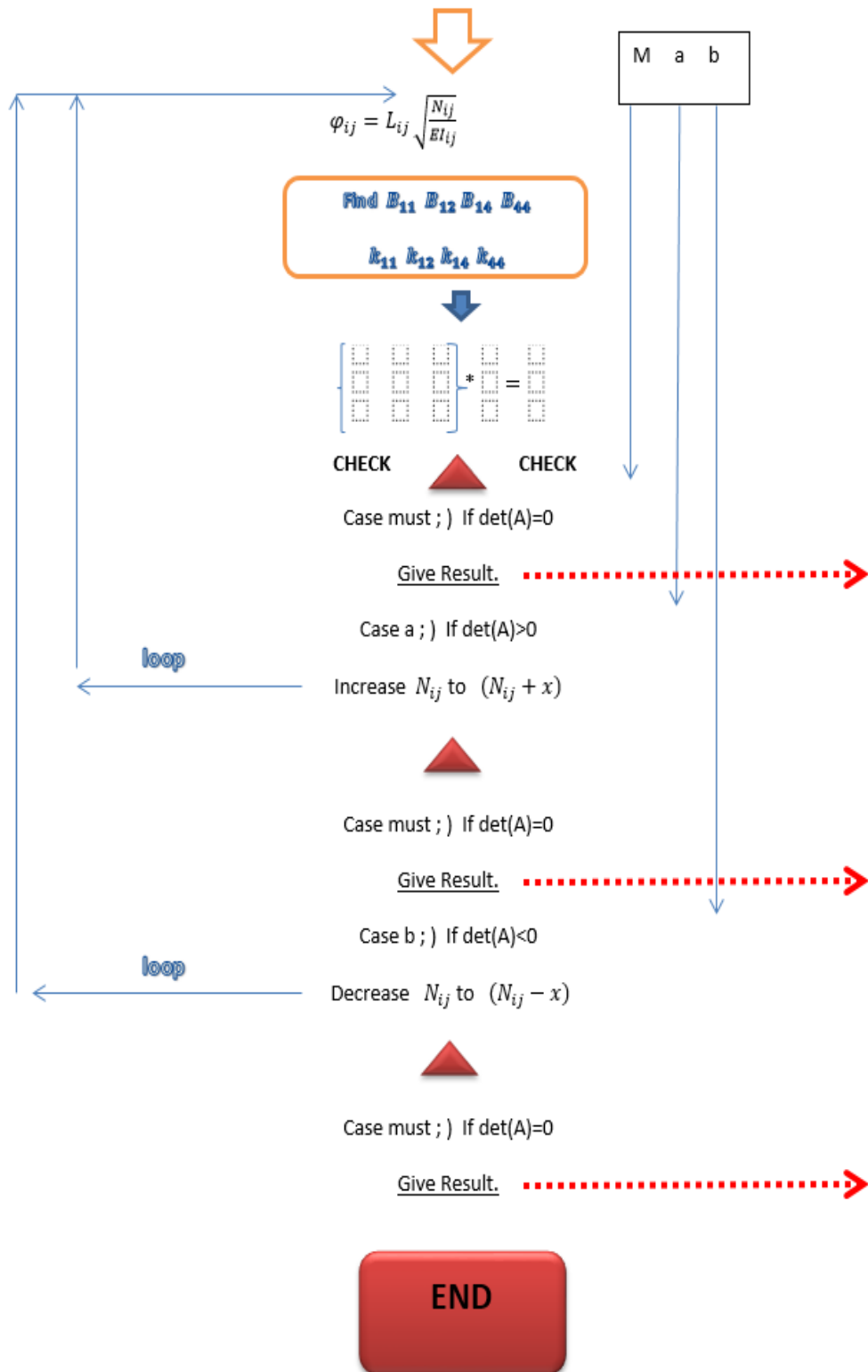
Chapter 6

Conclusion

Corrosion of steel bars is one of the main destructive effects on load-bearing capacity and serviceability of reinforced concrete structures. The effective cross sectional area of reinforcement reduces due to corrosion attack and the bond between reinforcement and concrete is lost in corroded RC structures. Corrosion reaction process effects the structural seismic behavior of the RC structures that's why the RC structures designed for the same seismic capacity could have different seismic performance especially during the earthquakes.

One reference and three reinforced concrete single bay single story 1/3 scale frame specimens were produced, subjected to natural corrosion and then tested under reversed cyclic load at the main campus of Istanbul Technical University. The bare frame and other specimens were constructed using special structural features such as low concrete quality with aggregate and sand coming from sea bed and non-ribbed mild steel to represents the existing RC structures stock built in Turkey before the existing earthquake codes and standards. This study is composed of primarily the theoretical and analytical works mainly based on experimental works. All frame specimens were tested up to failure point and the performance of specimens were studied through their failure modes, lateral load carrying capacity, initial stiffness and cumulative energy dissipation capacity. Different computer programs were used to analyse the structure and compare the overall results in terms of natural corrosion time effect. Also, confined/unconfined concrete

cylindrical specimens were tested as well for working on Poisson's ratio and stress strain relationships in descending branch.

Concrete core and reinforcement bar sample taken and tested to have an idea about the material mechanical properties. According to the study made after the experiments; characteristics of actual concrete and reinforcement model behavior defined. Probably corrosion was concentrated on stirrups, foundation and lower part of the column's longidutional bars. As seen according to the corrosion cleaning result given in Section 4.2.4.2, change in weight of stirrups specimens is %1.7 that is 3 times higher than the longiditional bars.

The reference frame and 15 years old frames had shear and bending type cracks formation during the tests. The cracks width are 0.1 mm at the beginning and 45 mm at the end of the experiments. During the displacement control based test, displacement protocol applied on the structure and the failure modes occurred at the stage of ultimate load level. Bending and shear failure occurred at column bottom/top ends of reference RC frame. Shear failure observed at left column ends of RCF-2 as shown Fig 4.46. The shear strength capacity of the column is low because of corrosion of the reinforcement effects the shear strength of columns as given figure above. This is because the failure occurred on the confinement reinforcement as given Fig 4.46 (b) in detailed.

The initial lateral stiffness of the reinforced concrete corroded frames increased compared with the references RC frame at just before the initial cracks observed in the structure. The initial stiffness of the frames are calculated from the base shear versus displacement graph as the tangent of maximum shear occurred during the cycles. Initial stiffness of the reference frame was 21.6 [kN/mm] and 25.4 [kN/mm] for specimen RCF-2.

The base shear carrying capacity kept constant level compared with the references RC frame as seen in Fig 4.40. The ultimate displacement capacity increased at 4 % story drift level for RCF-2 compared to the references RC frame.

The cumulative energy dissipation of the reference frame (specimen 1) at 3 percent story drift is 20.000 [kNmm]. The total energy dissipation of the RCF-2 at 3% story drift is 1.6 times bigger compared to the reference frame's as shown in Fig 4.44 The cumulative energy dissipation of reference frame at 0.03 story drift is 1.6 times increased compared to the RCF-2 shown in Fig 4.44.

The theoretical works that were achieved by several computer programs such as Sap2000, SeismoStruct and DC2B(v2) used to modelling the corroded RC frame. Nonlinear pushover analysis is carried out for corroded frame. The theoretical assumptions and corrosion behavior are based on the material test results of the experimental study. The theoretical results agree with the experimental results not only the maximum load capacity, target displacement, but also the similar damage propagation which is occurred during the experimental program given in detailed.

There were a lot of tests on 15 years old cylindrical 15/30 cm specimens has been conducted during the second stage of the experimental program to obtain Poisson's ratio and stress strain relationships in descending branch. The results have been compared by code proposals, the stress-strain relationships of confined/unconfined specimens have been compared paying attention on the descending branches as given in detailed at the section 4.4.

Results of the experimental and theoretical works prove that corrosion effects the structural behavior of reinforced concrete frames during the earthquake because of several reasons given in detailed at previous section. The experimental and theoretical findings of natural corrosion study are valuable information for the seismic performance analysis and development of retrofit strategies plan of existing natural corroded building stock.

Appendix A

Computer program code for buckling load

```
/*
* To change this license header, choose License Headers in Project Properties.
* To change this template file, choose Tools — Templates
* and open the template in the editor.
*/
package buck;


import java.io.BufferedReader;
import java.io.BufferedWriter;
import java.io.File;
import java.io.FileReader;
import java.io.FileWriter;
import java.util.ArrayList;
import java.util.Arrays;
import java.io.BufferedWriter;
import java.io.File;
import java.io.FileNotFoundException;
import java.io.FileReader;
import java.io.FileWriter;
import java.io.IOException;
```

```java
import java.util.ArrayList;

import java.util.Arrays;

import jxl.Workbook;

import jxl.read.biff.BiffException;

import jxl.write.Label;

import jxl.write.WritableSheet;

import jxl.write.WritableWorkbook;

import jxl.write.WriteException;


/**
 *
 * @author Isik
 */
public class BUCK
/**
 * @param args the command line arguments
 */
public static void main(String[] args) throws

FileNotFoundException, IOException, Exception

ArrayList<Double> f = new ArrayList<>();

ArrayList<Double> p = new ArrayList<>();

double K =100.56;

int delta_K = 1;

double d = 1.0;

do


int i = 1;

FileReader file1 = new FileReader("C:

Users

Isik
```

```
Desktop

DC2Bjava

DC-2B.dat");

BufferedReader reader = new BufferedReader(file1);

String text = "";

String line32 = "";

String lineUpdate = "";

String line = reader.readLine();

String n1 = System.getProperty("line.separator");

while (line != null)


// if (i == 32)
// line = line.substring(0, line.lastIndexOf(' ')) + " " + -1.4825 * K;
//
// if (i == 33)
// line = line.substring(0, line.lastIndexOf(' ')) + " " + -1.06 * K;
//
// if (i == 33)
// line = line.substring(0, line.lastIndexOf(' ')) + " " + 1.4825 * K;
//
if (i == 32)
line = "1 0 0.0 0.0 " + 1* K;


if (i == 33)
line = "2 0 0.0 0.0 " + 1* K;


text += line + n1;
line = reader.readLine();
i++;
```

```java
System.out.println(text);
reader.close();
try
File logFile = new File("C:
Users
Isik
Desktop
DC2B - java
DC-2B.dat");
BufferedWriter writer = new BufferedWriter(new FileWriter(logFile));
writer.write(text);
writer.close();
catch (Exception e)
e.printStackTrace();

try
//Runtime runTime = Runtime.getRuntime();
//Process process = runTime.exec("C:
Users
Isik
Desktop
DC2B - java
DC-2B-r24.exe");
Process process = Runtime.getRuntime().exec("C:
Users
Isik
Desktop
DC2Bjava
DC-2B-r49.exe", null, new File("C:
Users
Isik
```

```
            Desktop
            DC2Bjava
            "));
            process.waitFor();
        catch (Exception e)
            e.printStackTrace();



            FileReader file2 = new FileReader("C:
            Users
            Isik
            Desktop
            DC2Bjava
            DC-2B.son");
            BufferedReader reader2 = new BufferedReader(file2);


            String text2 = "";
            String line31 = "";
            i = 0;
            String line2 = reader2.readLine();
            while (line2 != null)
            text2 += line2 + n1;
            line2 = reader2.readLine();
            if (i == 30)
            line31 = line2;



            i++;
```

```
System.out.println(text2);

String[] output = line31.split(" ");

d = Double.parseDouble(output[3]);

System.out.println(d);

System.out.println(line31);

if ((K/d) ¿ 0)

f.add(d);

p.add(K);

K = K + delta_K;

else if ((K/d) ¡ 0)

K = K + delta_K * 0.5;




while (K/d ¿= 0.1);

System.out.println(Arrays.toString(f.toArray()));

System.out.println(Arrays.toString(p.toArray()));

createexcel(f,p);


public static void createexcel(ArrayList¡Double¿ x, ArrayList¡Double¿ p) throws
BiffException, Exception, WriteException

WritableWorkbook wworkbook;

wworkbook = Workbook.createWorkbook(new File("C:

Users

Isik

Desktop

n_java.xlsx"));

WritableSheet wsheet = wworkbook.createSheet("First Sheet", 0);

Label label = new Label(0, 2, "buckling load vs displacement ");

wsheet.addCell(label);

int h = 0;

for (int indx = 0; indx ¡ x.size(); indx++)
```

```
h = indx + 1;
jxl.write.Number number = new jxl.write.Number(3, 4 + h, x.get(indx));
wsheet.addCell(number);
jxl.write.Number number2 = new jxl.write.Number(4, 4 + h, p.get(indx));
wsheet.addCell(number2);

wworkbook.write();
wworkbook.close();
```

Appendix B

Computer program file DC2B for buckling load

run:

*** C3_SU_13

NOKTA;CUBUK;YUKLU CUBUK;GEVSEKLIK;YAY;YUKLU DUGUM

NOK.;SIFIR DEP. NOKTA SAY.

4 3 1 0 0 2 2

***** DUGUM NOKTALARI GEOMETRISI

NOKTA NO - X KOORDINATI - Y KOORDINATI

1 0.0 1.417

2 1.95 1.417

3 0.0 0.00

4 1.95 0.00

***** CUBUK ELEMAN BILGILERI

CUBUK - SOL UC - SAG UC - EI - EF - YAYILI YUK(1/0) - CUBUK TIPI -

GF - RSOL/L - RSAG/L -EKBILGI

1 1 2 2400.6 1152000.0 1 0 0.0 0.0 0.0 0.0

2 3 1 858.5 87280.0 0 0 0.0 0.0 0.0 0.0

3 2 4 858.5 87280.0 0 0 0.0 0.0 0.0 0.0

***** YUKLU CUBUK BILGILERI

IYUKTIP CUBUK NO - Z1 Z2 Z3 Z4 Z5 Z6 Z7 ALFA

0 1 0.0 0.0 1.95 0.0 3.44 0.0 0.0 0.0

***** CUBUK UC MAFSALLARI VE YAYLARI BILGISI

CUBUK GEV-1 GEV-5 GEV-6 GEV-2 GEV-3 GEV-4 YAY-1 YAY-5 YAY-6

YAY-2 YAY-3 YAY-4

0

***** YAY BILGILERI

NOKTA NO - X - Y - Z DOGRULTUSUNDAKI YAY SABITLERI

0

***** YUKLU DUGUM NOKTASI BILGILERI

NOKTA NO - IYUKTIPI P1 P2 P3 [kN]

1 0 0.0 0.0 100.56

2 0 0.0 0.0 100.56

***** TUTULMUS DUGUM NOKTASI BILGILERI

NOKTA NO - d1 d2 d3

3 1 1 1

4 1 1 1

References

[1] U. American Concrete Institute, "Aci-222r," *ACI-222R*, 2001.

[2] P. Desnerck, J. M. Lees, and C. T. Morley, "Bond behaviour of reinforcing bars in cracked concrete," *Construction and Building Materials*, vol. 94, pp. 126–136, 2015.

[3] W. Y. Zhang, R. Y. Zhang, and L. Xi, "Corrosion of reinforced concrete in accelerated tests," in *Advanced Materials Research*, vol. 610. Trans Tech Publ, 2013, pp. 485–489.

[4] R. Zhang, A. Castel, and R. François, "Concrete cover cracking with reinforcement corrosion of rc beam during chloride-induced corrosion process," *Cement and Concrete Research*, vol. 40, no. 3, pp. 415–425, 2010.

[5] O. T. Femi, "A contemporary review of the effects of corrosion of damaged concrete cover on the structural performance of concrete structure using cfrp strengthened corroded beam," *J Multidiscip Eng Sci Technol*, vol. 1, pp. 91–99, 2014.

[6] A. Al-Saidy, A. Al-Harthy, and K. Al-Jabri, "Effect of damaged concrete cover on the structural performance of cfrp strengthened corroded concrete beams," 2009.

[7] V. Kumar, R. Singh, and M. Quraishi, "A study on corrosion of reinforcement in concrete and effect of inhibitor on service life of rcc," *J. Mater. Environ. Sci*, vol. 4, no. 5, pp. 726–731, 2013.

[8] H. Yalçıner, "Predicting performance level of reinforced concrete structures subject to corrosion as a function of time," Ph.D. dissertation, Eastern Mediterranean University (EMU), 2012.

[9] G. Campione, F. Cannella, and G. Minafo, "A simple model for the calculation of the axial load-carrying capacity of corroded rc columns," *Materials and Structures*, vol. 49, no. 5, pp. 1935–1945, 2016.

[10] L. Berto, P. Simioni, and A. Saetta, "Numerical modelling of bond behaviour in rc structures affected by reinforcement corrosion," *Engineering Structures*, vol. 30, no. 5, pp. 1375–1385, 2008.

[11] C. Fu, N. Jin, H. Ye, X. Jin, and W. Dai, "Corrosion characteristics of a 4-year naturally corroded reinforced concrete beam with load-induced transverse cracks," *Corrosion Science*, vol. 117, pp. 11–23, 2017.

[12] W. Zhu and R. François, "Corrosion of the reinforcement and its influence on the residual structural performance of a 26-year-old corroded rc beam," *Construction and Building Materials*, vol. 51, pp. 461–472, 2014.

[13] J. Cairns, G. A. Plizzari, Y. Du, D. W. Law, and C. Franzoni, "Mechanical properties of corrosion-damaged reinforcement," *ACI Materials Journal*, vol. 102, no. 4, p. 256, 2005.

[14] C. Apostolopoulos and D. Michalopoulos, "The impact of chloride induced corrosion and low cycle fatigue on reinforcing steel."

[15] R. François, I. Khan, and V. H. Dang, "Impact of corrosion on mechanical properties of steel embedded in 27-year-old corroded reinforced concrete beams," *Materials and structures*, vol. 46, no. 6, pp. 899–910, 2013.

[16] L. X. Wang, X. and B. J. Deng, *Shanghai Jiaotong Univ (Sci.)*, 2012.

[17] A. Jayasuriya and T. Pheeraphan, "Prediction of time to crack reinforced concrete by chloride induced corrosion," *World Academy of Science, Engineering and Technology, International Journal of Civil, Environmental,*

Structural, Construction and Architectural Engineering, vol. 11, no. 9, pp. 1197–1203, 2017.

[18] C. Alonso, C. Andrade, J. Rodriguez, and J. M. Diez, "Factors controlling cracking of concrete affected by reinforcement corrosion," *Materials and structures*, vol. 31, no. 7, pp. 435–441, 1998.

[19] S. Ahmad, "Reinforcement corrosion in concrete structures, its monitoring and service life prediction—-a review," *Cement and concrete composites*, vol. 25, no. 4-5, pp. 459–471, 2003.

[20] H.-S. Lee, T. Noguchi, and F. Tomosawa, "Evaluation of the bond properties between concrete and reinforcement as a function of the degree of reinforcement corrosion," *Cement and Concrete research*, vol. 32, no. 8, pp. 1313–1318, 2002.

[21] C. Fang, K. Lundgren, L. Chen, and C. Zhu, "Corrosion influence on bond in reinforced concrete," *Cement and concrete research*, vol. 34, no. 11, pp. 2159–2167, 2004.

[22] K. Lundgren, M. Tahershamsi, K. Zandi, and M. Plos, "Tests on anchorage of naturally corroded reinforcement in concrete," *Materials and Structures*, vol. 48, no. 7, pp. 2009–2022, 2015.

[23] S. R. L, *Pacific Northest Tab 45*, 1980.

[24] S. M, *Sea water corrosion handbook*, 1979.

[25] T. Liu and R. Weyers, "Modeling the dynamic process in chloride contaminated concrete structures," *Cement and Concrete research,28(3),pp.365-379*, 1998.

[26] C. Andrade and C. Alonso, "Test methods for on-site corrosion rate measurement of steel reinforcement in concrete by means of the polarization resistance method," *Materials and Structures*, vol. 37, no. 9, pp. 623–643, 2004.

[27] H. Wang and Q. Li, "Prediction of elastic modulus and poisson's ratio for unsaturated concrete," *International Journal of Solids and Structures*, vol. 44, no. 5, pp. 1370–1379, 2007.

[28] A. Mirmiran and M. Shahawy, "Dilation characteristics of confined concrete. mechanics of cohesive-frictional materials," *MECH COHESIVE-FRICT MATER*, 1997.

[29] M. S. c. Azlan Adnan and I. M. Taib, "The mechanical properties of high strength concrete for box girder bridge deck," *Asia Pacific Structural Engineering Conference*, 2009.

[30] O. O. Olugbenga Ata, Kolapo Olusola and A. Olanipekun, "A study of compressive strength characteristics of laterite/sand hollow blocks," *Civil Engineering Dimension, Vol. 9, No. 1, 15–18, March 2007*, 2007.

[31] D. W. Dinehart and H. W. Shenton Iii, "Comparison of static and dynamic response of timber shear walls," *Journal of Structural Engineering*, 1998.

[32] "Turkish earthquake code," *Ankara*, 2007.

[33] "Turkish earthquake code," *Ministry of public works and settlement Ankara*, 2018.

[34] J. Mander and P. M. J. N., "Theoretical stress-strain model for confined concrete," *Journal of Structural Engineering*, 1988.